CORROSIVE PROPERTIES OF COMBUSTION GASES PRODUCED FROM LIQUID FUELS

by

AHMAD, SYED HABIBUDDIN,

B.Sc(Eng)(Hons); M.Sc(Eng)(London)

A thesis submitted to C.N.A.A. for the degree of Doctor of Philosophy in the Faculty of Engineering

Department of Fuel and Combustion Technology

Middlesex Polytechnic

Queensway, Enfield

JUNE, 1974

SUMMARY

The mechanism of formation of sulphur trioxide in combustion gases has been investigated using liquid fuel firing combustor with laminar pre-mixed flame.

The combustion chamber was constructed from a stainless steel tube for minimizing any affect of catalysis. A temperature controlled evaporating chamber was designed where liquid fuel was evaporated and mixed with total combustion air prior to entering the combustion zone. The vapour mixture then passed through a silica sintered disc and a flat flame was produced. Six sampling ports at 0.304m (1 ft) intervals along the combustion tube were used for sampling the gases for analysis and for the measurement of sulphur trioxide with respect to residence time. Diesel oil, Kerosine, Cyclohexane, n-hexane, and n-Pentane were used in the investigation. Sulphur content of these fuels were raised to 3.4% (wt.) by addition of appropriate amount of carbon disulphide (CS_2) in each fuel.

It was found that SO_3 was only formed when there was an excess oxygen in the combustion gases and under sub-stoichiometric conditions, no SO_3 could be detected.

An increase in the quantity of combustion air in excess of stoichiometric requirement lead to an increase in the concentration of SO_3 in the combustion gases. However, the level of SO_3-content in the flue gases reached a maximum at about 4% excess oxygen concentration in the flue gases.

It was established that ignition properties of fuels have an effect on the oxidation of SO_2. Ignition delay ν temperature curves for the fuels employed in the research programme were determined. This was done with the help of Ignition-Delay apparatus (PART II). It was found that fuels having shorter ignition delay times at temperatures prevailing near flame zone produced less SO_3 under identical combustion conditions.

The results of the effect of residence time of combustion gases in the high temperature zone showed that in the first instance amount of SO_3 formed was in excess of those predicted from thermodynamic considerations involving molecular oxygen. Sulphur trioxide thus formed began to dissociate back into sulphur dioxide and oxygen as the gases continued to pass along the combustion chamber. It was thought that oxygen atoms, produced in the flame, being a reactive oxidising species are responsible for the oxidation of SO_2. The theory proposed to explain the experimental results appear to be that of a consecutive reaction by

$$SO_2 + O \xrightarrow{K_1} SO_3 \xrightarrow{K_2} SO_2 + \tfrac{1}{2} O_2$$

where K_1 and K_2 are specific reaction rate constants for individual reactions (unit of K = sec^{-1}).

ACKNOWLEDGEMENTS

The author wishes to thank Dr. R. M. W. Rickett, B.Sc.,Ph.D., FRIC., Director, Middlesex Polytechnic, for granting permission to carry out research; to Mr. J. Osborne-Moss, Dean of Engineering, Science and Mathematics for taking interest in the work and for providing adequate facilities.

The author has great pleasure in acknowledging his thanks to Mr. D. F. Rosborough, Senior Research Scientist, ESSO Research Limited, Abingdon, for his discerning advice and help throughout the duration of research and for his constructive criticism to the draft thesis.

The author is grateful to Dr. B. J. Zaczek, Director of Studies for his supervision and guidance given throughout the investigation of the problem and taking a keen interest.

A word of thanks also to the Departmental technicians who helped in the work in their various capacities.

Last but not least, the author would like to record his thanks to his parents for their love and encouragement and to his wife for her understanding.

ABRIDGED CONTENTS LIST

TABLE OF CONTENTS

LIST OF FIGURES

LIST OF TABLES

LIST OF PLATES

CHAPTER 1

INTRODUCTION

With the refining of crude petroleum, high grade petrol is obtained leaving behind a high content of impurities in the residual fuel. The impurities contain substances like sulphur, vanadium, sodium etc., and it is basically these substances which are mostly responsible for fouling and corrosion in oil-fired installations. The sulphur content of the petroleum fuel products are generally much higher than other impurities and can vary in the range of 1.5 to 4 per cent (wt)[1].

During normal combustion, in the presence of excess air the sulphur in the fuel is oxidised to sulphur dioxide and a small portion to sulphur trioxide. It is generally accepted that occurrence of sulphur trioxide in an industrial combustion system is a major contributory cause to both high and low temperature corrosion of heat exchange surfaces.

High temperature corrosion occurs when metal surfaces are exposed to flue gases of about 650°C or over. In such conditions, even high grade steels are attacked and corrosion becomes a serious problem. Organic compounds of vanadium and sodium present in the residual fuel oil are considered to be worst offenders. Vanadium present in the fuel is converted during combustion to various oxides, the highest of which is vanadium Pentoxide. The condition can be further aggravated by the presence of other impurities like sodium sulphate which at a temperature of 630°C and above gives the following reaction[24]:

$$Na_2SO_4 + V_2O_5 \longrightarrow 2NaVO_3 + SO_3$$

Oxides of vanadium have relatively low melting point and therefore the ash is likely to be in a plastic state in the gases and will adhere to colder metallic surfaces. In case of super heater tubes of oil-fired boilers, the ash deposit will insulate the tubes and heat transfer will be reduced. Eventually the deposits will restrict gas passages and fouling will occur. In the molten state, these oxides of vanadium will attack even stainless steel alloys and will cause severe corrosion. It is therefore a major problem if the operating temperatures are above the sintering or softening temperatures of ash deposits when corrosion occurs through the fluxing action of vanadates.

Low temperature Corrosion :

When flue gases containing sulphur trioxide pass through cooler parts of boiler, the sulphur trioxide react with water vapour to form sulphuric acid and condenses on metallic parts which are near or below acid dew-point temperature of the combustion gases. Flue gases containing even traces of sulphur trioxide have high acid dew-point temperature, up to 170°C(350°F). The condensed liquid on the cold metal surfaces contain high concentration of sulphuric acid. Thus low temperature corrosion is mainly a sulphuric acid corrosion and occurs in case of oil-fired boilers, mostly in economisers, air heaters and flue stacks where temperatures are relatively low and may fall below acid dew-point temperature of the flue gases.

It is evident that in order to reduce low temperature corrosion, the formation of sulphur trioxide has to be suppressed and therefore, an understanding of the mechanism of formation of SO_3 and factors influencing it has to be studied.

This thesis is mainly concerned with this problem and an attempt has been made to investigate factors affecting the formation of SO_3 in a non-catalytic combustor with laminar pre-mixed flame when only chemical aspect of reaction can be investigated with the exclusion of other variables.

CHAPTER 2

LITERATURE SURVEY

The behaviour of oxides of sulphur during combustion

2.1 Introduction

It is important first to consider impurities present in crude oil. This contains a number of elements other than carbon and hydrogen, but the majority of them occur only in trace quantities[1] (See Table 2.1). A minority of crudes contain less than 0.5 per cent sulphur, but the majority contain 0.5 - 3.0 per cent and in some cases it may contain as much as 7 per cent. Sodium, chlorine and vanadium concentrations in the crude oil are generally up to 100 ppm. Table 2.2 gives a comparison of the ash, sulphur and asphaltene contents of various crude oils. The three elements present in greater concentration, sulphur, sodium and vanadium are mainly responsible for most of the corrosion and fouling encountered in oil-fired installations.

The need for the understanding of mechanisms of corrosion and the associated problems have been the subject of intensive research for many years and a great number of publications have appeared reviewing the progress[2,3,4,5,23]. Here in the literature survey an attempt is made to study the behaviour of sulphur present in the fuel during combustion, in the light of the published data.

2.2 The formation of SO_3.

A number of mechanisms have been proposed to explain the formation of sulphur trioxide in the flue gases when fuel containing sulphur as an impurity, is burned.

Laxton[7] has listed four possible theories which are as follows:-

a) The reaction of sulphur dioxide with atomic oxygen in a high temperature flame zone[8,9,10]

b) The heterogeneous catalysis of the SO_2/SO_3 reactions on the boiler surfaces [11]

c) The homogeneous gas phase reactions between SO_2 and O_2[12]

d) The low temperature oxidation of sulphur dioxide on metal surfaces below acid dew-point[14,15]

Undoubtedly all four theories are valid but their relative importance varies from one plant to another. However, one can make one general statement that the mechanism (a) is the most important because if the formation of SO_3 in the flame is reduced then the catalysts necessary for the mechanisms (b) and (d) will be reduced.

2.2.1 Atomic Oxygen theory.

The flame or atomic oxygen theory was first proposed by Dooley and Whittingham[8] in 1946 and Gaydon and Whittingham[13] in 1947. (Fig. 2.1). Further work by Whittingham using small diffusion flames of carbon monoxide, hydrogen and methane, containing SO_2 showed that there was a marked difference in

the degree of oxidation of sulphur dioxide with different flames. (Fig. 2.2). He observed that the increasing order of conversion of SO_2 into SO_3 was in the methane, hydrogen and then carbon monoxide flame - which is in the same order as that of increasing atomic oxygen concentrations in these flames, as observed by Gaydon[16]. Gaydon also described the reaction occurring in a flame when nitric oxide is injected and expressed it in the following equation:

$$NO + O = NO_2 + \text{light energy}$$

Dooley and Whittingham[8] argued that if atomic oxygen is involved in the formation of SO_3 in the flame, then the introduction to the flame of a substance known to react with atomic oxygen will suppress the formation of SO_3. On the above assumption they introduced different percentages of NO to the flame and confirmed experimentally the suppressed formation of SO_3 (Fig. 2.3). More evidence of SO_3 formation in flames was offered by Crumbey and Fletcher[17] (1956) (Fig. 2.4 and Fig. 2.5) and by Hedley[12] (1962). Hedley used an oil fired laboratory furnace where the temperature and mixing history of the gases were known, and carried out a quantitative investigation of the oxidation of SO_2 to SO_3. The results showed that the concentrations of SO_3 were in excess of those that one might expect from normal thermodynamic considerations involving molecular oxygen (Fig. 2.6; 2.7). The results were in agreement with those predicted by Whittingham and Hedley thus proposed a mechanism in which atomic oxygen reacts with

SO_2 to form SO_3 which then dissociates to give SO_2 and molecular oxygen.

Levy and Merryman[20] (1965) working with $H_2S - O_2 - X$ flat flames (where $X = N_2$ or Ar) showed that (a) SO_3 was formed about one flame length thickness past the visible flame zone, and (b) the formation of SO_3 in the flame was directly related to the oxygen concentration through the reaction zone (Fig. 2.8 and 2.9). Fig. 2.10 shows the O-atom profile for two different flames.

Barrett, Hummell and Reid[21] (1966) investigated formation of SO_3 in a stainless steel combustor while burning natural gas hydrogen sulphide mixture and operating at a maximum wall temperature of 260°C (500°F). The concentration of SO_3 was measured at distances of 3 to 24 in. (7.6 cm. to 61 cm.) from burner plate with excess air levels of 1 to 12 per cent. No significant variation of SO_3 concentration was observed along the combustor at any excess air level. It was concluded that all of the SO_3 was formed in the first 3 inches (7.6 cm) of the combustor, or about within visible flame (Fig. 2.11). Fig. 2.12 shows their results when 15% excess air was added 9 inches (22.86 cm) downstream from the burner plate and SO_3 concentration were meausred at various positions.

Halstead[23] (1970) reviewing the progress made in this field agrees that most of the SO_3 present in the flue gases of a combustion system originates in the flame. He further states that on leaving the flame, the concentration of atomic

oxygen decreases rapidly, and the formation of additional SO_3 downstream of the flame becomes increasingly dependent on intermolecular reactions. He adds that molecular re-oxidation of SO_2 ($SO_2 + \frac{1}{2} O_2 \rightleftharpoons SO_3$) as the temperature falls is considered to be very slow[5,9], though its rate can be increased by catalysts, both gaseous (i.e. nitrogen oxides)[25] and condensed phase (i.e. iron oxides)[64]. He concludes that the net result is that the steady state SO_3 concentration in the flue gases is normally of the same order or slightly less than that generated in the flame.

2.2.2 The heterogeneous catalysis of SO_2/SO_3 reaction on boiler surfaces.

The formation of sulphur trioxide in boilers by a heterogeneous catalysis was probably first proposed by Harlow[11,26] (1944). The use of ferric oxide (Fe_2O_3) to promote the oxidation of SO_2 to SO_3 is well known and Harlow suggested that the presence of SO_3 in the boiler flue gases was due to the catalytic oxidation of SO_2 over hot boiler surfaces. This cannot however explain the existence of SO_3 found by other workers[6,9] within the combustion chamber before the gases came into contact with catalytic surfaces. Work done by Barrett[6] does show that Fe_2O_3 - covered surfaces catalyse oxidation of SO_2 to SO_3 at temperatures near (1200°F) (650°C) (Fig. 2.13) (Fig.2.14). The indications are that some SO_3 is formed during the passage of flue gases through the boiler, especially at high temperatures and when excess oxygen is available.

2.2.3 The homogeneous gas phase reaction between SO_2 and O_2.

Oxides of nitrogen have been used as catalysts in the manufacture of sulphuric acid in the lead chamber process. But this is essentially a low-temperature operation and gases are cooled to nearly 200°F (93°C) before entering the reaction chamber. It has been suggested[8,9,12] that the presence of nitrogen oxides in the flame gases is more likely to reduce the amount of SO_3 formed because of the removal of oxygen atoms from the system (Table 2.3).

2.2.4 The low temperature oxidation of sulphur dioxide on metal surfaces below acid dew-point.

Low temperature oxidation of sulphur dioxide is a very commonly encountered phenomenon. Rylands and Jenkinson[14] (1954) proposed that economiser deposits especially ferric sulphates, can catalyse the oxidation of sulphur dioxide. During trials at Bromborough Power Station, Alexander et. al.[15] confirmed an increase in the conversion of SO_2 to SO_3 during the passage of flue gases through the economiser and reported this as evidence for the hypothesis suggested by Rylands and Jenkinson.

After examining the various mechanisms of the formation of sulphur trioxide it is useful to establish the effect of some factors on the degree of SO_3 formation.

The following list gives some conditions which are known to have an effect on the oxidation of sulphur:

a) The sulphur content in the fuel

b) The excess of combustion air used

c) The method of introducing air into the combustion zone

d) The nature of the fuel

e) The flame temperature

f) The method of atomisation

This is by no means a complete list of the possible factors to be investigated but even with this short list one cannot make firm general statements with confidence. One can only be very positive about the first three points.

a) It is generally agreed that the form in which sulphur is present in the fuel has no effect on the production of SO_3 during combustion[17,27,28]. The work of Crumley and Fletcher[17] (Fig. 2.5) shows that, with the increase of sulphur content in the oil, SO_3 formation increases; the increase gradually reducing at higher values of sulphur content. Other investigators obtained very similar results[28,21,33] (Figs. 2.15, 2.17, 2.18).

b) The effect of air/fuel ratio has been thoroughly investigated and there is ample evidence that the formation of SO_3 will decrease by the reduction of excess air. The reduction of excess air will result in the reduction of acid build-up and direct low-temperature corrosion[34,15,35,39]. Tests at Marchwood Power Station showed a reduction in air-preheater corrosion and acid smuts emission.

Glaubitz[37] demonstrated the elimination of bonded deposits on superheaters. Similar work has also been reported by Chaikivsky and Siegmund[36]. Rosborough[41] drew some interesting comparison between SO_3 formation in power stating and domestic oil-fired boilers (See Fig. 2.19). A steep rise in the percentage oxidation of sulphur dioxide to trioxide near 4% excess oxygen in the flue gases was observed by Fielder et. al.[40] (1960) (Fig. 2.20). Neipenberg[38] (1966) reported that, by decreasing the air ratio to stoichiometric, the SO_3 content of the flue gases was reduced to zero. Fig. 2.21 shows the results of his measurements. Further work showed that the sulphur content of the fuel oil and fuel oil quality affected the formation of SO_3, Fig. 2.22. He observed that the effect of excess air on the SO_3 formation in the combustion gases has the same tendency irrespective of the size of the steam boiler plant (32 to 400 ton/h evaporation), but the absolute values varied widely, Fig. 2.23. Rees et.al.[42] also found that SO_3 formation could be brought about to zero with no injection of excess air. Results are shown in Fig. 2.24, 2.25. Recently, however, Holland and Rosborough[43] (1971) describing the experimental programme of high temperature corrosion trials at Marchwood Power Station stated that they found no evidence from those trials to suggest that very low excess air operation, 0.2 to 0.3% excess oxygen above stoichiometric, made any significant effect on high temperature superheater corrosion. Their observations were in some disagreement with the works of other workers

described earlier, but this was thought to be due to differencein vanadium to sodium ratio of the fuels employed. Their argument explains how source of fuel used can determine whether very low excess air operation is likely to have any significant effect on high temperature corrosion. They suggested that vanadium after being fully oxidised forms vanadium pentoxide V_2O_5 which has a melting point of 675°C. This vanadium pentoxide combined with sodium oxides to form various low-melting phases, particularly sodium vanadyl-5-vanadate ($Na_2O . V_2O_4 . 5 . V_2O_5$) which has a melting point of 625°C and comparatively rare 5-Sodium-vanadyl-11-vanadate ($5 . Na_2O . V_2O_5 . 11 . V_2O_5$) which has a melting point of 535°C. Thus high temperature corrosion is a real possibility when melting point of these substances are exceeded since most protective metal oxides are soluble in molten vanadium salts.

c) Method of injection of excess air.

It is also generally known that air entrainment into a combustion system effects SO_3 formation depending upon the temperature of the combustion gases[9,6,44,37]. Glaubitz[37] noted that if the additional air was added in such a way that it could still participate in combustion, i.e. very near the flame, then the dew-point increased immediately and the formation of SO_3 was immediately noticed. The same air when added $\frac{1}{4}$ flame length beyond the end of the flame, no increase in dew-point was noticed. Work of Barrett[6], et. al. reported earlier also showed that when excess air

was added downstream from the flame, where the gas temperature was still above 1150°C, the SO_3 concentration increased at the point of air addition. It was concluded that the addition of excess air further downstream at lower gas temperatures around 950°C, had little effect on further oxidation of SO_2 to SO_3, although it was thought possible that it may still contribute to the formation of SO_3 by catalytic means.

The use of two-stage combustion where fuel is gasified in a first stage spray combustor operating with deficiency of air producing a hot combustible reducing gas and burning near stoichiometric conditions in the second stage combustor had been reported[45]. Recently Archer and Eisenklam[46] (1970) reported their work on two-stage combustion giving operating data on a pilot spray combustion chamber burning high vanadium content residual fuel oil. This chamber formed part of a two-stage system with interstage heat removal. In the second stage, fresh air was mixed in the combustion chamber with cooled products from the first stage after releasing its heat to water-cooled heat exchange tubes. In the second stage a spontaneous combustion reaction was initiated. The results suggested that oxidation to CO_2 was completed within the residence time in the chamber and was further reduced by carbon formation and production of CO according to equation

$$2C + O_2 \begin{cases} \nearrow 2\,CO + 221\ MJ & \text{heat release} \\ \searrow CO_2 + C + 394\ MJ & \text{heat release} \end{cases}$$

Under gasification conditions with air atomization, SO_3 was not detected in the combustion gases.

They suggested that in a competitive situation oxygen would react preferentially with carbon and hydrogen species instead of with sulphur dioxide. Another reason against SO_3 formation was considered to be the known inhibition resulting from the presence of carbon[47].

d) Nature of fuel.

It has been found that burning of coal produced less SO_3 formation than oil having same sulphur content[26]. It has also been shown that fuel oil containing different per centages of impurities has different affects on the formation of SO_3 (Fig. 2.22). Ratio of sodium to vanadium in fuel oils has been found to have an effect on high temperature corrosion[43].

e) Flame temperature.

Enough literature could not be traced to assess the effect of flame temperature on SO_3 formation. One of the difficulty is that changes in flame temperature are a result of changing other variables, e.g. excess air, and the role of flame temperature in isolated condition is difficult to ascertain. If SO_3 formation takes place primarily due to intermolecular oxidation of SO_2, less SO_3 will be expected to form at higher flame temperature since at higher temperatures oxygen molecules will dissociate, thereby decreasing its concentration in the gases. Crumley and Fletcher[17] showed that concentration of SO_3 increased with flame temperature up to about 1750°C and then remained more or less constant (Fig. 2.4). Flame temperature was varied by varying the amount of preheat to

the combustion air, maintaining the other variables constant.

f) Method of atomisation.

It was reported[17] that fineness of oil atomisation probably had an effect on SO_3 formation and it was found that a 25 per cent reduction in SO_3 formation could be achieved by using a burner head giving coarser atomisation. A flame which favoured production of SO_3 was blue in colour while flames which gave less SO_3 were slow burning and luminous. But excellent oil atomization is necessary for obtaining complete combustion with a minimum of air which is known to reduce the production of SO_3. Marskell[49] (1959) reported the experiences with some boilers fitted with steam atomizers which was found free from back-end corrosion and steam atomization was considered a better method of atomizing fuel in large burners. More recently Exley[44] (1970) recommended that oil temperature should be maintained as high as possible for good atomization to allow oil particles to be very fine for intimate mixing required for stoichiometric condition. He stressed the importance of atomization and recommended very close periodic inspection of the burner by operators, and also by other means if available, such as furnace television, smoke recorders, or stack television.

2.3 Effect of additives on the formation of SO_3.

A vast literature is available concerning additives used to suppress low and high temperature corrosion and many claims

extraordinary performance without explaining the mechanism of its working. Additives introduced in the system is expected to act in one of the three ways to remove ill-effects of SO_3 :

a) to physically adsorb SO_3,

b) to react with atomic oxygen present in the flame, and thereby inhibit oxidation of SO_2,

c) to combine chemically with SO_3 once it has already formed, to form non-corrosive compounds.

The effectiveness of metallic zinc and magnesium additives was shown by Laxton[50]. The effect of zinc injection into the combustion chamber of No. 1 boiler (60 MW) at Tilbury Power Station was investigated with the idea that burning metal will react preferentially with atomic oxygen and would reduce the tendency of SO_3 formation. An approximate linear relationship was obtained between the maximum-acid-deposition and the rate of injection of zinc at the fixed value of oxygen concentration (See Fig. 2.27). Similar trials were carried out with magnesium and it was found that magnesium compared with zinc, is nearly ten times more efficient. Compounds of Mg and Ca, mainly their oxides, hydroxide and carbonates are considered to be important additives[42,43]. These additives cannot only react with H_2SO_4 condensed on cooler parts of the plant,

$$CaO + H_2SO_4 \rightleftharpoons CaSO_4 + H_2O$$

but also are capable of reacting with V_2O_5 to form vanadates with melting point higher than 1000 C[51].

$$MgO + V_2O_5 \rightleftharpoons MgV_2O_6$$

Silica[52] and Kaolin[53] have also been reported to be used with some success. On laboratory scale Whittingham[54] showed that carbon and silica smoke reduced the acid dew-point.

The use of heterocyclic tertiary amines for the control of corrosion by flue gases was reported by Barrett-Davies and Alexander[55], as a laboratory work on a pilot-plant scale and on a full scale boiler plant. It was concluded that economiser, air heaters, flues and ancillary ferrous equipments of boiler installations burning fuels of high sulphur content could be protected by the injection into the flue gases of 0.03 per cent of heterocyclic tertiary amines by wt. of the rated fuel capacity of the installation. Zaczek[56] also reported the use of amines in suppression of low-temperature corrosion.

Lee, Friedrick and Mitchell[57] reported the use of a Mg : Al formulation as chemically neutralizing agent of SO_3. He considered this as preferable to using magnesia or alumina separately since its use results in forming a porous deposit having more chemically active surface exposed to SO_3 and sulphuric acid. It was claimed that with additive-treated oil, any H_2SO_4 in soot was physically and/or chemically inhibited at all O_2 levels up to 5%.

Lowell[58] (1971) while evaluating oxides of different elements as absorbent for the removal of SO_2 from flue gases noted that oxides of vanadium and iron had strong catalytic

effect on SO_2 and also the oxides of copper and titanium. Macfarlane[59] reported that experience with zinc additive in full scale engine tests had shown that deposited material can cause intergranular corrosion of nickel-based alloys. The use of magnesium also introduced problems of deposit build-up on turbine blade surfaces, the severity of which depended largely on the vanadium content of the fuel and the proportion of magnesium to vanadium used.

Barrett[6] working on a laboratory scale furnace showed that introduction of a MgO-coated specimen reduced the concentration of SO_3 in the flue gases from its original value of 38 ppm to 18 ppm, but after 5 hour exposure, it gradually increased to its original value of 38 ppm. He investigated the catalytic effect of various materials and found that Kaolin, Mg SO_4, fly ash, sulphate mixture are not catalytic compared with Fe_2O_3, when applied to clean mild steel surfaces at 660°C. He concluded that coating the steel with Mg O or other non catalytic materials apparently served mainly to slow the rate at which catalytic oxide layers were formed on the surface of the metal, and once the layer was formed, the coating interfered partially with the rate at which SO_2 and O_2 could reach the catalytic layer. His investigations stressed the role of SO_3 because this material was involved inextricably in every case where corrosion occurs or harmful deposits are formed.

2.4 Summary of Literature Survey

Most residual fuels contain complex organic compounds of

vanadium, sodium and sulphur. Most of the sulphur in oil is oxidised during combustion to form sulphur dioxide. Usually 1[60,44] to 5%[12,61] of the SO_2 is converted to SO_3 under conditions of high excess air. Sulphur trioxide (SO_3) gas exists at temperatures above the acid dew-point, but sulphuric acid is formed by condensation at the cold end of a boiler as gases pass along cooler metal surfaces. Presence of SO_3 in the system is considered to be a contributory cause to both high and low-temperature corrosion of heat exchange surfaces.

A number of paths have been identified[23] whereby SO_3 may be formed in the flue gases and a number of research workers[8,10,12] suggested that it may be formed mainly in flames. Harlow[11] suggested the formation of SO_3 by the hetrogeneous catalytic oxidation of SO_2 on metal surfaces, basing his arguments on field experiences. A third mechanism was put forward by Raylands and Jenkinson[62], based on the earlier work of Johnstone[63] suggesting that once corrosion effects the cooler parts of a boiler system, the corrosion products can themselves act as catalysts to promote the formation of further quantities of acid. Although from recent works[10 12], a much clearer picture is emerging of the various factors responsible for the formation of sulphur trioxide, literature on non-catalysed oxidation of SO_2 is scant. No literature could be traced where oxidation of SO_2 has been studied ensuring absence of any physical delay of evaporation and mixing in the combustion zone under non-catalytic conditions.

Considering the flame theory that oxidation of sulphur dioxide takes place primarily in flames at high temperatures by combination of atomic oxygen, a very short time will be available for this to take place. If sulphur dioxide can pass through this zone unaffected by excess oxygen, or atomic oxygen has longer time to combine preferentially with species other than SO_2, then the reduction of SO_3 can be achieved. It is then probable that treating a fuel with a chemical additive which changes the ignition characteristic of the fuel to ignite it a fraction of a second earlier, will suppress the oxidation of SO_2.

TABLE 2.1

ASH ELEMENTS IN CRUDE OILS (REFERENCE 1)

Crude oils from	United States		Venezuela				East Indies		Middle East		
Element	Parts per million in Crude Oil										
Aluminium	0.1	0.3	1.0	0.8	nil	0.3	6	1.9	7	0.3	0.6
Calcium	12	1.2	12	1.7	1.8	9	3	1.7	3	nil	0.4
Chromium	0.1	0.2	0.05	1.4	nil	nil	0.2	trace	0.1	0.1	trace
Cobalt	1.6	nil	nil	nil	nil	nil	nil	1.9	nil	trace	nil
Copper	0.2	0.5	1.9	0.2	7.3	7	0.4	1	5	0.1	0.7
Iron	3.0	4.6	5.7	30	1.2	0.4	61	15	5	1	3.7
Lead	0.7	0.2	2.1	0.3	nil	nil	0.6	0.7	nil	0.1	nil
Magnesium	2.0	0.5	1.7	0.6	0.6	1.2	1.7	0.8	7	0.2	0.1
Manganese	nil	nil	nil	nil	nil	nil	nil	trace	nil	trace	nil
Molybdenum	0.1	nil	nil	0.3	nil	nil	0.6	0.2	nil	0.2	nil
Nickel	0.8	1.2	6	0.3	5.5	10	0.4	1	30	6	0.4
Potassium	nil	2.9	2.1	nil	trace	nil	nil	nil	nil	0.5	0.7
Silicon	0.1	0.5	0.7	1.7	0.1	0.8	6.9	3.5	1	0.2	0.4
Sodium	38	2.7	33	24	13	9.4	15	6	0.1	0.5	0.2
Tin	nil	0.1	0.5	nil	nil	0.3	0.9	0.2	nil	nil	nil
Titanium	0.1	0.2	0.3	nil	nil	nil	trace	0.3	4	0.1	nil
Vanadium	1.9	0.7	24	nil	30	72	nil	nil	100	27	3
Zinc	2.1	1.2	3	0.2	nil	nil	0.3	0.6	2	nil	nil

TABLE 2.2

A comparison of the ash, sulphur and asphaltene contents of various crude oils. (Reference 1)

Crude Oil	Contents of		
	Ash (p.p.m.)[a]	Sulphur (% wt.)	Asphaltine (% wt.)
Venezuela			
i	1130	2.59	5.8
ii	425	1.27	1.3
iii	168	0.92	0.19
iv	138	0.14	< 0.1
v	107	0.55	0.97
Trinidad			
i	820	2.22	3.6
ii	80	0.99	0.7
United States			
i	490	0.24	0.04
ii	184	0.29	0.4
iii	85	0.26	0.1
iv	31	0.34	-
Middle East			
i	240	1.57	2.1
ii	60	2.5	0.8
iii	17	1.61	0.8
East Indies			
i	183	0.15	-
ii	68	0.21	trace
Columbia	177	0.95	1.0
Africa			
i	50	0.18	< 0.05
ii	20	0.13	< 0.08
Canada	30	0.16	0.05

[a] p.p.m = parts per million parts of crude oil.

TABLE 2.3

Effect of Nitric oxide addition on oxidation of SO_2 in flames (Reference 8)

SO_2 in gases = 0.05%

Per cent NO added	Per cent oxidation of SO_2
0.0	7.5
0.1	7.3
0.5	6.0
1.0	4.5
2.0	4.3

TABLE 2.4

Effect of varying concentration of SO_2 on % oxidation to SO_3 (Reference 8)[2]

Per cent SO_2 in exit gases	Per cent oxidation to SO_3	Dew point ^oC
0.02	10.0	110
0.04	8.2	140
0.11	4.5	165
0.15	3.8	170
0.50	1.8	176
1.00	1.0	180

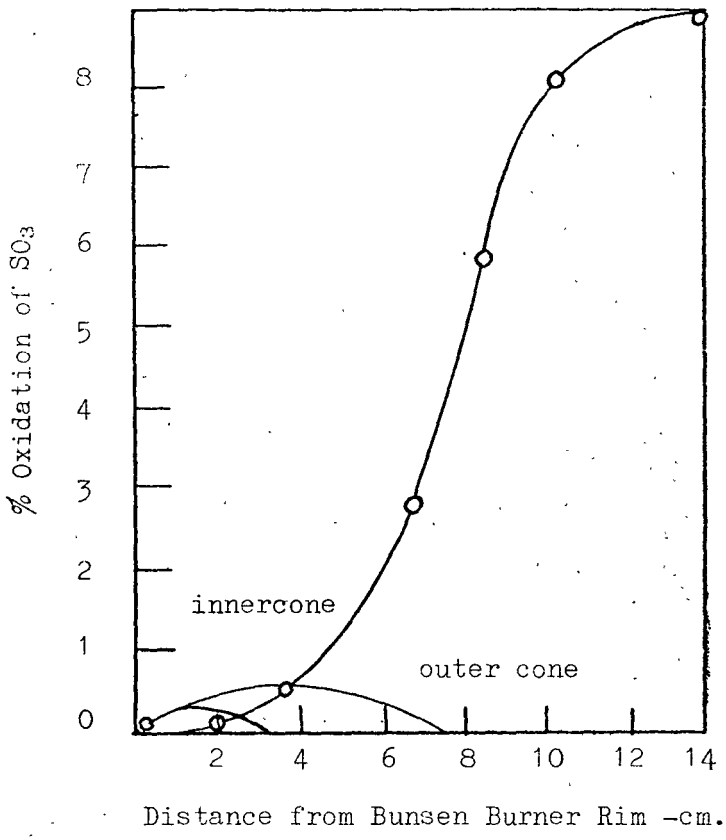

FIG. 2.1 Variation of % oxidation of SO_2 with distance from Bunsen burner rim. After Dooley and Whittingham, reference 8.

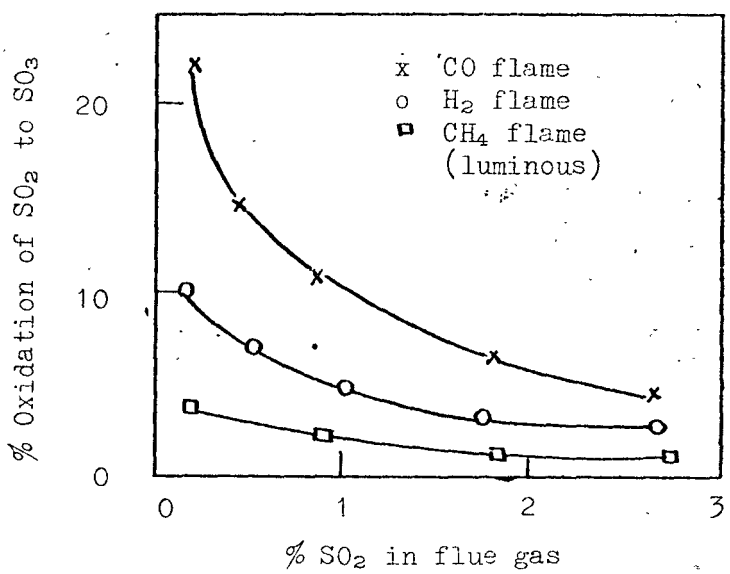

FIG. 2.2 Oxidation of SO_2 in flames from different flue gases, reference 8.

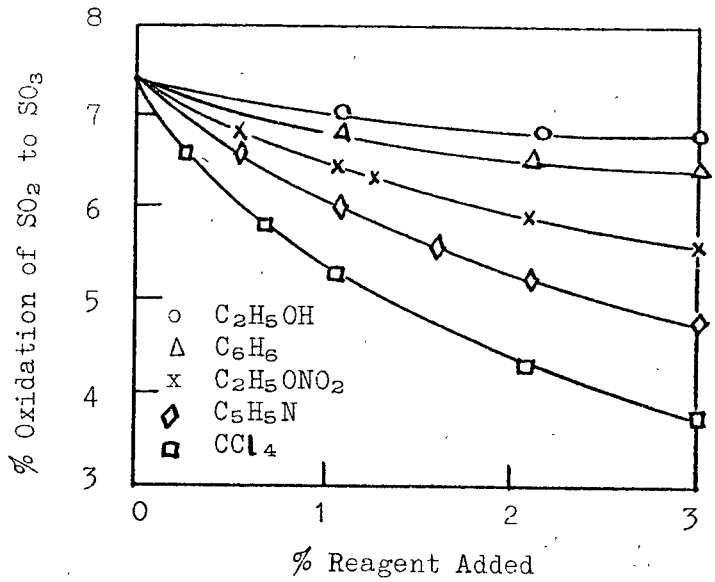

FIG. 2.3 Effect of various substances on the oxidation of SO_2 in a bunsen flame. After Dooley and Whittingham, reference 8.

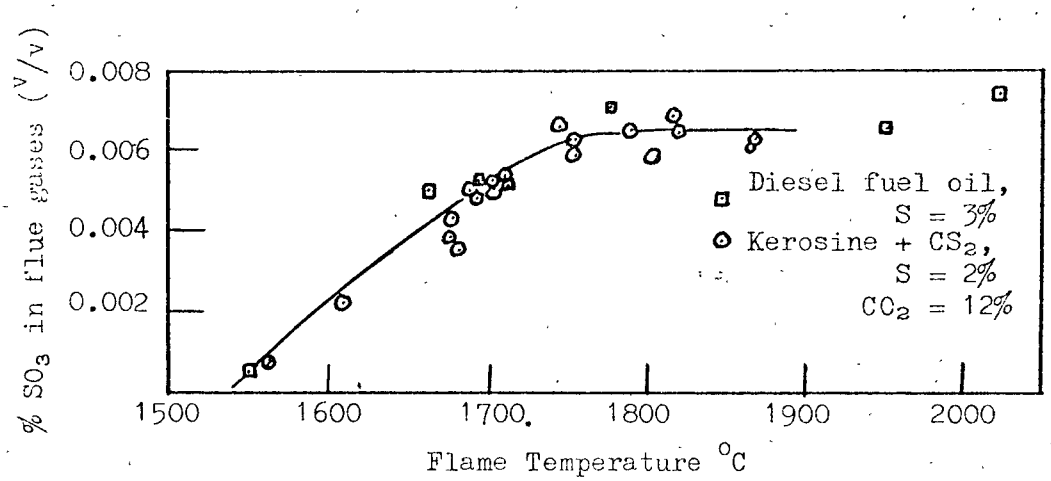

FIG. 2.4 Variation of SO_3 content of flue gases with flame temperature. After Crumley and Fletcher, reference 17.

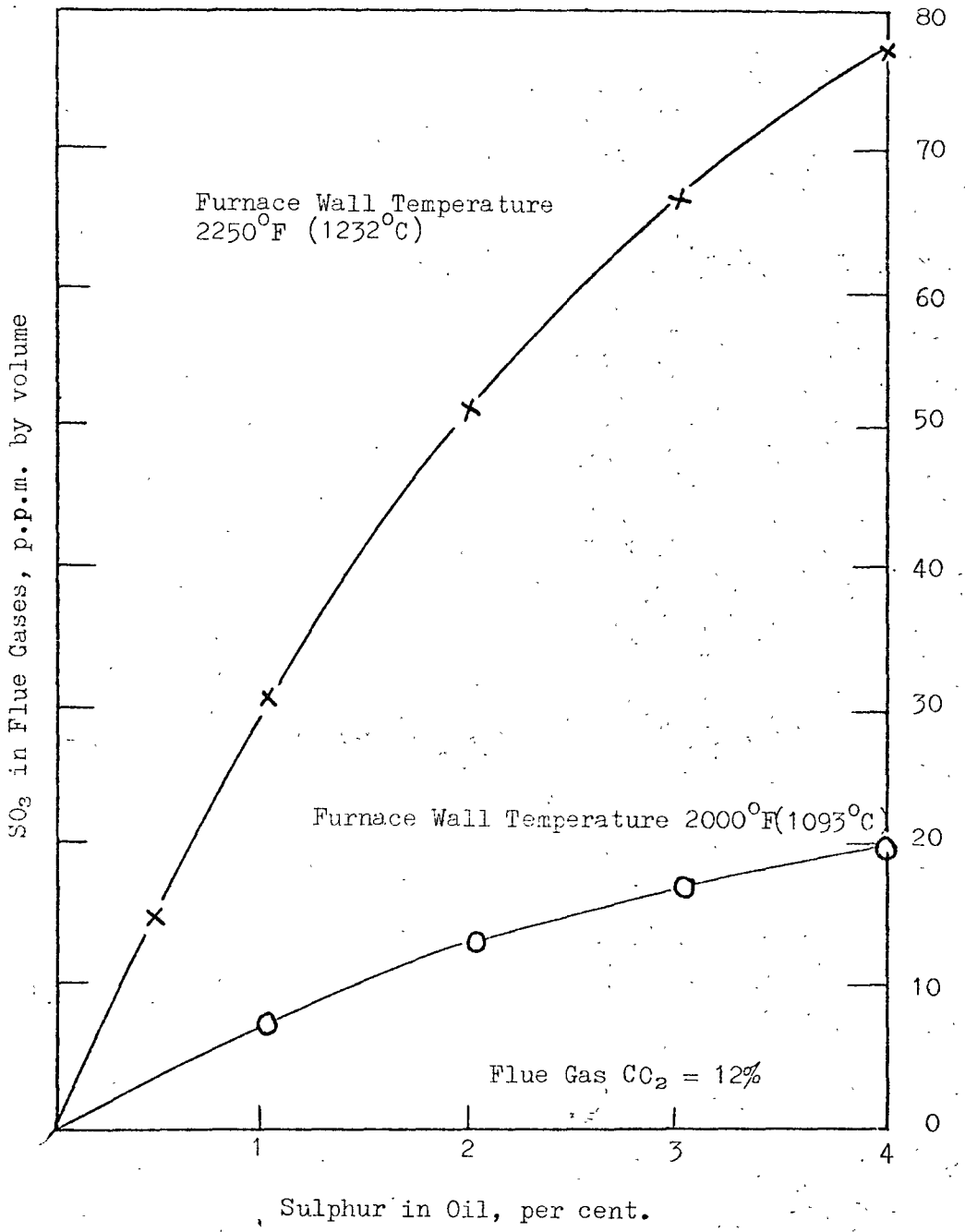

FIG. 2.5 Variation of flue gas SO_3 with sulphur content of the oil. Reference 17

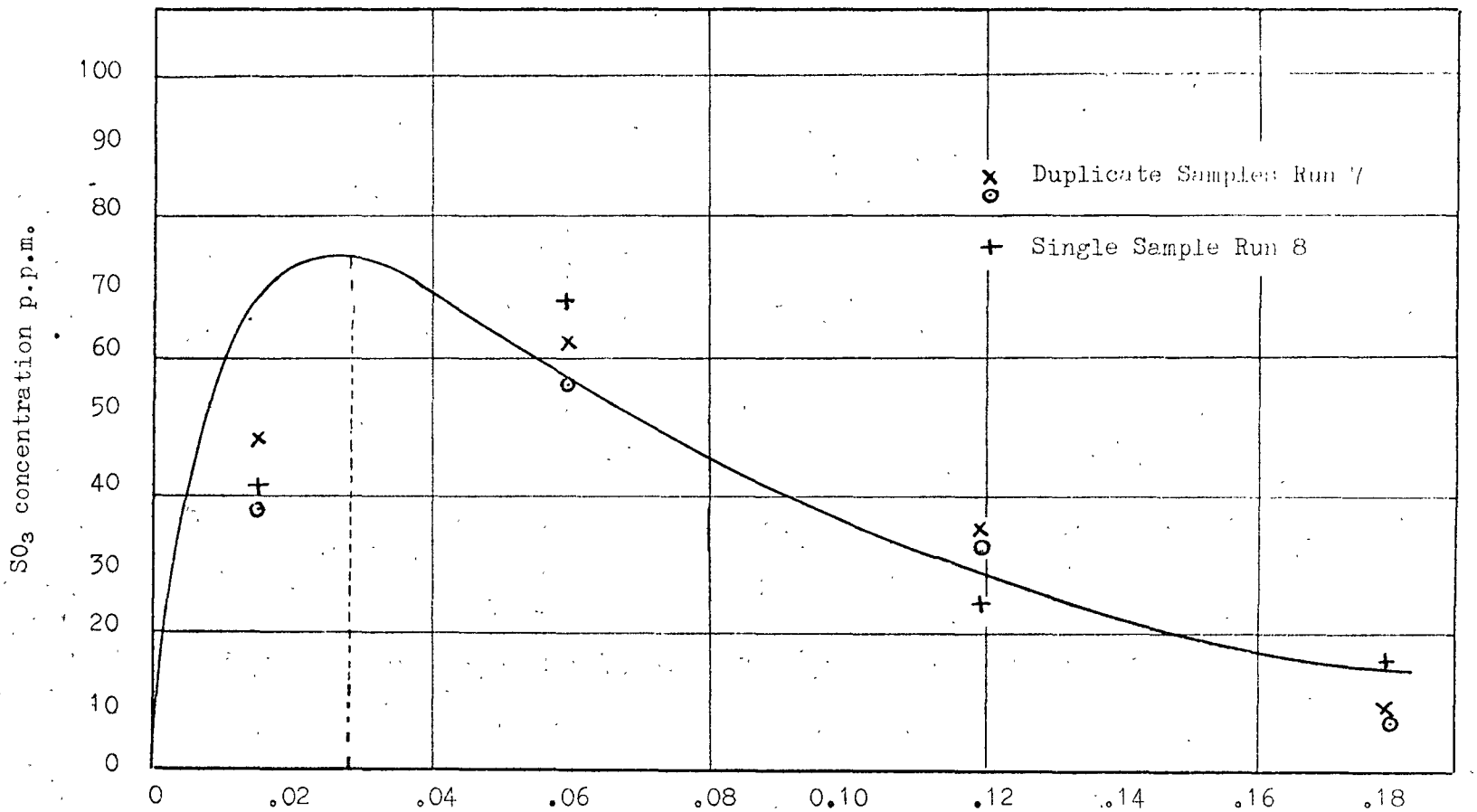

FIG. 2.6 Variation of SO_3 concentration with time (Reference 18)

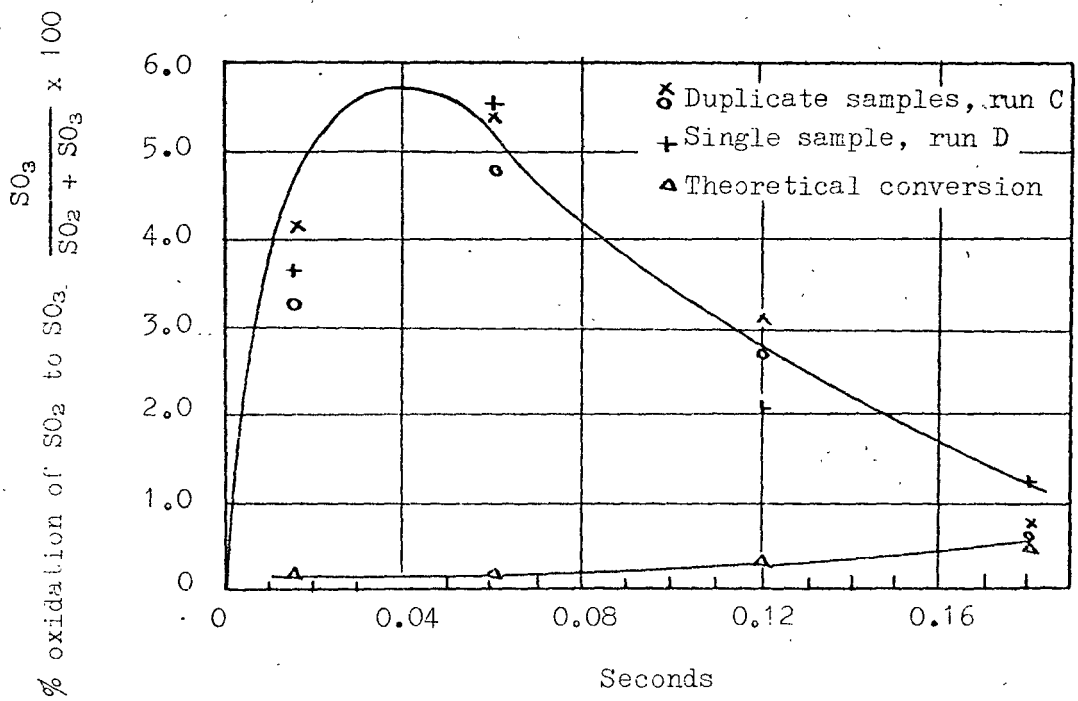

Fig. 2.7 Variation of % oxidation of SO_2 with time in a homogeneous plug flow reactor. After Hedley, reference 18.

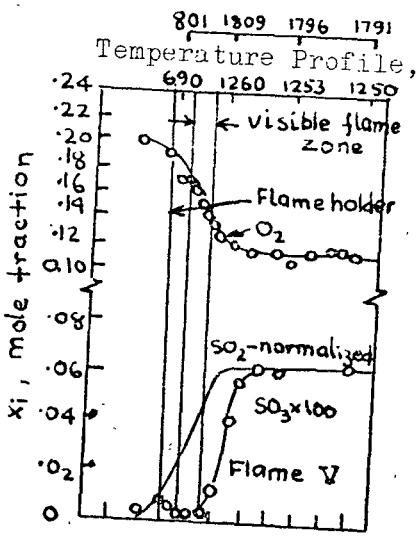

FIG. 2.8 SO_2, O_2, SO_3 composition. Flat-flame profile. A mixture of oxygen, hydrogen and H_2S was fed to the flameholder. After Levy and Merryman, reference 20.

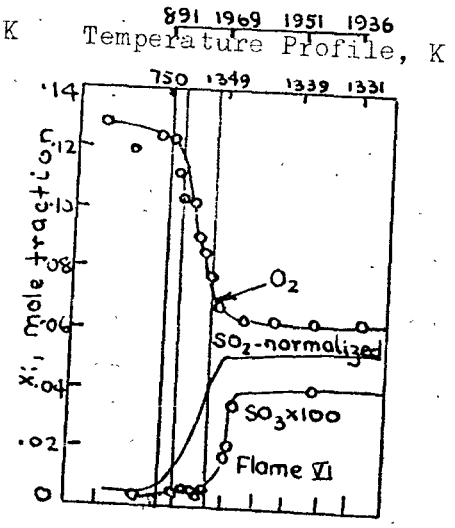

FIG. 2.9 SO_2, O_2, SO_3 composition. Flat-flame Profile. After Levy and Merryman, reference 20.

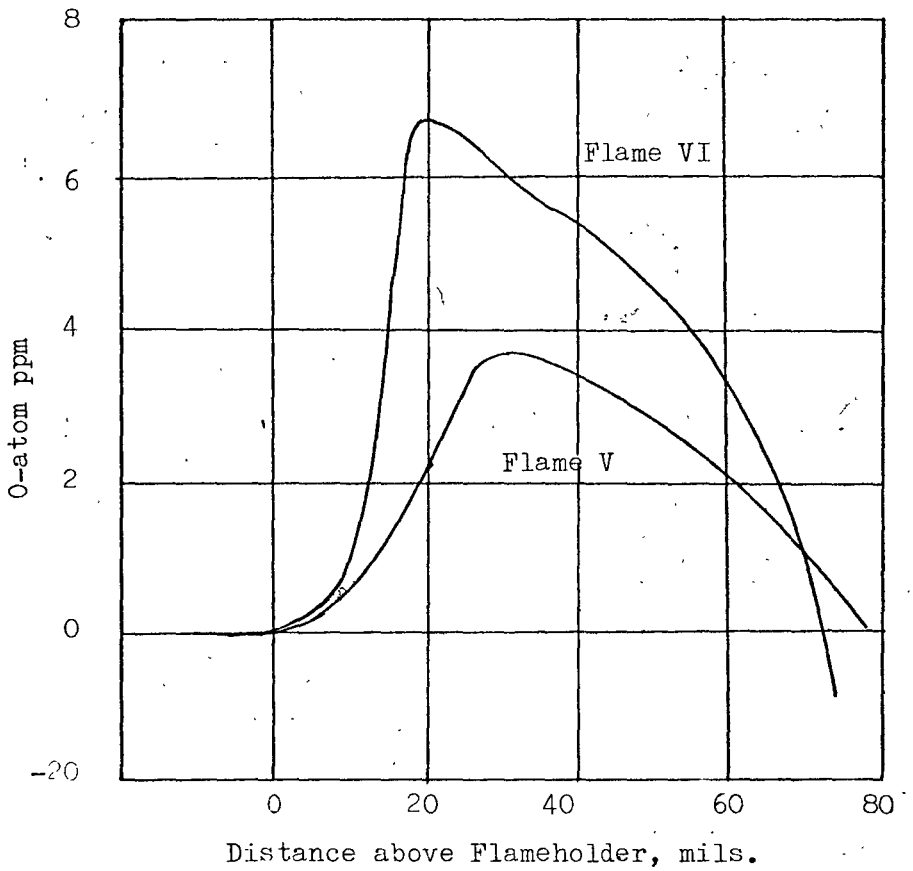

FIG. 2.10 O-Atom profiles. After Levy and Merryman, reference 20.

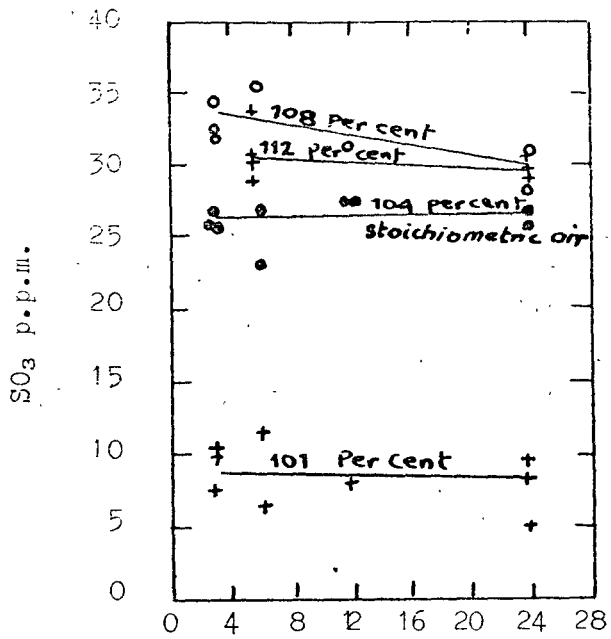

FIG. 2.11 SO_3 concentration at various distances from burner plate. Reference 21.

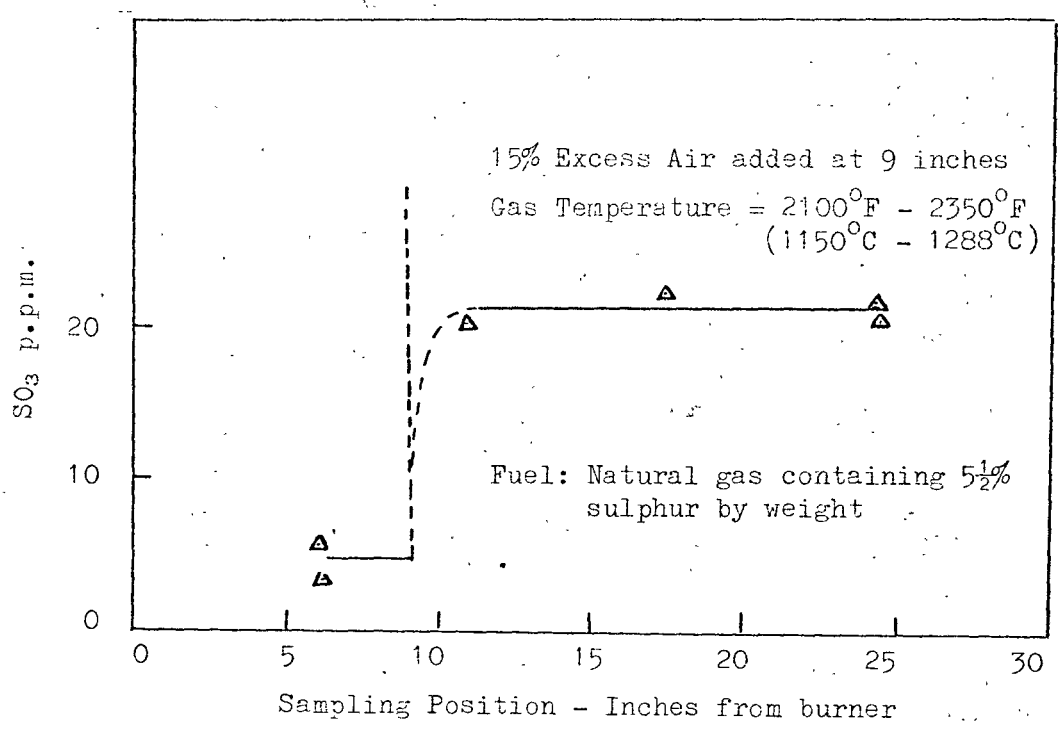

FIG. 2.12 SO_3 concentration when adding post flame air. Reference 21.

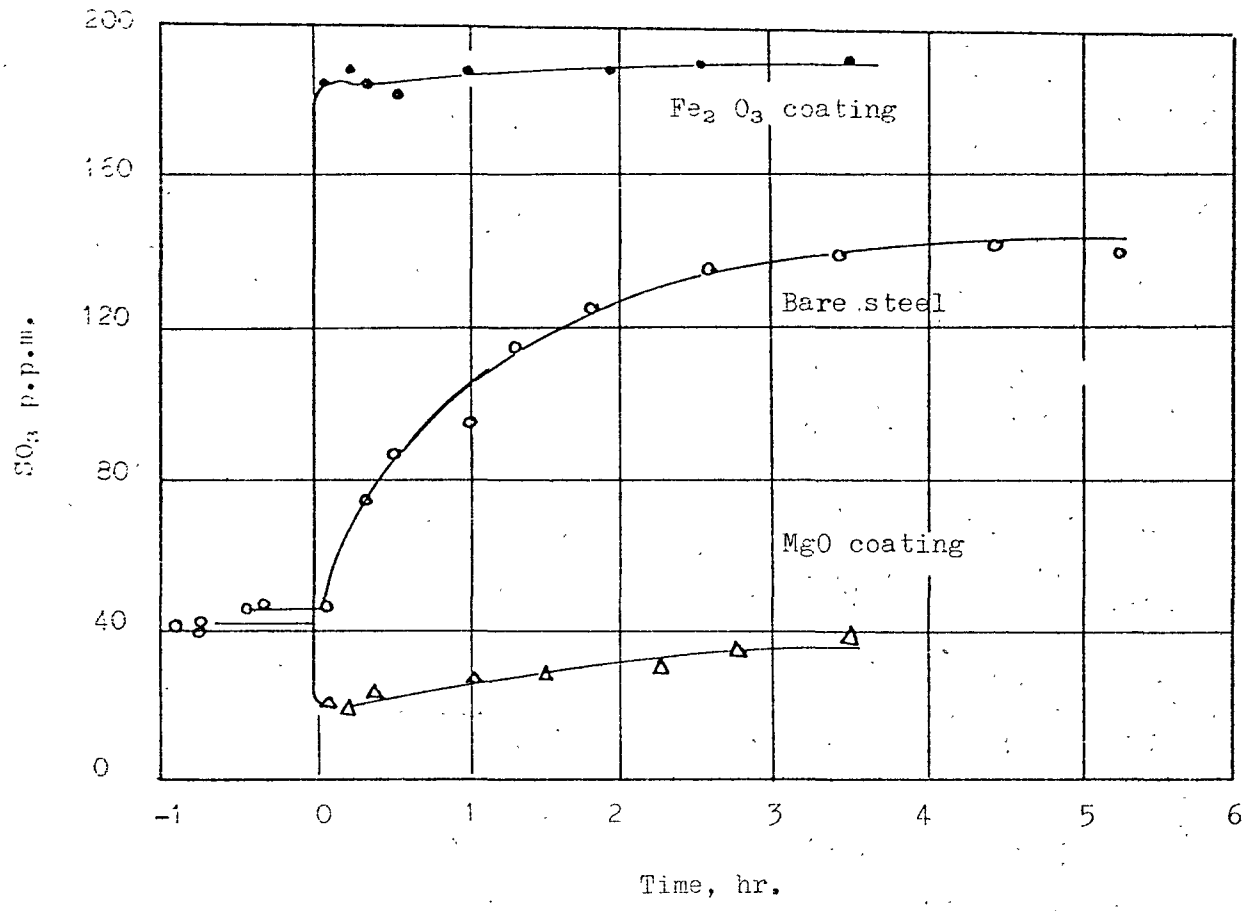

FIG. 2.13 SO_3 - concentration downstream of bare and coated mild-steel specimens. Reference 6.

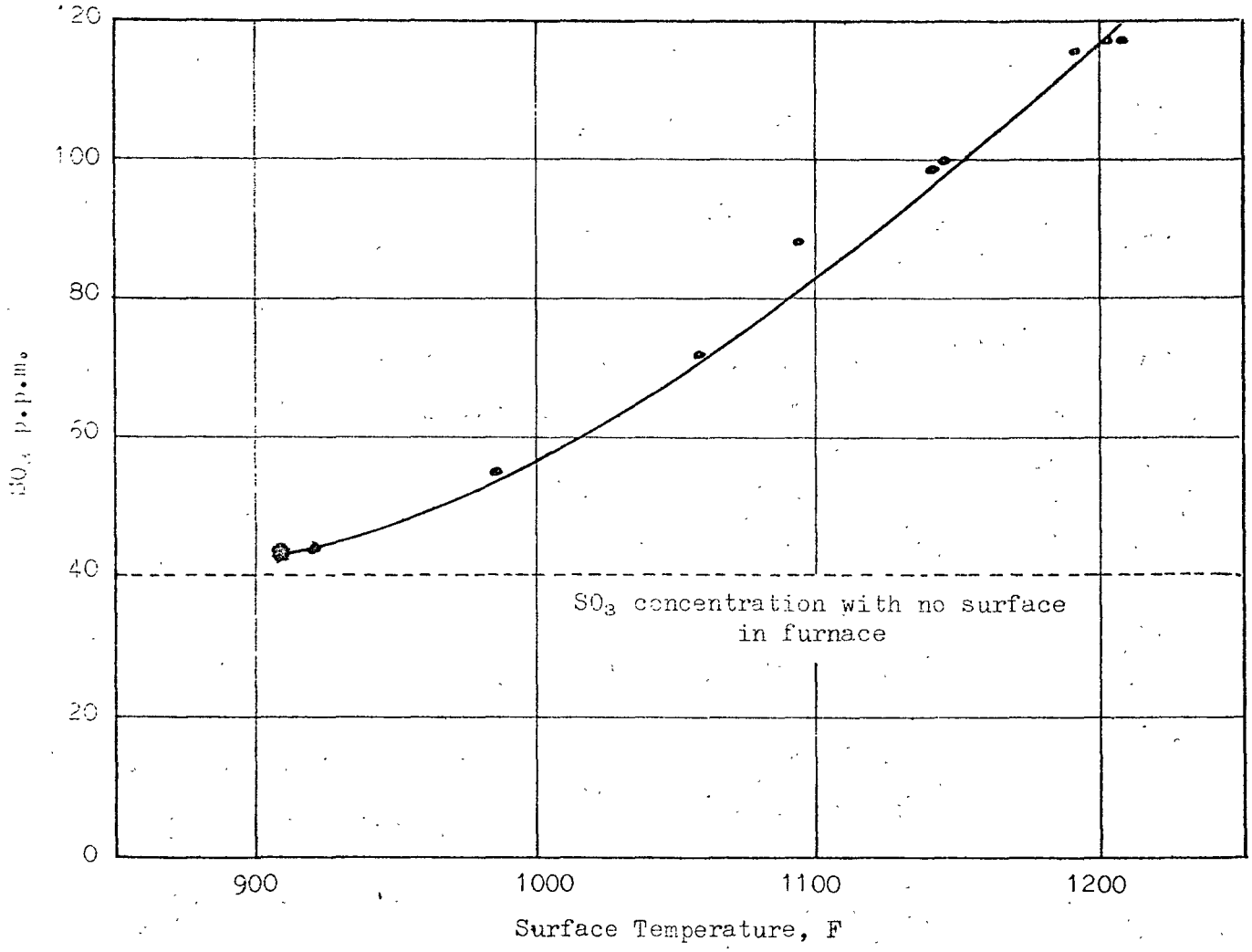

FIG. 2.14 SO_3 concentrations downstream of an Fe_2O_3-coated surface at several temperatures. Reference 6.

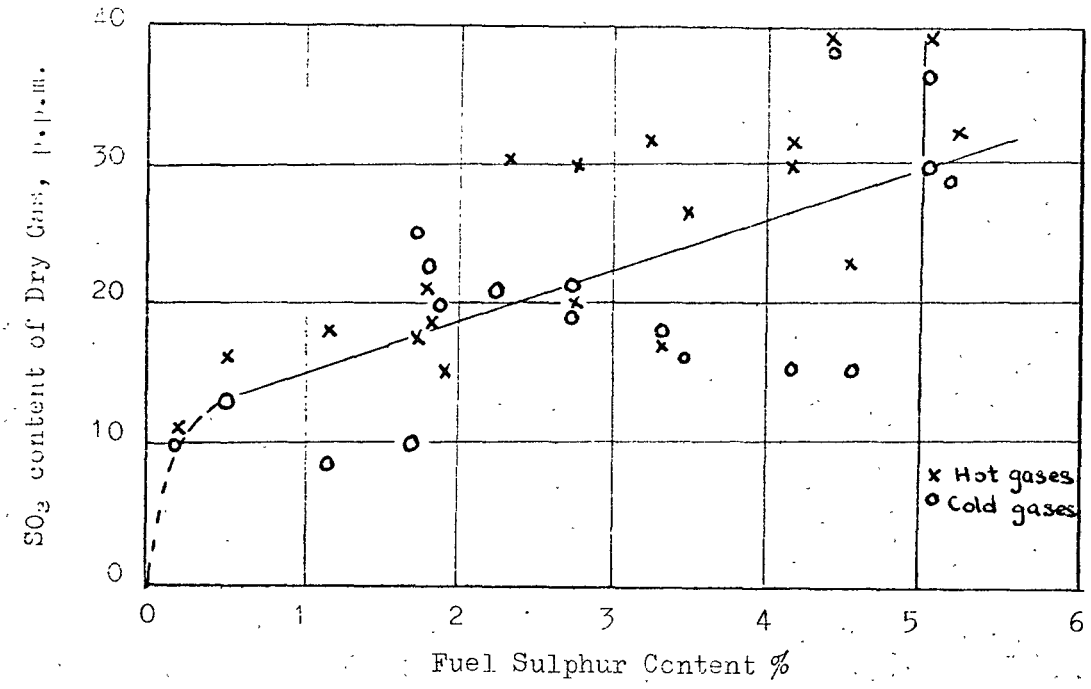

FIG. 2.15 Relation of SO_3 content of flue gases to fuel sulphur content. Reference 18.

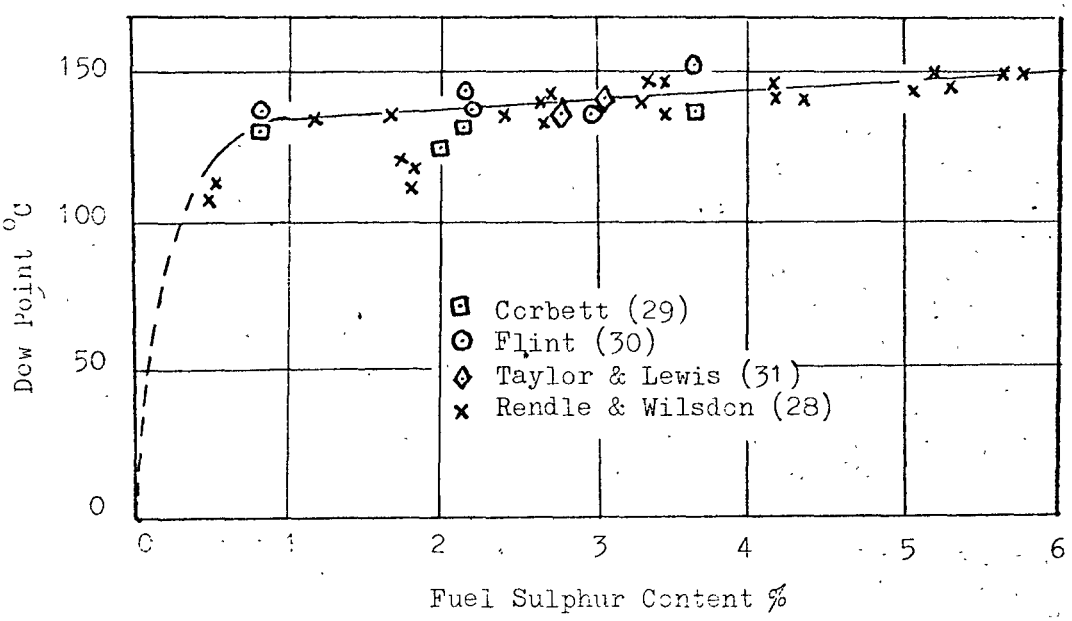

FIG. 2.16 Relation of dew point to fuel sulphur content. Reference 12.

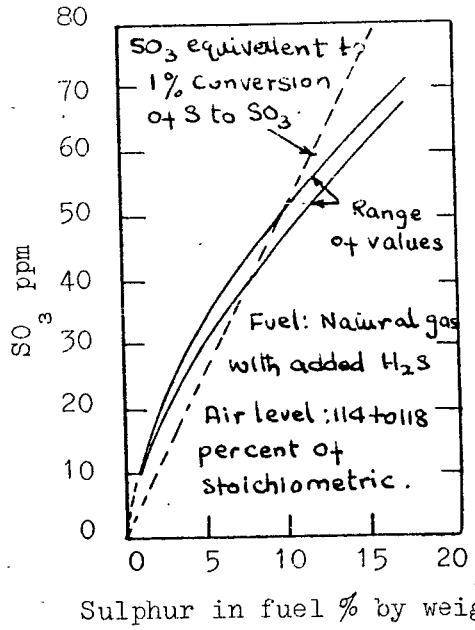

FIG. 2.17 Effect of sulphur content on formation of SO_3. Reference 21.

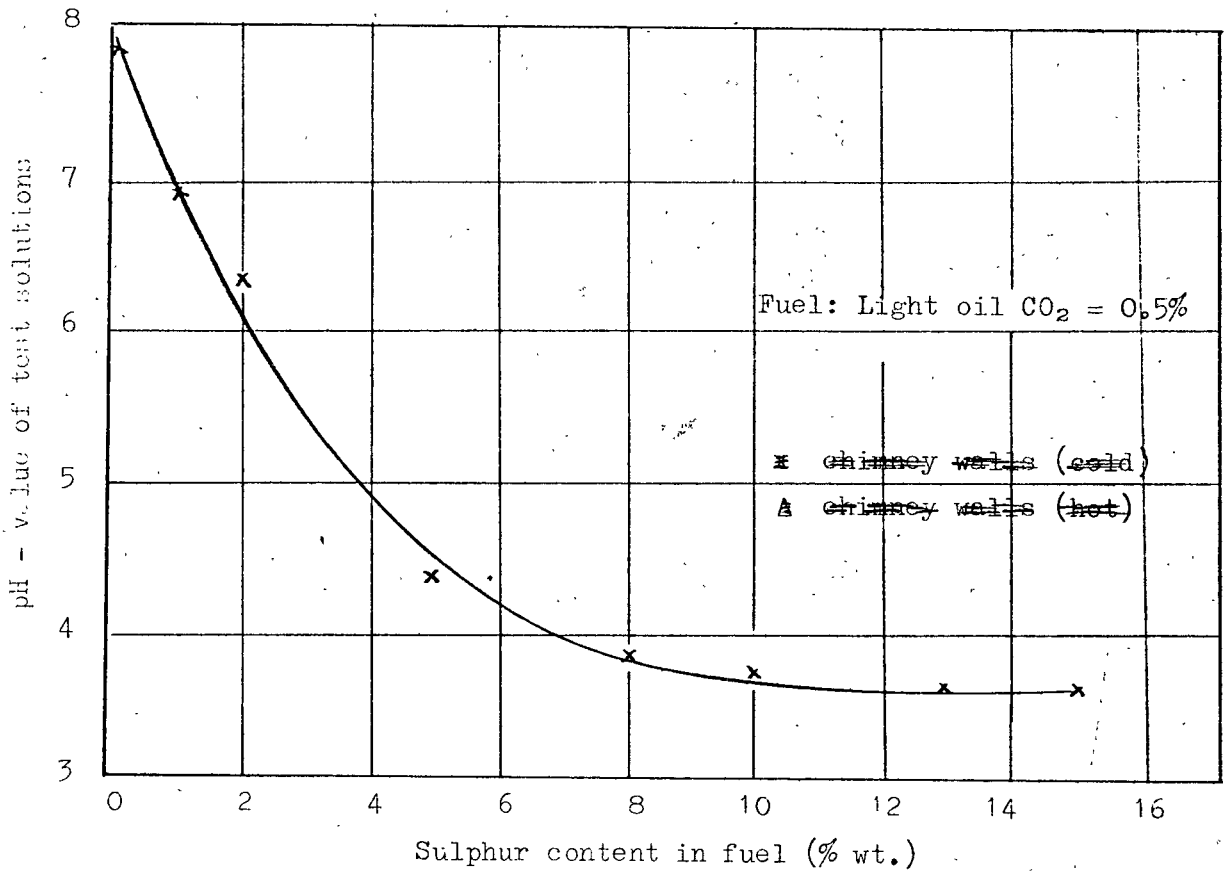

FIG. 2.18 Effect of sulphur content of fuel on acidity of flue gases. After Ahmed, reference 33.

Relationship between SO_3 and boiler oxygen
with different sulphur content fuels

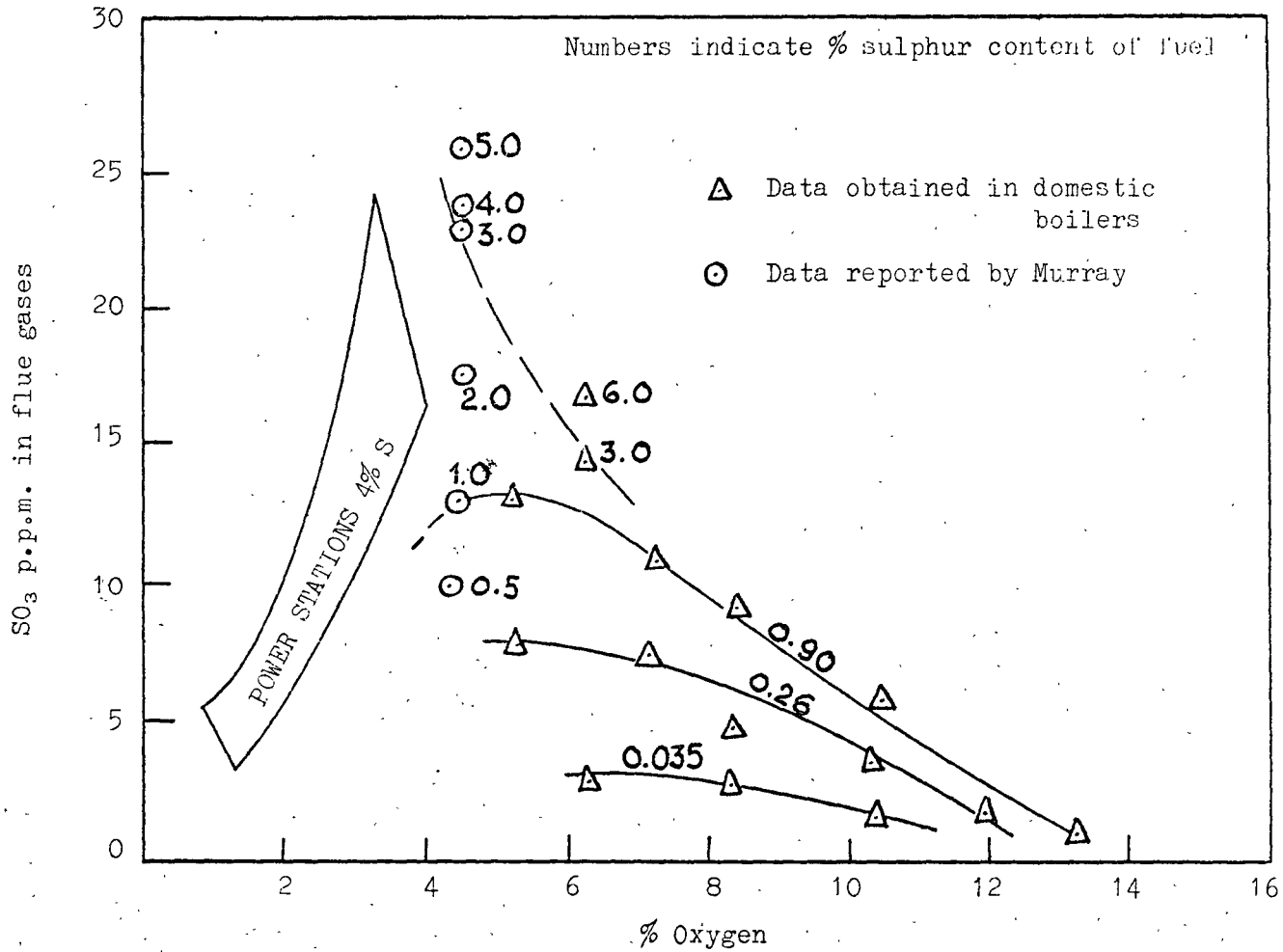

FIG. 2.19

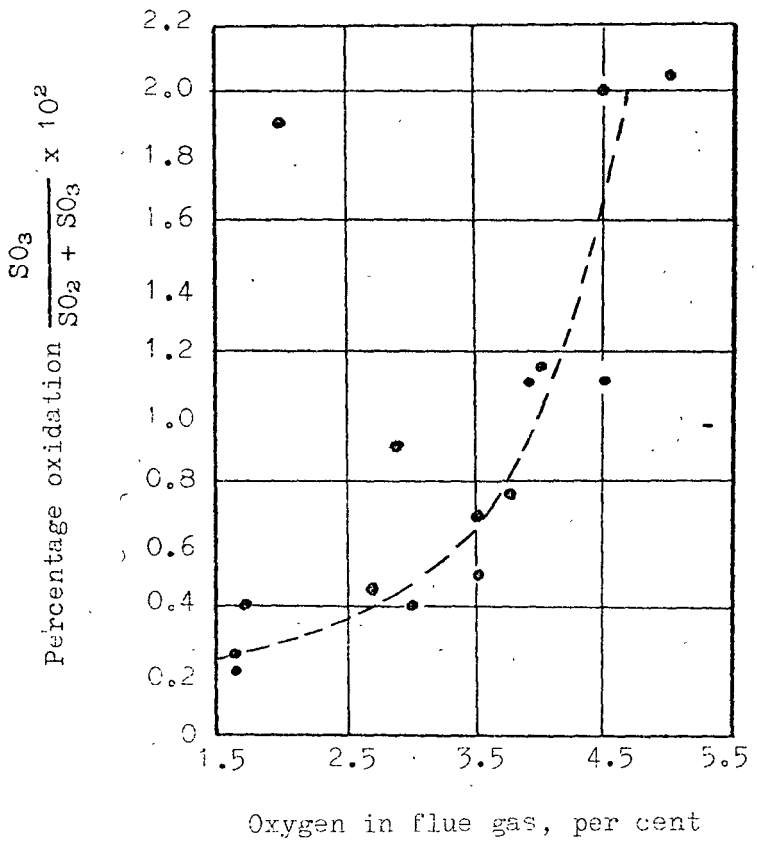

FIG. 2.20 Relation between percentage oxidation and oxygen content of the flue gas: No. 1 boiler Ince, air heater inlet, no additive. Reference 40.

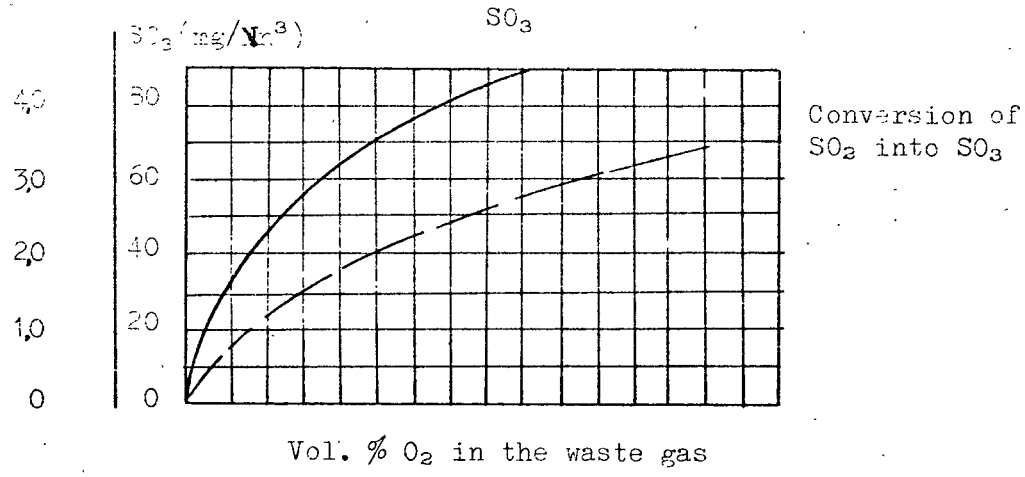

FIG. 2.21 Formation of SO_3 and conversion of SO_2 into SO_3 plotted against excess-air coefficient (measured values). Reference 38.

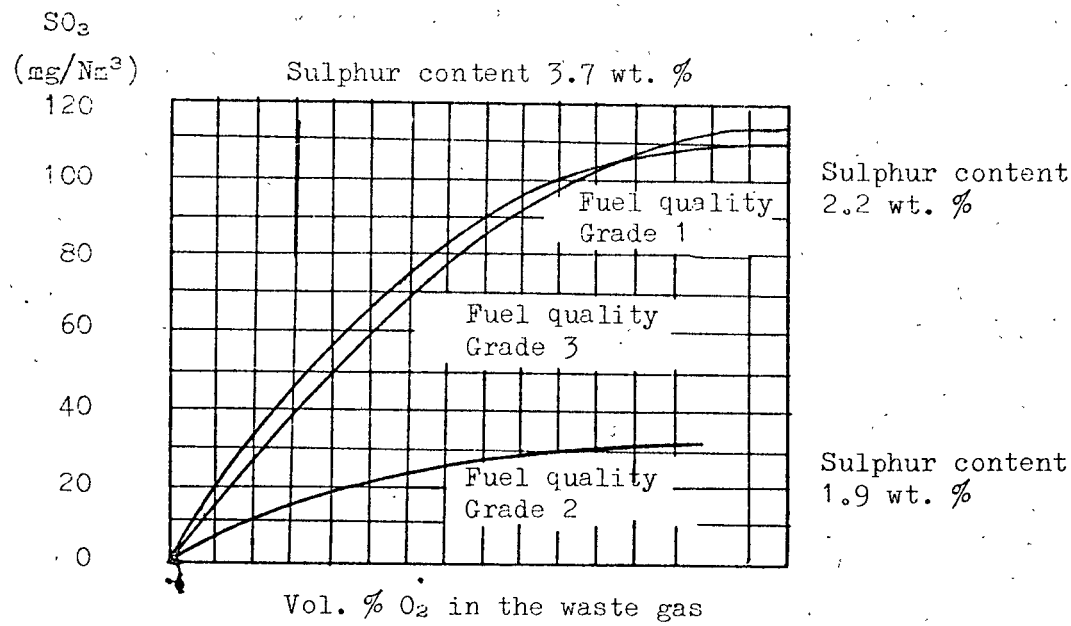

FIG. 2.22 Formation of SO_3 plotted against fuel quality grade, excess-air coefficient, and sulphur content. Reference 38.

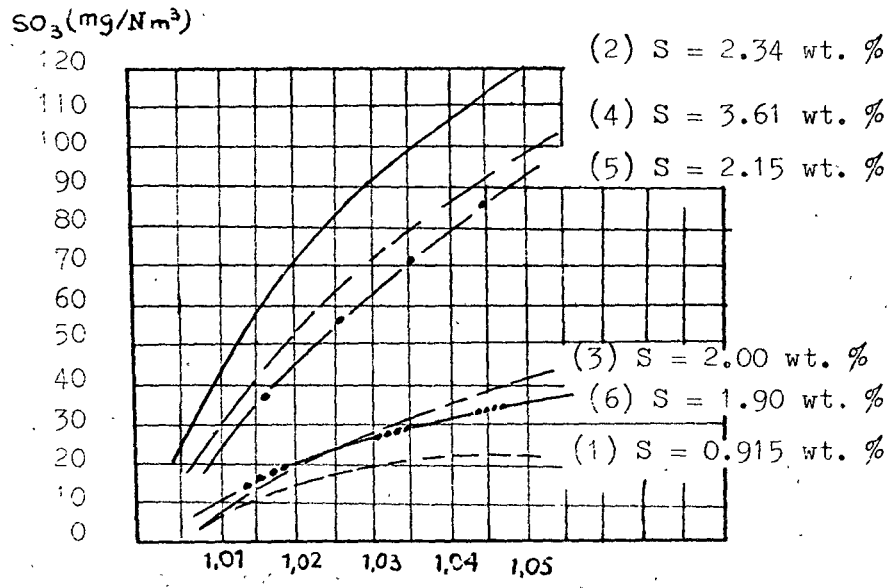

(1) = 400 t/h steam output 18 front burners each abt. 1600 kg/h
(2) = 400 t/h steam output 18 front burners each abt. 1600 kg/h
(3) = 50 t/h steam output 4 front burners each abt. 1000 kg/h
(4) = 32 t/h steam output 3 front burners each abt. 850 kg/h
(5) = 32 t/h steam output 3 front burners each abt. 850 kg/h
(6) = 32 t/h steam output 3 front burners each abt. 850 kg/h

FIG. 2.23 Formation of SO_3 at different load in front-fired steam generators plotted against excess-air coefficient and sulphur content. Reference 38

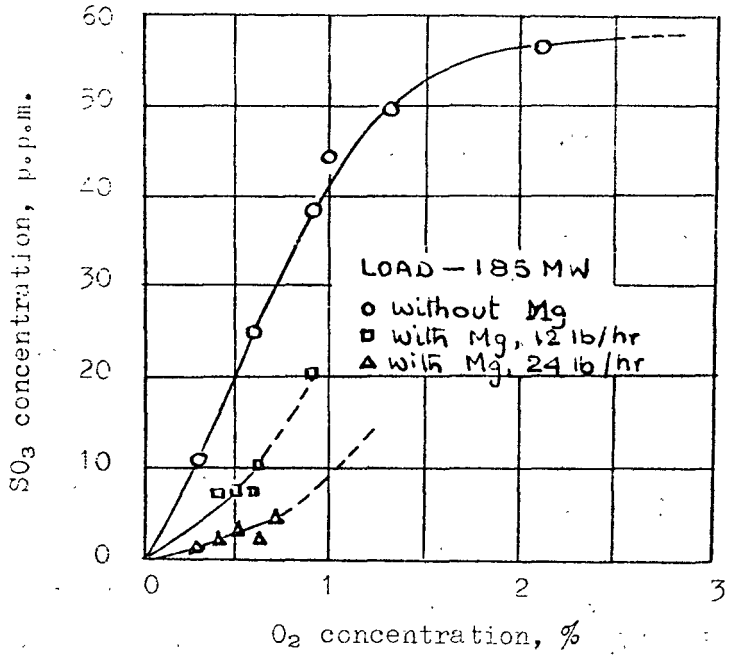

FIG. 2.24 SO_3 concentration as a function of O_2 concentration for full load (185-mW) operation both with and without magnesium addition. Reference 42.

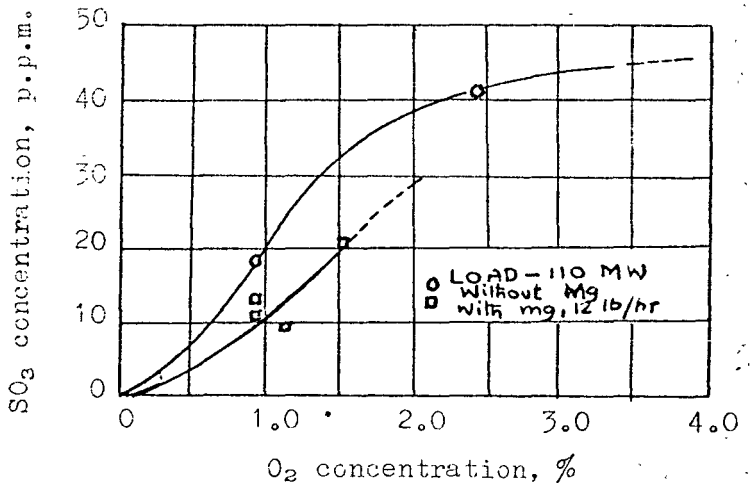

FIG. 2.25 SO_3 concentration as a function of O_2 concentration for 110-mW operation both with and without magnesium addition. Reference 42.

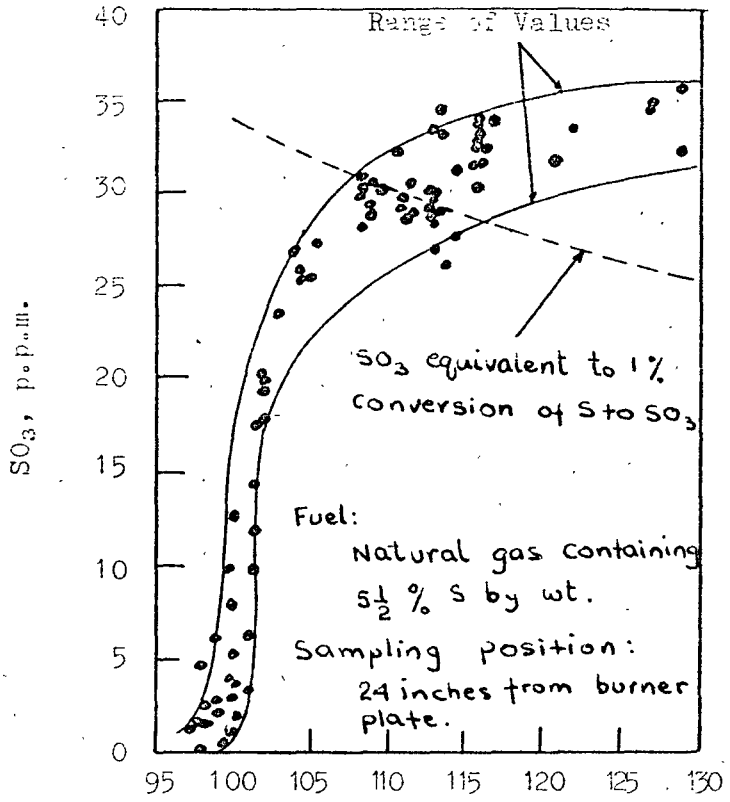

FIG. 2.26 Effect of excess air on formation of SO_3. Reference 32.

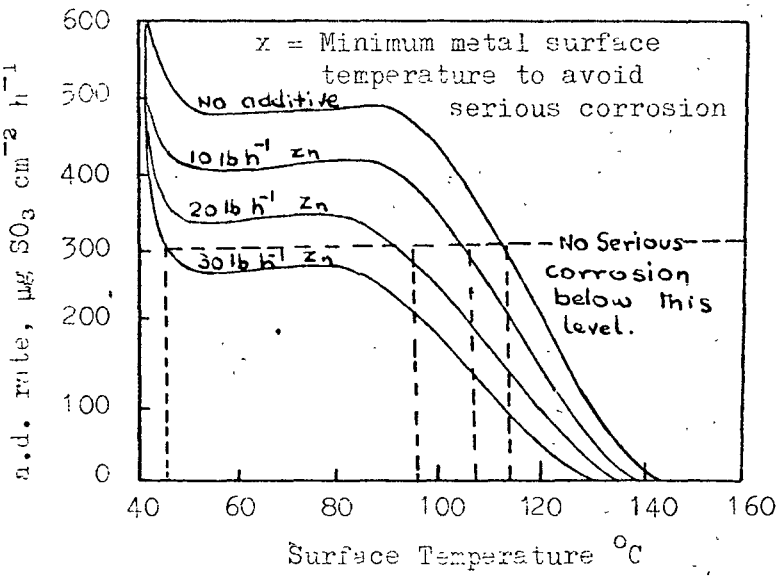

FIG. 2.27 Dependence of acid deposition rate on additive injection rate. Reference 30.

CHAPTER 3

OBJECTIVE OF RESEARCH PROGRAMME

From the study of the works of various research workers in this field, it appears that a number of factors are responsible for the formation of sulphur trioxide in a combustion system. These factors are summarised in the earlier chapter. Two theories have emerged as possible mechanism of formation of sulphur trioxide, viz, the flame or the atomic oxygen theory and the catalyst theory. Although it has been shown that boiler deposits can cause oxidation of SO_2 to SO_3, some work on laboratory scale combustion system has also shown that SO_3 can be formed in flame. However no information is available when investigation of SO_3 is carried out under non-catalytic condition with pre-mixed flame which will eliminate any physical affects of atomisation of fuel. Investigation of the effect of ignition properties of fuel on the formation of SO_3 in flame has never been attempted.

Therefore it is vital to verify conclusively whether SO_3 is formed in the high temperature zone where purely chemical effects are involved with the exclusion of all physical affects of atomisation of fuels.

Furthermore, it has been reported that sulphur dioxide competes with other species present in the flame for combination with atomic oxygen. Therefore fuels tending to initiate early reactions may allow greater time for CO to combine with available atomic oxygen in preference to sulphur dioxide and its (SO_2) oxidation may be suppressed. This involves the measurement of ignition delay times of the fuels employed.

The present research programme describes the construction and use of appliances to study factors effecting formation of SO_3 in the hot zone of the combustion chamber using various liquid fuels and the measurement of ignition delay times of these fuels and interpretation of these results.

CHAPTER 4

FACTORS INFLUENCING THE CHOICE OF EXPERIMENTAL SYSTEM AND EXPERIMENTAL PROGRAMME

4.1 Choice of Flame.

Mixing and recirculation processes which occur in conventional jet flames under turbulent conditions may interfere with the study of chemical reaction producing sulphur trioxide. It was therefore decided to separate physical effect of evaporation and mixing from chemical effects, this led to the choice of pre-mixed laminar flame. So it was possible to investigate chemical reactions involving sulphur dioxide oxidation.

The basic assumptions made of the system are as follows:

a) A pre-mixed flat flame is produced in a circular combustion chamber and the hot gases completely fills the entire length of the tube.

b) There is no recirculation of hot gases back into the earlier stages of the flame.

c) Velocity, temperature and mass concentration profiles across the flame are flat.

4.2 Choice of Fuel.

It was decided to use the following fuels which could be easily evaporated and mixed with combustion air in the evaporating chamber.

a) Diesel oil

b) Kerosine

c) Cyclohexane

d) n-hexane

e) n-pentane

In each case, sulphur content of the fuel was raised to 3.4%(wt.) by addition of appropriate amount of carbondisulphide (CS_2). Related properties of these fuels are given in Table 6.1.

4.3 Method used for the determination of SO_2 and SO_3 content of the flue gases

It was decided to use a chemical method developed by Gcksoyr and Ross[68] for the determination of SO_2 and SO_3. Accuracy and limitation of this method were investigated and is reported in Chapter V. The method consists of passing known quantity of flue gases through a glass helical coil condenser and titrating the candensate with NaOH solution. The description of apparatus and detailed procedure is given in Chapter 5.5.

EXPERIMENTAL PROGRAMME (PART I & PART II)

PART I

1. Design and Construction of evaporating burner.
2. Determination of concentration traverse curves.
3. Determination of temperature profiles across sections of the combustion chamber.
4. Determination of the effect of air/fuel ratio on the combustion products using two fuels.
5. Determination of the effect of excess oxygen concentration in the combustion gases on the SO_3 formation using two fuels.
6. Determination of the effect of burning various hydrocarbons with different ignition properties on the formation of SO_3 at various excess oxygen concentrations.
7. Determination of the effect of residence time of combustion gases on the formation of SO_3.
8. Calculation of the theoretical percentage oxidation of SO_2 to SO_3 at several oxygen concentration under equilibrium conditions.

PART II

9. Design and construction of ignition delay measurement apparatus.
10. Determination of ignition delay curve for Kerosine droplets with respect to change in surface temperature.
11. Determination of ignition delay curves of different hydrocarbons used in the previous programme of experiments.
12. Determination of minimum ignition temperature of Kerosine, Cyclohexane, n-hexane and n-Pentane and comparison with the results of other workers.

CHAPTER 5

DESCRIPTION OF APPARATUS AND EXPERIMENTAL PROCEDURE

The general arrangement of the apparatus is shown in Plate 5.1 and the diagrammatic view is given in Fig. 5.1.

5.1 Burner System

5.1.1 Fuel Tank.

This consisted of a 1.75×10^{-3} m^3 trapiziodal container, constructed from a 3mm thick stainless steel plate with three openings at the top mounted on a Dixian stand. The openings are meant for pressurizing the fuel tank, for supply of fuel to evaporating chamber and for the observation of pressure in the fuel tank. For safety reason, the use of nitrogen cylinder was made for pressurizing fuels.

5.1.2 Evaporating Chamber.

This was constructed from stainless steel, the dimensions are given in Fig. 5.1.2 and Plate 5.1.2 shows its front view. The chamber was heated by means of an electric heating element covering the outside wall of the chamber. This was of 0.5 kw capacity. Liquid fuel from the tank entered the heated evaporating chamber through a small opening directly in the path of the air stream from an air-compressor. Heated mixture of fuel vapour and air passed through a Grade 3 sintered stain-

less steel disc, thus a pre-mixed flat flame was produced beyond the sintered filter disc.

5.1.3 Combustion Chamber

The combustion chamber was made from a stainless steel tube of 32mm internal diameter and of 3mm wall thickness. It was 2m long having 10mm diameter tapped holes at 304.8mm (1 ft) intervals for sampling of combustion gases. These holes were kept closed when not in operation. Six additional holes of 3mm diameter at right angles to the sampling holes were drilled for the introduction of thermocouples. The combustion tube was supported on four brackets mounted on a steel frame. A long Dixian table held the entire apparatus. The combustion tube was lagged with 'Kerlane' heat insulating blanket of total thickness of 51mm.

5.2 The Fuel, air and Water supply

5.2.1 The Fuel Supply

Fig. 5.1 shows the arrangement for the supply of fuel and air to the combustion chamber (see also Fig. 5.2). The pressure over the surface of the oil in the fuel tank was kept at 0.17×10^5 N/m^2 (2.5 lbf/in^2). The pressurized oil flowed through a filter and a needle value. A 'Rotameter' manufactured by G.E.C. Elliot's, model 1100, range 0-19cc was used for the control of oil flow and a quick visual means of checking the oil flow.

i) Calibration of 'Rotameter'

The Rotameter was calibrated for every fuel used by cutting off the oil supply to the evaporating chamber and allowing it to collect in a measuring cylinder. The time taken for a specific volume of oil collected, was noted and flow was calculated.

5.2.2 Air Supply

A reciprocating air compressor connected with pressure operated relays supplied the necessary combustion air at a constant supply pressure of 0.68×10^5 N/m^2. A pressure regulating value was used to give the constant pressure. A liquid trap and a filter was also used in the air supply system.

The air supply was metered by means of an 'Air Rotameter' manufactured and calibrated by G. A. Platon Ltd., of range $0\text{-}50 \times 10^{-3}$ m^3/min. (0-50 litres/min) at N.T.P.

5.2.3 Water Supply

Water was supplied through the mains for circulation in the gas cooler which was inserted in the test gas line of the INFRALYT GAS ANALYSER (Appendix 4).

5.3 Temperature Measurements

Temperature of combustion gases was measured by means of Ni Cr/Ni Al thermocouples placed every 1 ft. (304.8mm) along

the chamber. They were connected through compensating leads to a six point switch and a 'Cambridge' temperature indicator of 0-1200°C range.

The investigation was concerned with comparative temperatures only, the accuracy of thermocouples was therefore considered acceptable.

5.4 External heating of Combustion Chamber

In order to raise the temperature of the combustion gases to 950-1000°C through the whole length, it was found necessary to externally heat near the exit of the tube. A 3 kw electric heating element was used and was controlled by means of a variable volt/regulator.

5.5 Gas Sampling Apparatus

CO and CO_2 content of the flue gases were measured by means of infra-red absorption gas analyser and oxygen content was measured by means of magnetic oxygen analyser. These were standard instruments supplied by Elliot's Automation Ltd. General principles of operation of these instruments are given in Appendix 4.

Measurement of SO_2 and SO_3 were made by means of Goksyr and Ross[68] Method. A schematic arrangement of the sampling system is given in Fig. 5.1. Gaseous combustion products were drawn through a quartz tube (3mm diameter bore, 3mm thick and 140mm long). The tube had a 'quick-fit' ground glass connection

at one end which was connected to the sulphur trioxide collector. The tube was externally heated by means of 'electrothermal' heating taps to maintain the gas sample at a temperature not below 250°C, to prevent condensation of sulphuric acid in the tube. The residence time of combustion gases in the probe was calculated to be of the order of 0.02 seconds compared with the total residence time of 0.6 seconds in the combustion chamber. A measured volume of hot flue gases was drawn through the glass coil and a Grade 4 glass disc, both enclosed in a glass jacket filled with water (SO_3 collector), maintained at a temperature between 60°C and 90°C. (Plate 5.1.3). This temperature range which is below the acid dew-point of the gases, ensured that all sulphuric acid condensed on the wall of the coil. However the temperature was high enough to prevent any condensation of water vapour. Any acid particles left in the gas stream were retained by the sintered glass filter. The acid was then washed out with a mixture at pH 4.6 of distilled water, 5% by volume of isopropanol (IPA) and bromophenol blue indicator (2 drops per 50cm^3 solution). The washed solution was then titrated with N/50 sodium hydroxide solution. The exit gas from the sulphur trioxide collector was passed through the SO_2 absorber - and bubbled through 100cm^3 of 3% hydrogen Peroxide solution. 1-2 drops of bromophenol blue indicator was added to the solution and the content was titrated with standard N/10 N_a OH solution until the blue end-point was reached. SO_2 and SO_3 contents by volume of the flue gases were calculated by means of the following equation.

$$SO_2 \text{ or } SO_3 = \frac{T \times N \times 11.2 \times 10^6}{V}$$

p.p.m. by volume of dry gas

where T = titration value, cm^3

N = normality of N_a OH solution

V = volume sampled, cm^3 of dry flue gas corrected to $0^{\circ}C$ and 760mm Hg.

An accuracy of $\pm$ 2p.p.m. of SO_3 was obtained when $\frac{N}{50}$ N_a OH solution was used for titration of washed acidic solution and the rate of flow of sampling gases was 5×10^{-3} m^3/min for a period of 20 minutes. This was as recommended by Goksyr and Ross.

5.6 Velocity Measurement

Since the quantity of fuel and air supplied for combustion could be metered accurately, it was decided to rely on the calculated values of velocity. Effect of temperature of gases at each sampling port were taken into account in the calculation of velocity at that port. Sample calculations are shown in Appendix 1.

5.7 Procedure during Run

The burner was allowed to run for a period of $1\frac{1}{2}$ hours to warm up the apparatus before the actual commencement of the test. This helped to maintain the temperature constant throughout the length of the tube. Fuel flow rate and air

flow rate were then accurately set, and CO, CO_2 and O_2 concentration in the flue gases were measured. This was repeated at intervals of 5 minutes until constant readings were obtained. The test was then started for the determination of SO_2 and SO_3 at various ports.

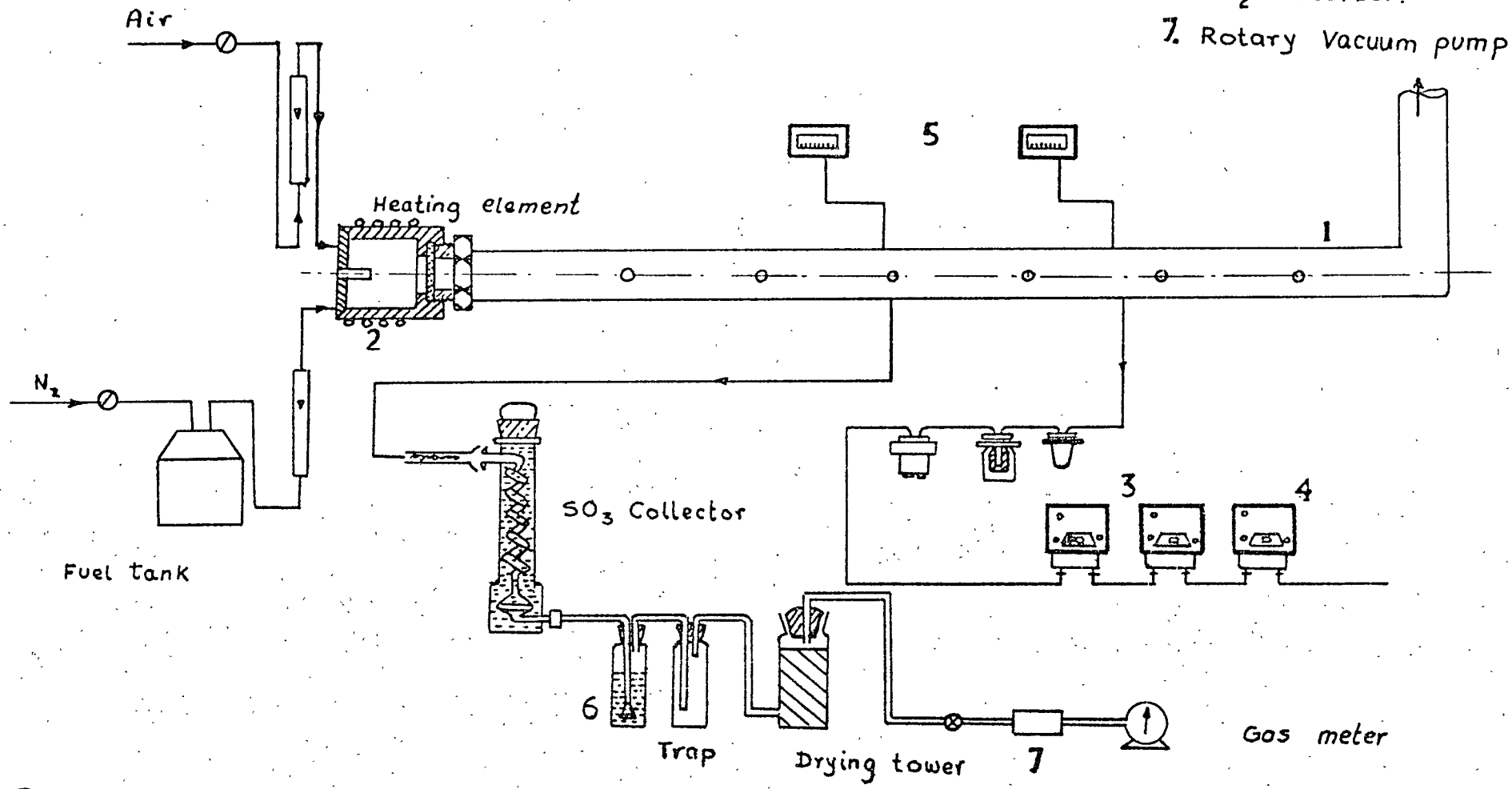

FIG.5.1 DIAGRAMMATIC VIEW OF APPARATUS.

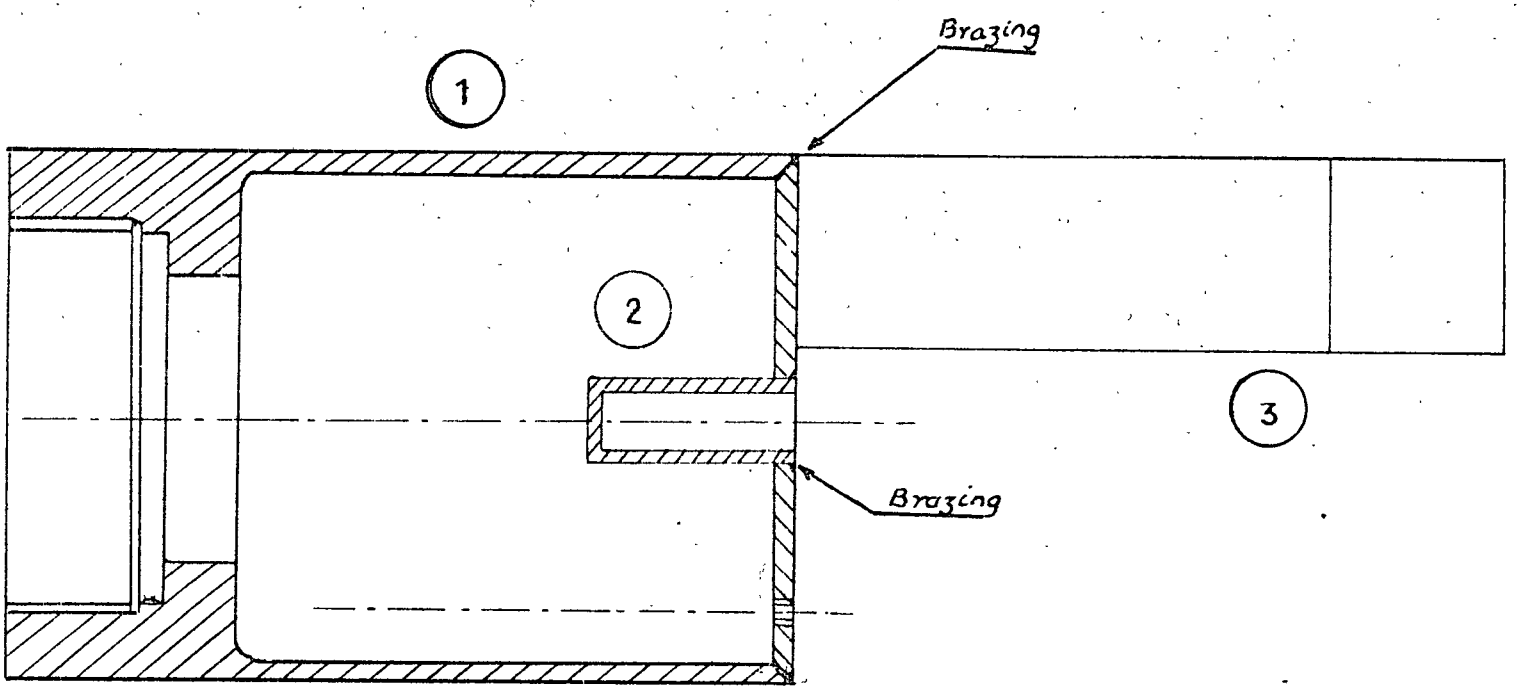

SCALE FULL SIZE

1. Evaporating chamber -- Stainless steel.
2. Pipe for thermo pole -- "
3. ½" wide plate for fixing -- "

Fig. 3.1.1. Sectional view of Evaporating chamber.

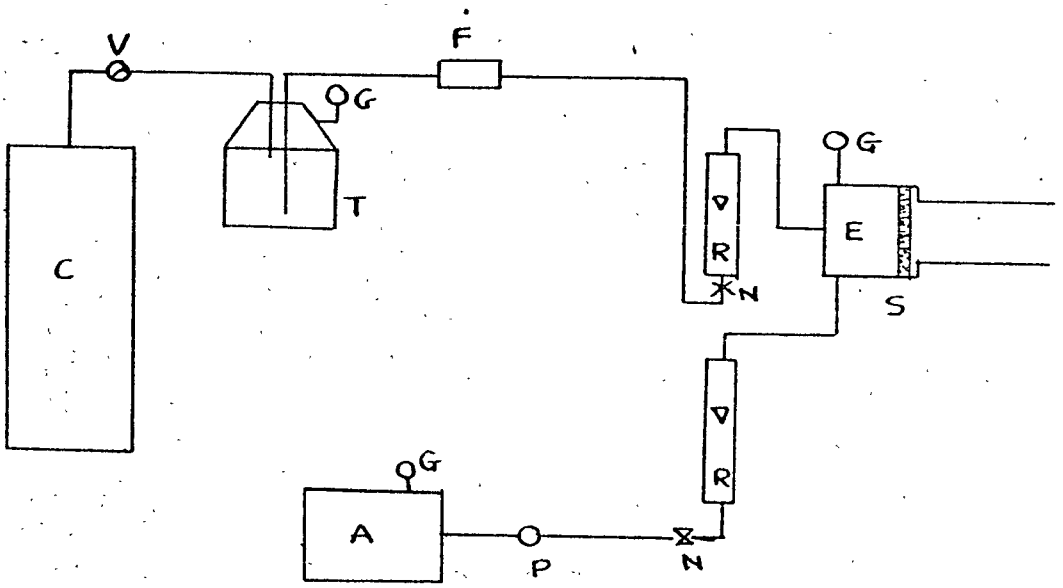

C	Nitrogen Cylinder
V	Pressure valve
T	Fuel tank
G	Pressure gauge
F	Filter
N	Needle valve
R	Rotameter
E	Evaporating tank
S	Stainless steel filter
A	Air compressor
P	Constant pressure valve

FIG. 5.2 Schematic diagram of fuel and air supply system.

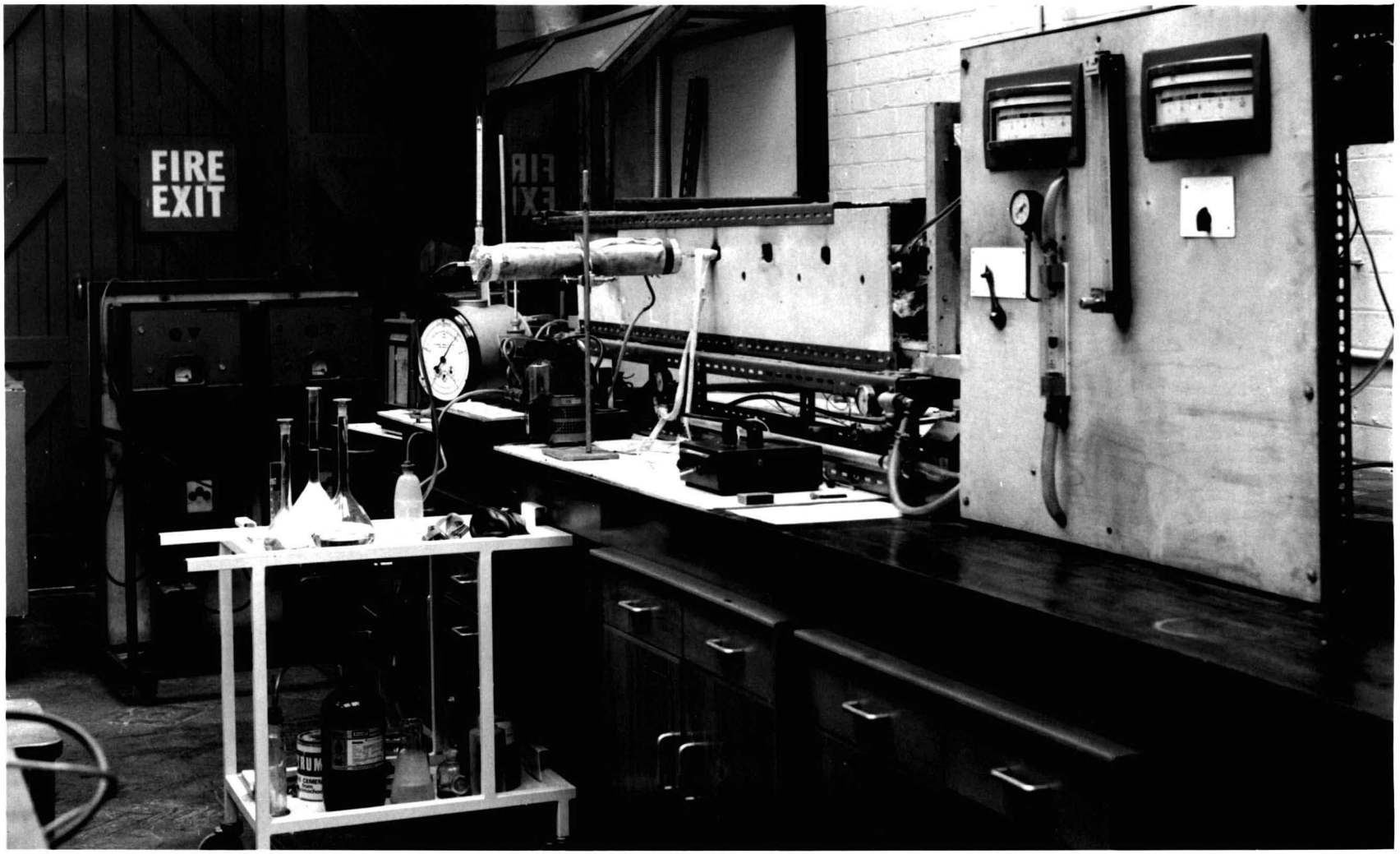

PLATE 5.1 General view of the Apparatus

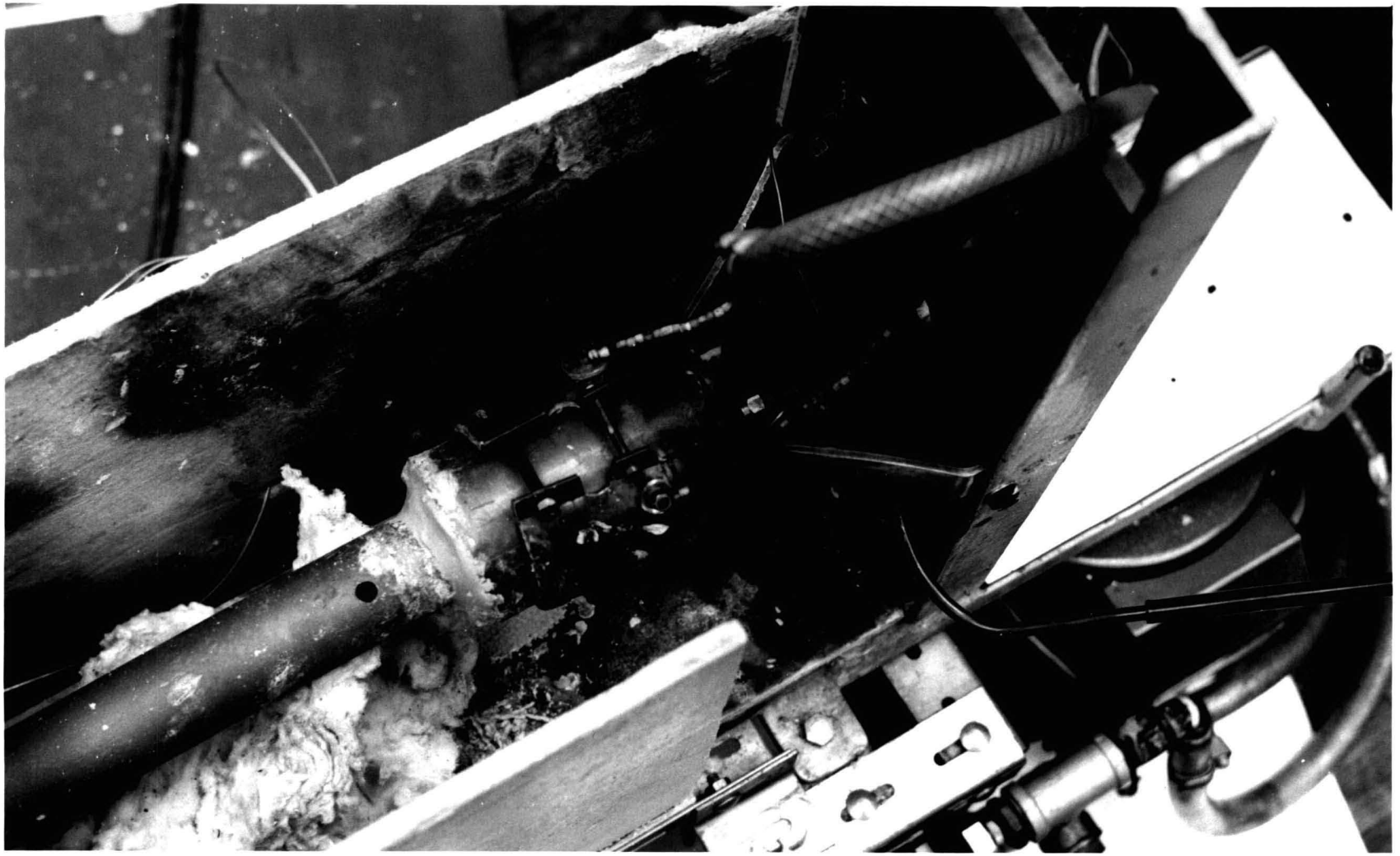

PLATE 5.1.2 Front view of the evaporating chamber.

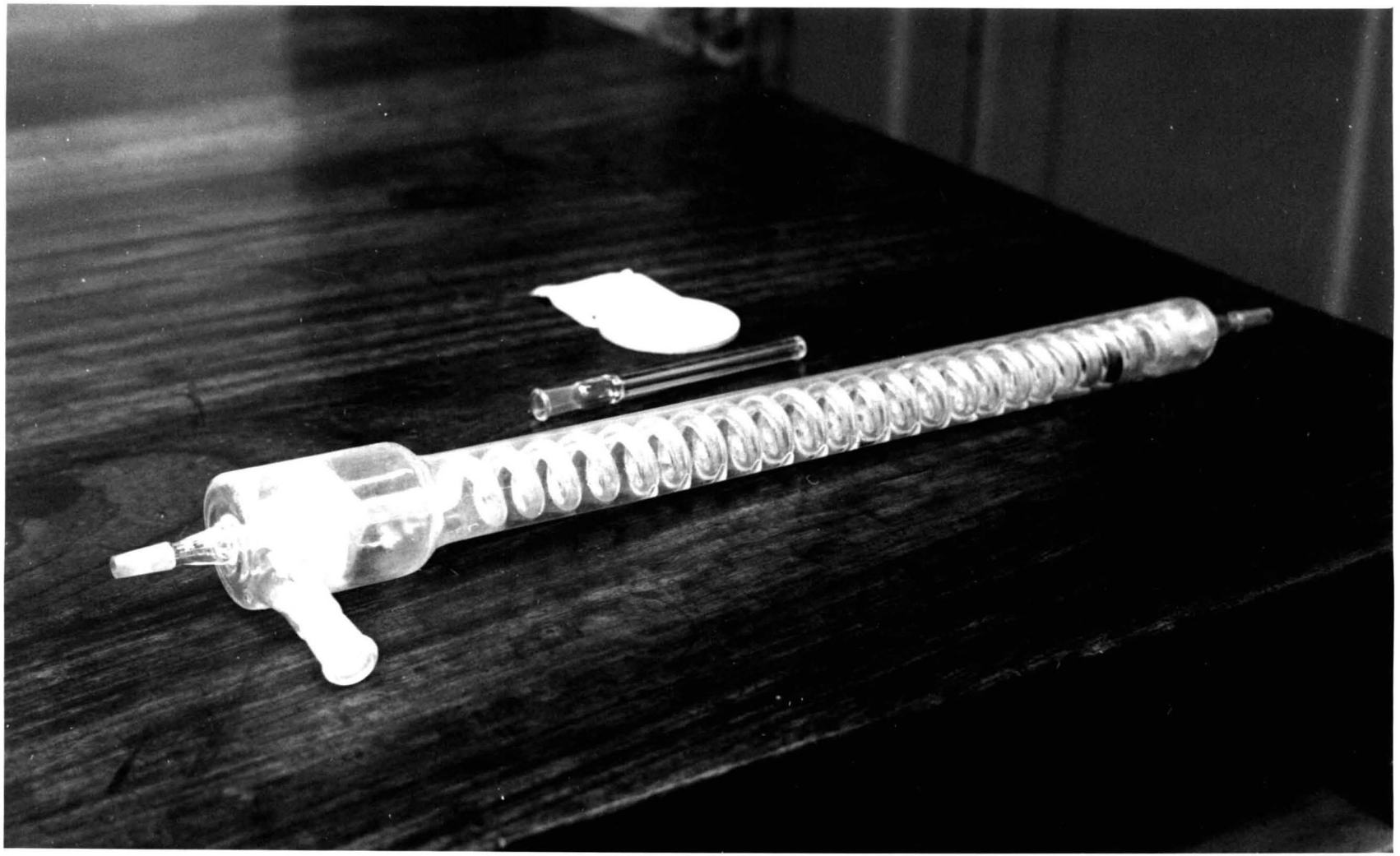

PLATE 5.1.3 General view of :-

a) SO_3 collector
b) Quartz sampling tube
c) Stainless steel sintered disc.

CHAPTER 6

EXPERIMENTAL RESULTS

6.1 Measurement of combustion conditions through the length of the tube

Concentrations of CO, CO_2 and O_2 in the combustion gases were measured at all sampling points to confirm that combustion was completed well within the first sampling port. Temperature measurements were also taken at each sampling port. Fuel and air-flow were kept constant throughout the run. The operating conditions are given in Table 6.2. It can be seen that CO_2 content did not rise appreciably and it was confirmed that combustion was completed almost immediately. Also, carbon monoxide could not be detected at any sampling port and a near constant value of 4.5% excess oxygen was observed.

6.2 Gas Analysis at various air-fuel ratios

Carbon dioxide and oxygen concentrations in the flue gases were measured at different air-fuel ratios. Fuels used were Diesel oil and Kerosine. The results are graphically represented by Figs. 6.1 and 6.2. Gas samples were taken at a distance of approximately 1 metre from the centre of the flame.

6.3 Effect of excess oxygen concentration in the combustion gases on the formation of SO_3

A number of runs were conducted and duplicated to find the reliability of the apparatus under investigation and to co-relate the findings of other workers. SO_3 measurements were made at different excess oxygen concentration in the flue gases and the results are given in tabular form in Table 6.3 and Table 6.4. They are also represented graphically by Fig. 6.3. It can be seen that with no excess oxygen i.e. under stoichiometric condition, SO_3 formation reduced to zero. With the increase of excess oxygen in the combustion system, SO_3 formation began to rise. The rate of increase of SO_3 with increase in excess oxygen concentration remained nearly constant up to about 3.5% excess oxygen. Maximum SO_3 formation was found at around 4% excess oxygen concentration in the combustion gases. These results are in general agreement with the findings of Glaubitz, Hedley and Laxton, described in literature survey (Chapter 2).

6.4 Effect of ignition properties on the formation of SO_3

Liquid hydrocarbons of different ignition properties were used to investigate any effect on the formation of SO_3, the results were compared with those of Kerosine, all fuels having same sulphur content, and under identical combustion conditions. Hydrocarbon chosen for the investigation were cyclohexane, n-hexane, and n-Pentane, some of their properties

6.3 Effect of excess oxygen concentration in the combustion gases on the formation of SO_3

A number of runs were conducted and duplicated to find the reliability of the apparatus under investigation and to co-relate the findings of other workers. SO_3 measurements were made at different excess oxygen concentration in the flue gases and the results are given in tabular form in Table 6.3 and Table 6.4. They are also represented graphically by Fig. 6.3. It can be seen that with no excess oxygen i.e. under stoichiometric condition, SO_3 formation reduced to zero. With the increase of excess oxygen in the combustion system, SO_3 formation began to rise. The rate of increase of SO_3 with increase in excess oxygen concentration remained nearly constant up to about 3.5% excess oxygen. Maximum SO_3 formation was found at around 4% excess oxygen concentration in the combustion gases. These results are in general agreement with the findings of Glaubitz, Hedley and Laxton, described in literature survey (Chapter 2).

6.4 Effect of ignition properties on the formation of SO_3

Liquid hydrocarbons of different ignition properties were used to investigate any effect on the formation of SO_3, the results were compared with those of Kerosine, all fuels having same sulphur content, and under identical combustion conditions. Hydrocarbon chosen for the investigation were cyclohexane, n-hexane, and n-Pentane, some of their properties

are given in Table 6.1. SO_3 concentration in the combustion gases was determined at various excess oxygen concentrations in the flue gases. The results are represented graphically in Fig. 6.4. Tables 6.5, 6.6 and 6.7 also show these results. Fig. 6.4 also contain graph of SO_3 concentration v. oxygen concentration for Kerosine doped with sulphur. The effect of use of n-Pentane as an additive was also investigated although the results are not conclusive. Table 6.8 shows the results with the use of 1% n-Pentane in Kerosine doped with carbondisulphide. Effect of aniline as an additive was also investigated and results are tabulated in Table 6.9 which shows a small reduction of SO_3 formation.

6.5 Effect of residence time on the formation of SO_3

6.5.1 Introduction.

The experimental programme consisted of five series of tests, namely A, B, C, D and E, which represent the different rates of fuel combustion from 2.3 cm^3/min to 6.0 cm^3/min. O_2 concentration was kept constant by keeping the air-fuel ratio constant throughout the series of experiments. It was found necessary to externally heat the exit of the combustion tube for the series E (Fuel flow rate - 6 cm^3/min) of the experiment to keep the temperature along the tube constant. Temperature measurements were made at each sampling port, at the centre of the tube for each run of tests to determine

temperature history of the gases (Fig. 6.5). In order to find variation of temperature across the section of the tube, measurement of temperatures were made at distances of 5mm, 10mm and 25mm from the wall of the tube. Measurements were made at three different ports. The results are graphically represented in Fig. 6.6.

6.5.2 Experimental runs A, B, C and D.

Tables 6.12 to 6.15 show the experimental data and analysis of combustion gases for sulphur dioxide and sulphur trioxide at different ports of the combustion tube. The duration of a complete run lasted several days and tests were repeated for reliability.

The aim of these experiments was to study the effect of residence time of combustion gases on the formation and decay of SO_3.

Gas temperatures shown in the tables was the average gas temperature through the length of the combustion tube.

Experimental results of A and B are shown graphically in Fig. 6.7, that of runs C and D are shown in Fig. 6.9, where SO_3 is plotted against the residence time.

6.5.3 Experimental Run E.

This series of experiments was similar to the previous runs, except that higher gas temperature was obtained by means

of higher fuel rate of burning and external heating near the end of the combustion tube in order to keep constant temperature throughout the length of the tube. The excess air was kept constant by keeping O_2 concentration in the flue gases at 4.5% (vol). There was also no change in sulphur content of Kerosine used, which remained at 3.4% (wt) by addition of CS_2.

The results of these experiments are shown in Fig. 6.12.

TABLE 6.1.

Properties of some liquid hydrocarbons

Name	Formula	Mol. wt.	sp. gravity at 15°C	B.P. Range (95%)	Minimum Ignition Temp. °C (in air)
Kerosine	-	-	0.79	160-290	254
Cyclohexane	$CH_2(CH_2)_4CH_2$	84.16	0.776	80- 82	274
n-hexane	$CH_3(CH_2)_4CH_3$	86.18	0.670	67- 70	248
n-Pentane	$CH_3(CH_2)_3CH_3$	72.15	0.625	35- 37	284

TABLE 6.2

Gas analysis results for a test run

Run No.	Sampling Port	Distance from burner plate ft	CO_2 % (vol.)	CO % (vol.)	O_2 % (vol.)
1	1	1	11.2	Nil	4.5
2	2	2	11.3	Nil	4.5
3	3	3	11.2	Nil	4.5
4	4	4	11.4	Nil	4.4
5	5	5	11.3	Nil	4.5
6	6	6	11.2	Nil	4.5

Fuel: Kerosine + 3.4% S(wt).

Fuel Flow Rate = 6 cc/min.

Air Flow Rate = 55 lit/min.

TABLE 6.3

Fuel: Diesel oil + 3.4% S(wt.)

Fuel Flow Rate: 2.55 cc/min.

Temp. of gas near sampling point: 380°C - 410°C

Run No.	Air flow Rate lit/min	Air/Fuel Mass Ratio	Gaseous Combustion products			SO_2	SO_3
			CO	CO_2	O_2		
1	29.0	17.8	Nil	11.9	4.1	1610	40
2	25.0	15.1	Nil	13.9	1.2	1723	12
3	27.0	16.3	Nil	12.7	2.6	1480	22
4	27.0	16.3	Nil	12.9	2.6	-	23
5	23.0	13.9	0.5	15.3	0.0	-	0
6	24.6	14.8	Nil	14.2	0.7	1900	10
7	24.6	14.8	Nil	14.5	0.7	1980	9
8	32.8	19.8	Nil	11.1	5.5	1970	39
9	25.2	15.2	Nil	13.8	1.3	-	8
10	26.7	16.1	Nil	13.2	2.7	1790	30
11	26.8	16.15	Nil	13.0	2.8	-	33
12	37.2	22.4	Nil	9.5	7.7	1852	18
13	37.1	22.35	Nil	9.5	7.7	1670	25.5
14	35.0	21.1	Nil	9.8	7.0	1610	16
15	26.8	16.15	Nil	13.4	2.5	1900	22
16	26.8	16.15	Nil	13.4	2.5	1630	23
17	34.0	20.5	Nil	9.8	6.5	1852	27
18	26.2	15.75	Nil	13.8	2.0	1700	20

TABLE 6.4

Fuel: Kerosine + 3.4% S(wt.)

Fuel Flow Rate: 2.55 cc/min.

Temp. of gases near suction point: 380°C - 450°C

Run No.	Air Flow Rate lit/min	Air/Fuel Mass Ratio	Gaseous combustion products % volume			SO_2 p.p.m.	SO_3 p.p.m.
			CO	CO	O		
1	24.8	16.1	0.0	13.8	0.15	-	1.3
2	25.4	16.5	Nil	13.2	0.8	1752	4.5
3	26.2	17.05	Nil	12.9	1.3	1648	12.0
4	26.5	17.2	Nil	12.9	1.6	-	17.5
5	27.3	17.5	Nil	12.7	2.4	-	25
6	27.8	18.1	Nil	12.6	2.6	1615	26.5
7	29.0	18.9	Nil	11.9	3.4	1840	39
8	33.8	22.0	Nil	9.9	5.8	1583	34
9	36.2	23.5	Nil	9.5	6.8	1689	29
10	23.0	14.9	0.3	15.0	0.0	1731	0
11	23.0	14.9	0.5	14.9	0.3	-	0
12	25.0	16.2	Nil	13.8	0.8	1656	2
13	30.1	19.6	Nil	11.6	4.2	1725	43
14	30.0	19.45	Nil	11.7	3.75	-	44
15	27.4	17.8	Nil	12.8	2.4	1670	27.5
16	34.0	22.1	Nil	10.0	6.0	1590	33.5

TABLE 6.5

Fuel: Cyclohexane + 3.4% S(wt.)
Fuel Flow Rate: 2.5 cc/min.
Temp. near suction = 400°C

Runs	Excess oxygen (% vol.)	SO_3 p.p.m.
1	5.5	26.8
2	4.5	39
3	3.4	30
4	2.9	23

TABLE 6.6

Fuel: n-hexane + 3.4% S(wt.)
Fuel Flow Rate: 2.5 cc/min.
Temp. of gases near suction: 440°C

Runs	Excess oxygen (% (vol.)	SO_3 p.p.m.
1	4.5	22.8
2	3.0	13.5
3	1.2	0.6
4	2.0	5.0
5	4.5	23
6	7.0	14
7	5.5	21
8	3.4	20

TABLE 6.7

Fuel: n-Pentane + 3.4% S(wt.)

Fuel Flow Rate: 2.5 cc/min.

Temp. of gases near suction: 400-450°C

Runs	Excess oxygen % vol.	SO_3 p.p.m.
1	4.3	33
2	3.9	29
3	5.0	29
4	4.8	30
5	4.0	31

TABLE 6.8

Fuel: Kerosine + 3.4% S(wt.) + 1% n-Pentane (vol.)

Fuel Flow Rate: 2.5 cc/min.

Temperature of gases near suction: 400°C

Run	Excess Oxygen (% vol.)	SO_3 p.p.m.	SO_3 p.p.m. (Untreated) from graph
1	4.25	42	44.8
2	4.5	41	44.5

TABLE 6.9

Fuel: Kerosine + 3.4% S(wt.) + 1% aniline

Fuel Flow Rate: 2.5 cc/min.

Temperature of gases near suction: 400°C

Run	Excess Oxygen (% vol.)	SO_3 p.p.m.	SO_3 p.p.m. (Untreated) from graph
1	4.4	35.7	45.0
2	4.5	40	44.5
3	2.5	10	25.0

TABLE 6.10

Combustion Products Analysis

Run B

Expt.No.	Ports	CO_2	CO	O_2
1	1	11.5	0.02	4.5
2	2	11.5	Nil	4.5
3	3	11.5	Nil	4.3
4	4	11.5	Nil	4.5
5	5	11.8	Nil	4.4
6	6	11.4	Nil	4.4

TABLE 6.11

Gas temperature measurement along the length of the tube for Runs A, B, C, D and E

Run	Gas temperature ^{o}C					
	Port 1	Port 2	Port 3	Port 4	Port 5	Port 6
A	725	645	590	580	574	553
B	740	658	610	604	600	580
C	765	680	600	590	600	600
D	778	700	620	600	590	580
E	1080	990	1000	1040	970	860

TABLE 6.12

Run A

Fuel: Kerosine + 3.4% S(wt.)

Fuel Flow Rate: 2.3 cc/min.

Air Fuel Ratio: 18.4

Av. Gas Temp. up to 1ft. length; 800°C; Rest - 600°C

Velocity V_1 = 8.38ft/sec; V_2 = 5.98ft/sec.

Gas analysis: CO - NIL; CO_2 - 11.5%; O_2 - 4.5%

	Run No.	Sampling Port					
		1	2	3	4	5	6
SO_3 p.p.m.	A	76	102	89			65
	B		105	92		68	
	C	80		94			71
SO_2 p.p.m.	A	1620	1661	1683			1650
	C	1680		1603			1700
% conversion of SO_2 to SO_3	A	4.49	5.78	5.00			3.78
	C	4.54		5.54			4.00
Residence time secs.		.119	.334	.502	.668	.836	1.00

TABLE 6.13

Run B

Fuel: Kerosine + 3.4% S(wt.)

Fuel Flow Rate: 2.5 cc/min.

Air Fuel Ratio: 18.4

Av. Gas Temp. 1ft. from flame 800°C ; Rest - 600°C

Gas analysis: CO - NIL ; CO_2 - 11.5% ; O_2 - 4.5%

	Run No.	Sampling Ports					
		F	1	2	3	5	6
SO_3 p.p.m.	A	34	80			74	
	B			110	94		60
	C	32			96		
SO_2 p.p.m.	A		1743			1641	
	B			1684	1693		1703
% oxidation of SO_2	A		4.37	6.14	5.26	4.31	3.4
	B			6.14			3.4
Residence Time sec.		0.045	0.11	0.31	0.465	0.77	0.93

F = approximately 1" from flame front.

TABLE 6.14

Run C

Fuel: Kerosine + 3.4% S(wt.)

Fuel Flow Rate: 2.8 cc/min.

Air Fuel Ratio: 18.4 (mass)

Av. gas Temp. up to 1ft. length: 850°C ; Rest - 600°C

Gas analysis: CO - NIL ; CO_2 - 11.5% ; O_2 - 4.5%

	Run No.	Sampling Ports					
		1	2	3	4	5	6
SO_3 p.p.m.	A	72	106	99			
	B	80	110	103			89
	C	76	108	96		70	65
SO_2 p.p.m.	A	1830	1800	1792			1722
	B	1810	1685	1728		1643	1683
% oxidation of SO_2 to SO_3	A	3.76	5.56	5.19			4.9
	B	4.24	6.14	5.61		4.1	3.72
Residence time, secs.		0.1	0.28	0.42		0.7	0.84

TABLE 6.15

Run D

Fuel: Kerosine + 3.4% S(wt.)

Fuel Flow Rate: 3.5 cc/min.

Air Fuel Ratio: 18.4

Av. gas temp. up to 1ft. length: 850°C ; Rest - 600°C

Gas analysis: CC - NIL ; CO_2 - 11.5% ; O_2 - 4.5%

	Run No.	Sampling Ports						
		1	2	3	4	5	6	F
SO_3 p.p.m.	A		108	106			60	
	B	72	105					33
	C	61	110					
SO_2 p.p.m.	A			1683			1707	
	B	1631	1603					
	C		1781					
% oxidation of SO_2	A	3.6	6.15				3.4	
	B		5.9					
	C		5.84					
Residence time, secs.		.077	.218	.326	.435	.54	.54	0.033

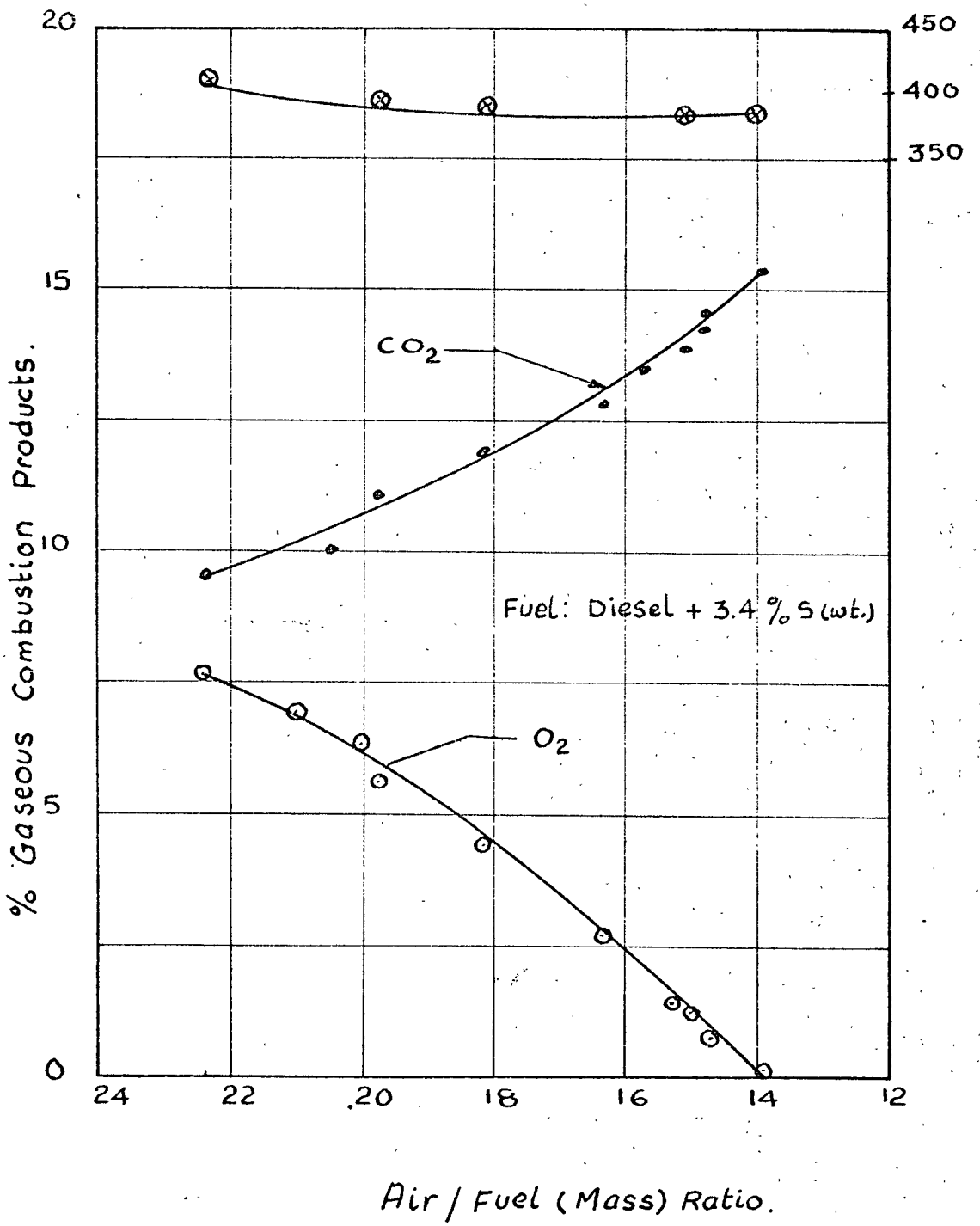

FIG. 6.1 Variation of combustion products with air/fuel ratio burning Diesel fuel.

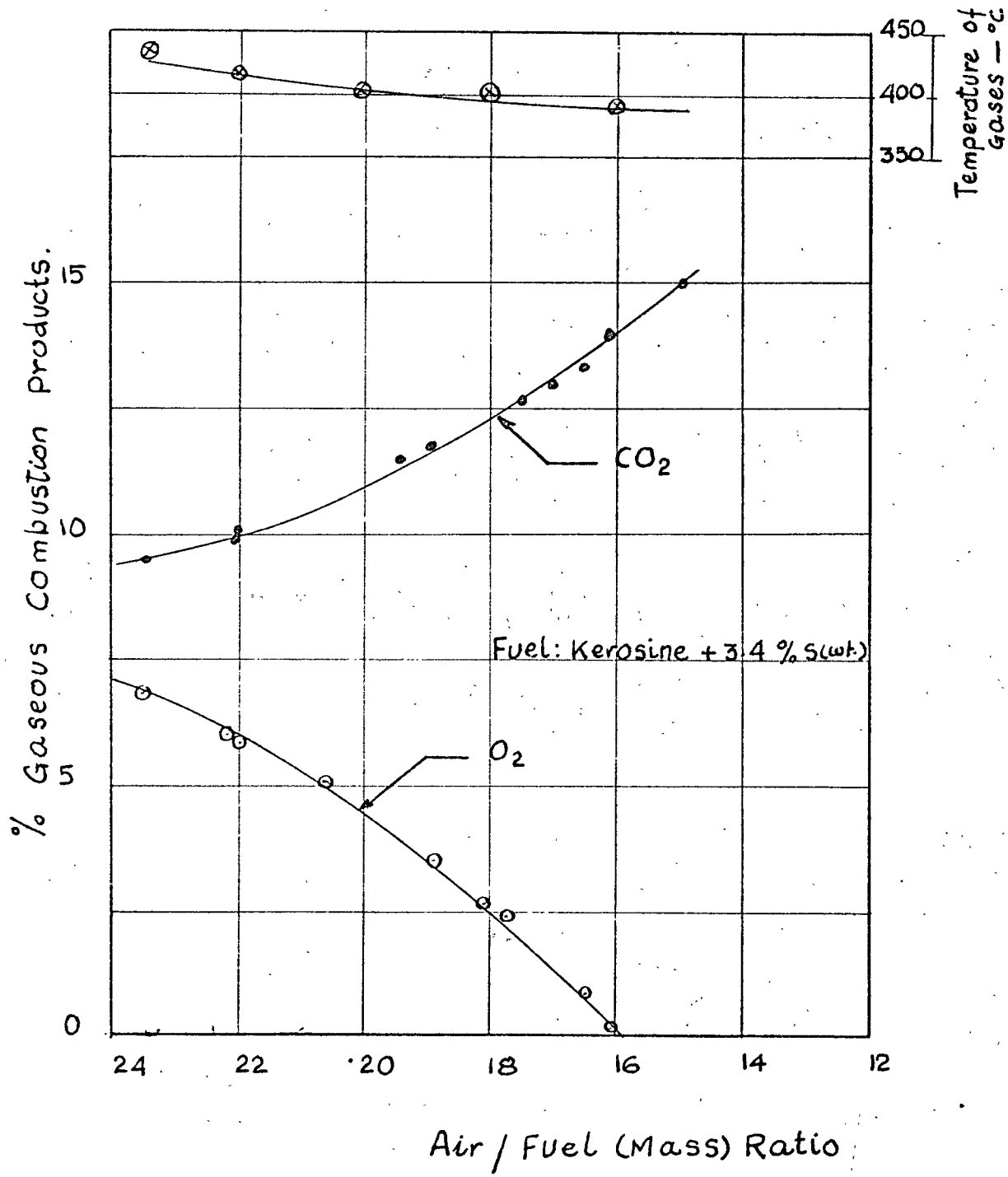

FIG. 6.2 Variation of combustion products with air/fuel ratio burning Kerosine as fuel.

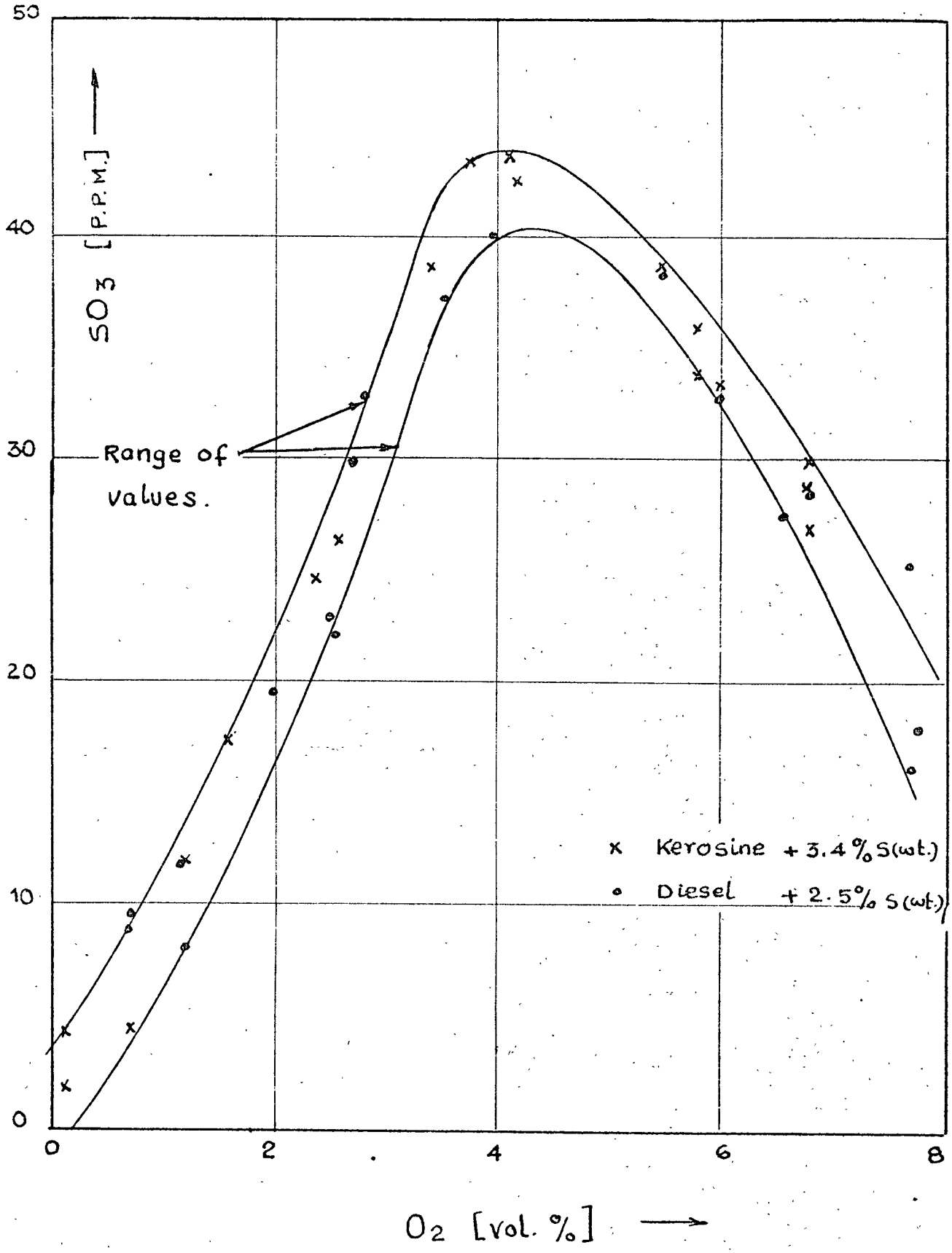

FIG. 6.3 Effect of excess oxygen on the formation of SO_3 for Kerosine and Diesel fuels.

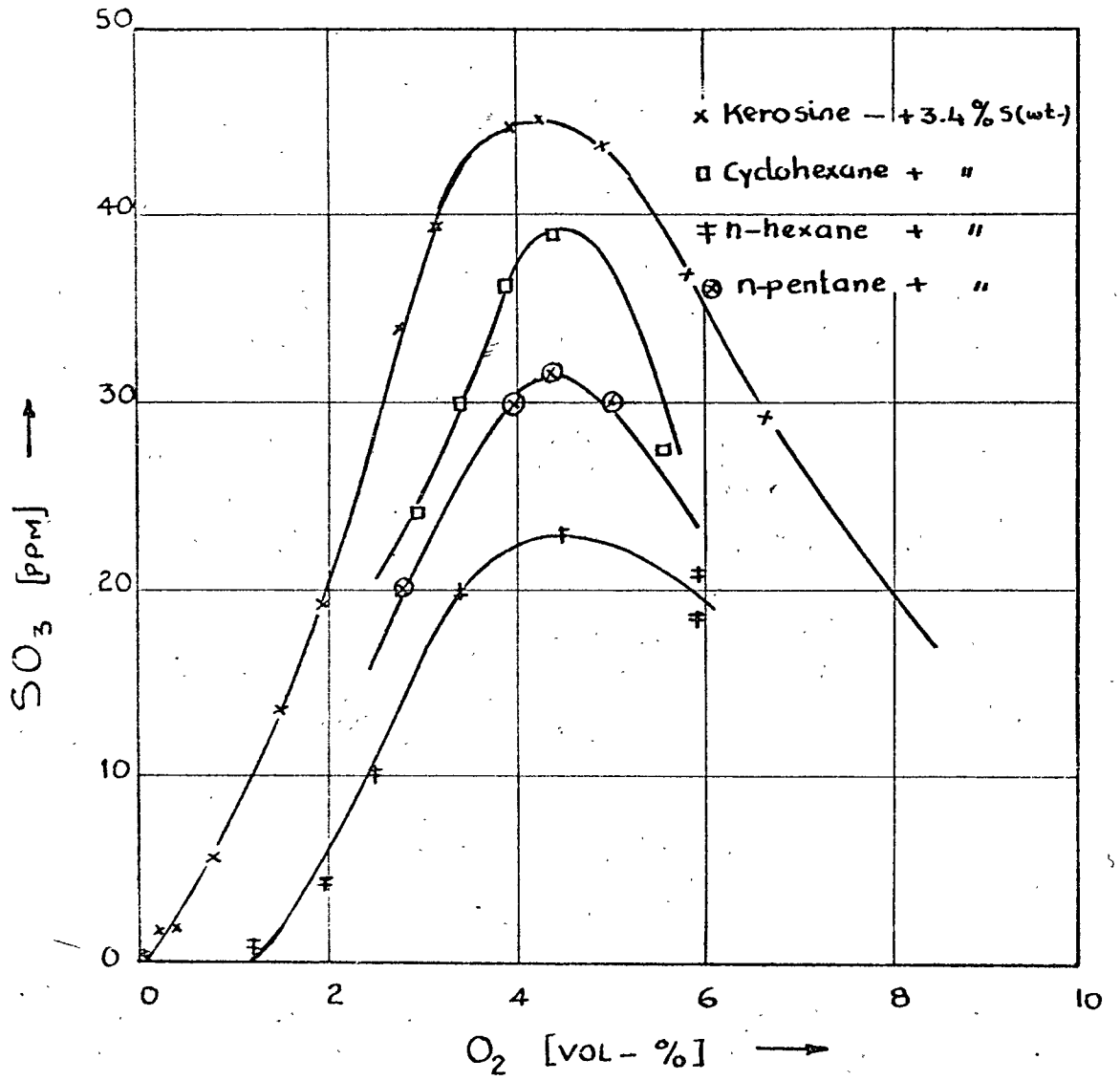

FIG. 6.4 Variation of SO_3 content with excess oxygen in the combustion gases for various hydrocarbons doped with same amount of sulphur.

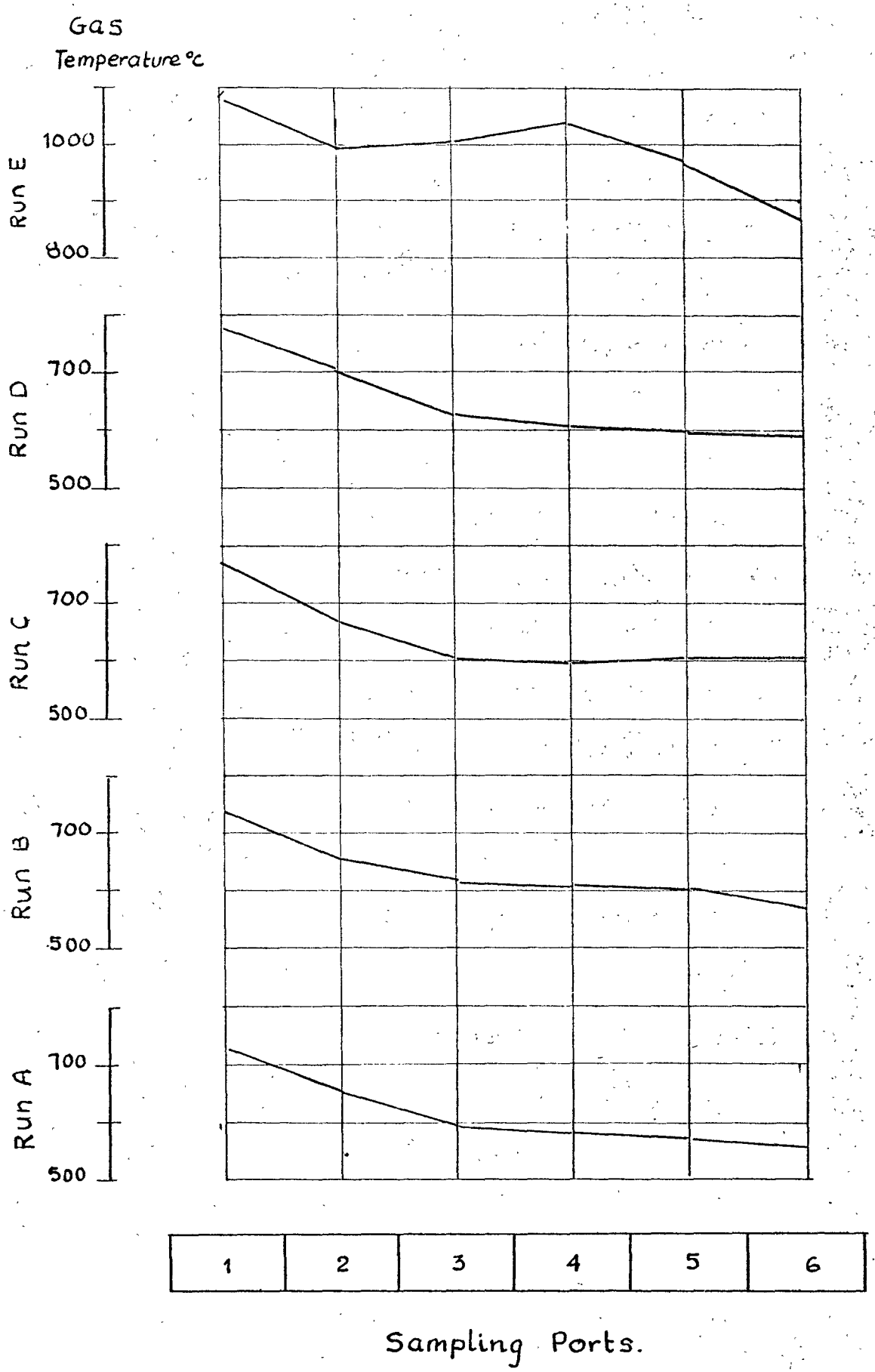

FIG. 6.5 Temperature history of combustion gases.

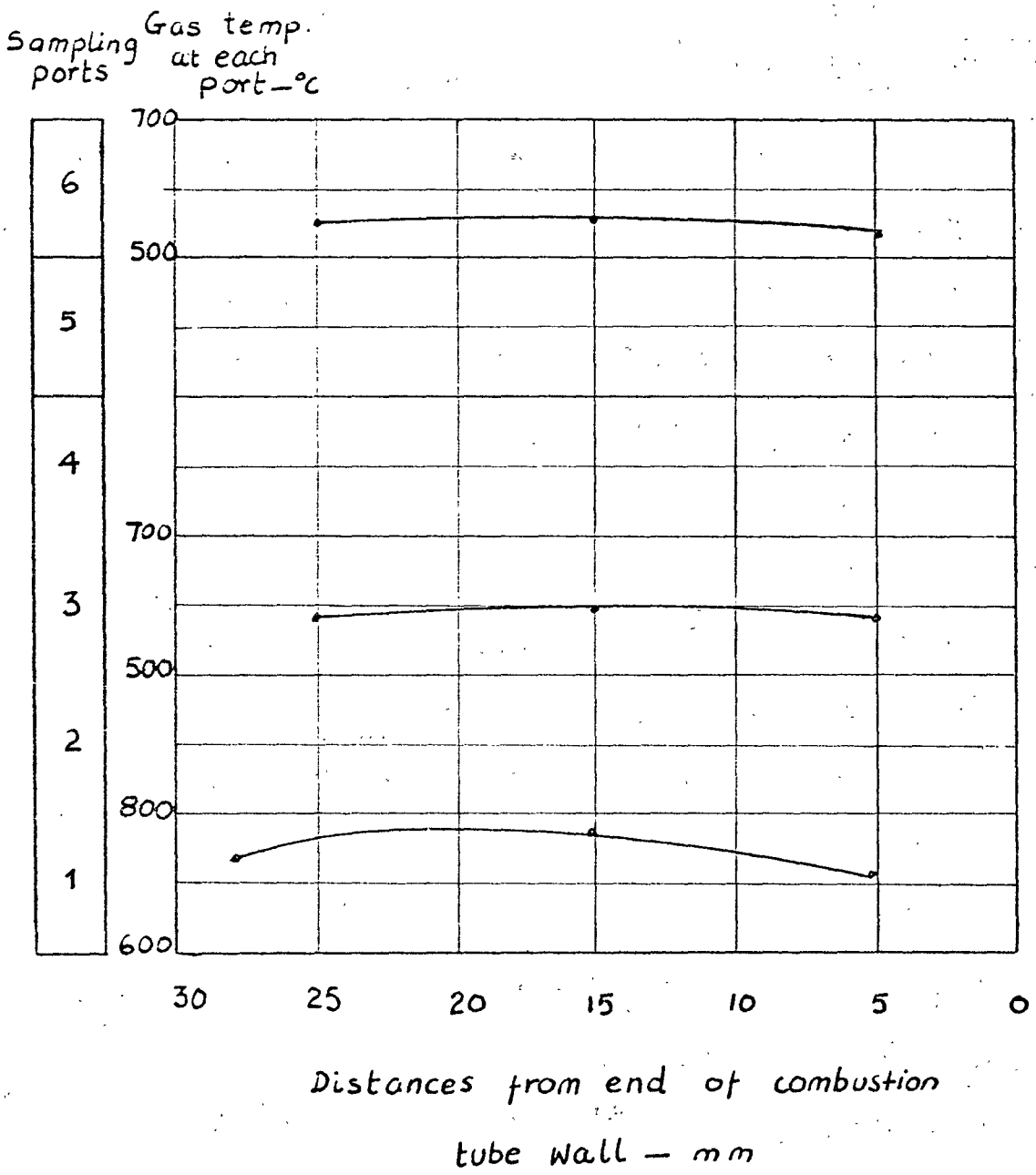

FIG. 6.6 Temperature traverse across the combustion tube for combustion conditions of Run C.

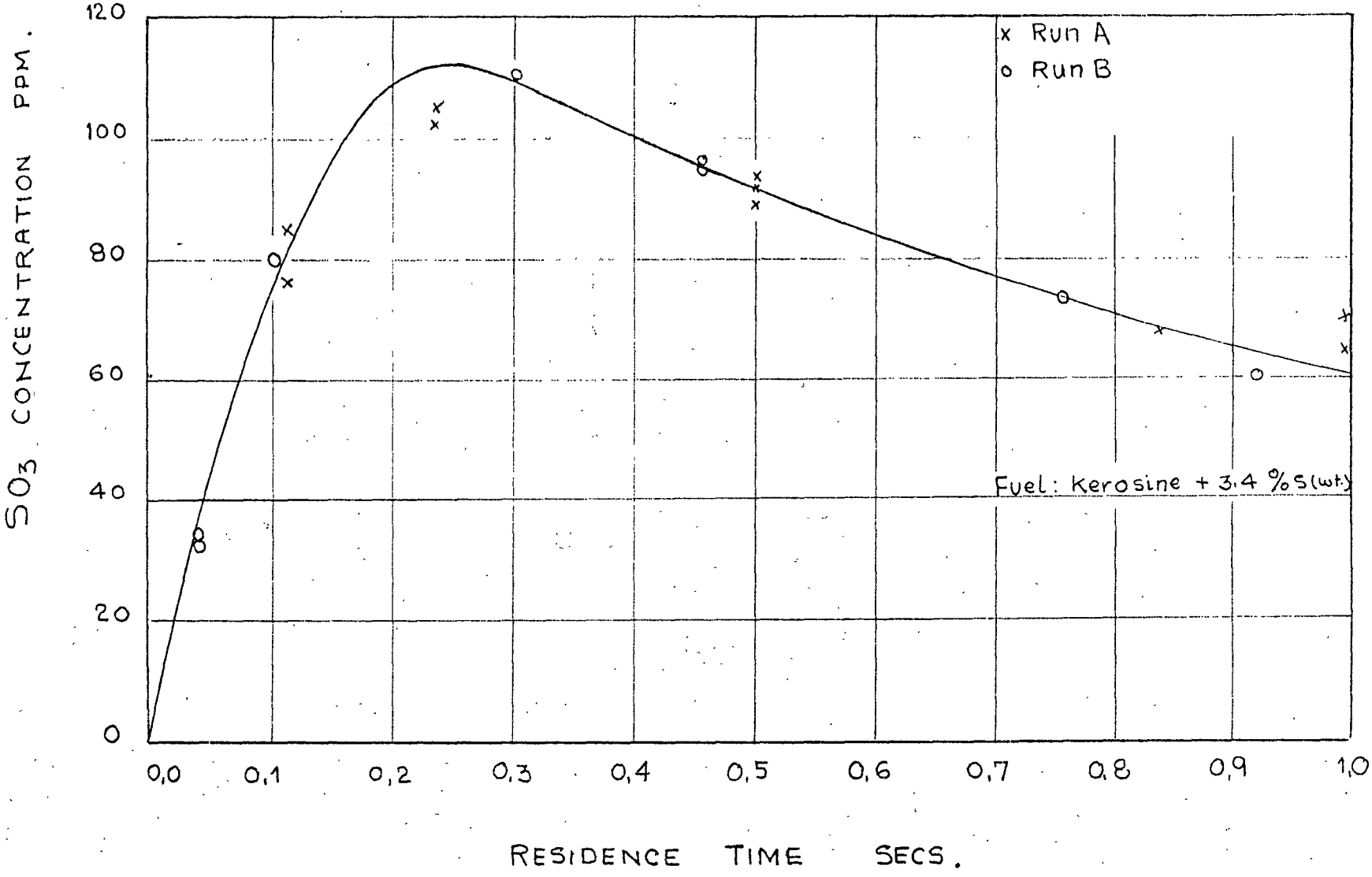

FIG. 6.7 Variation of SO_3 concentration with time.

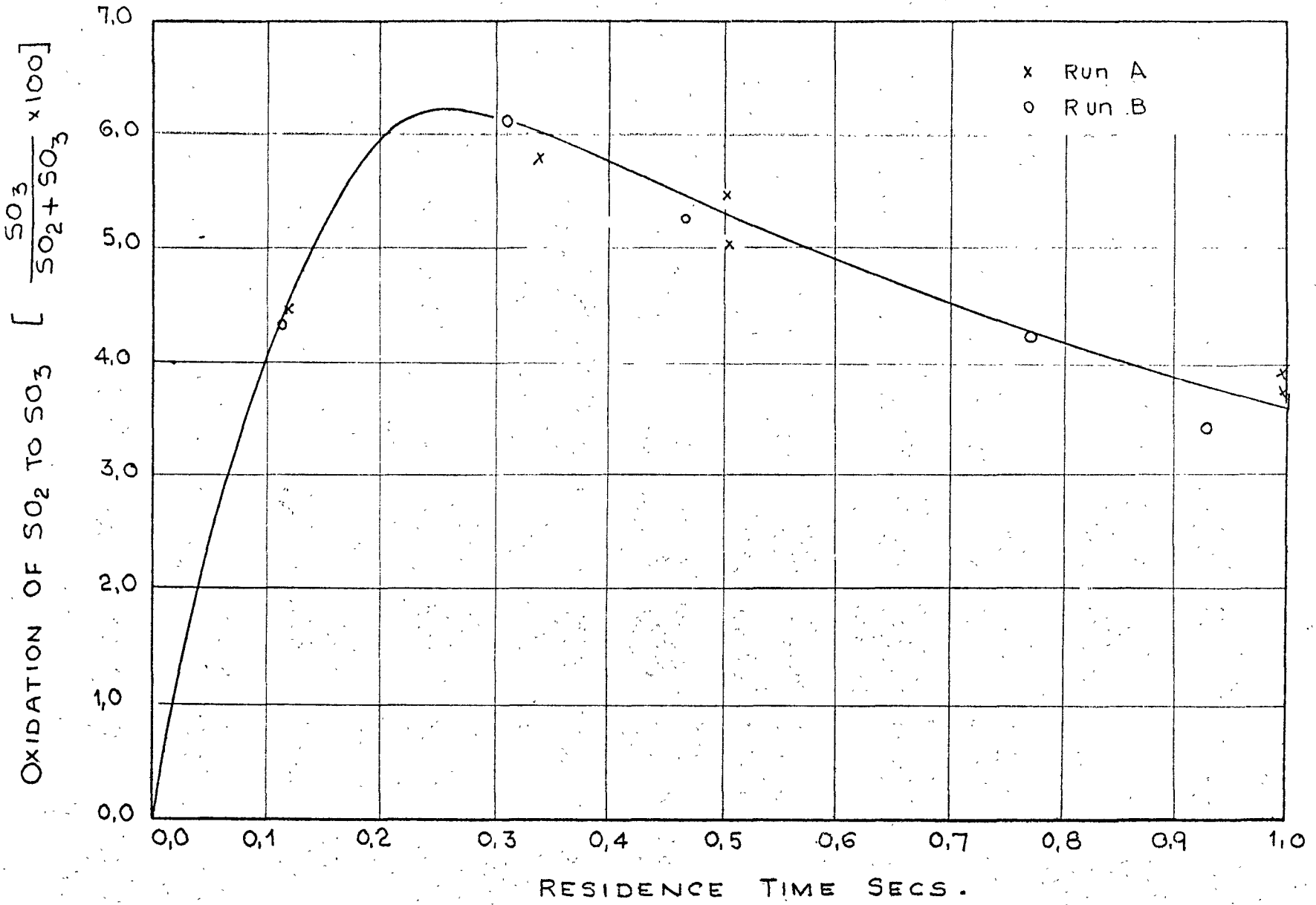

FIG. 6.8 Variation of percentage oxidation with time.

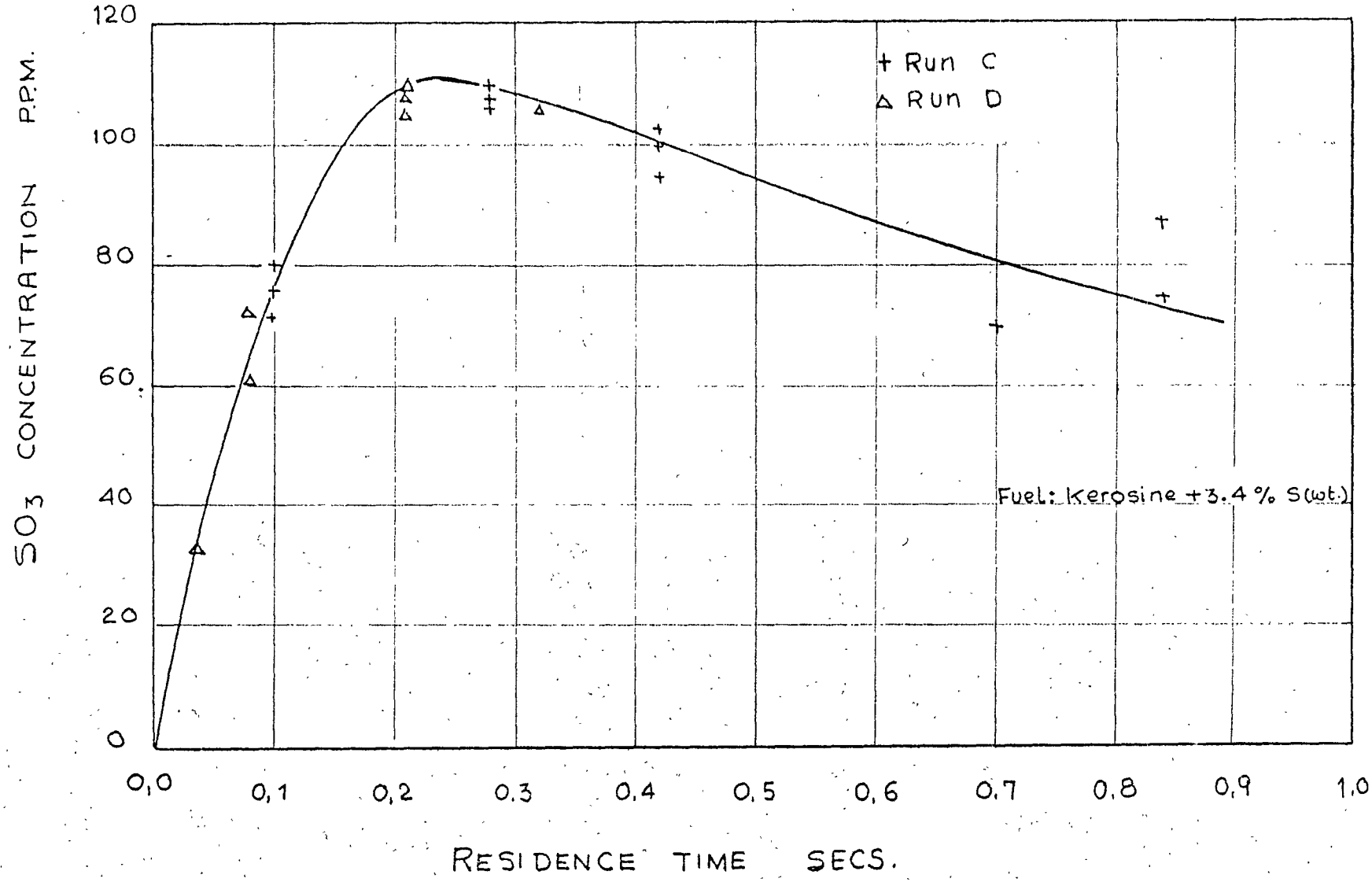

FIG. 6.9 Variation of SO_3 concentration with time

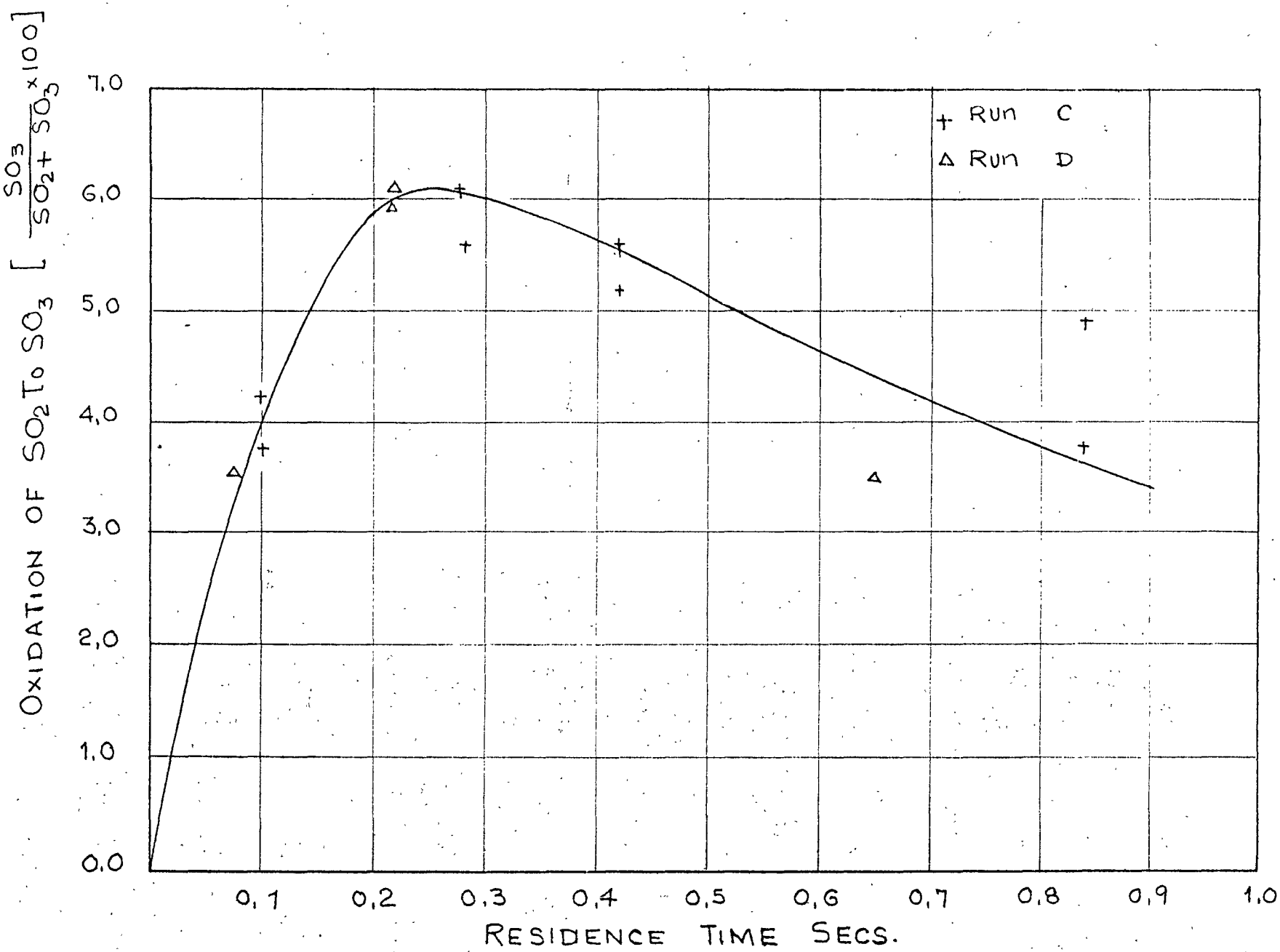

FIG. 6.10 Variation of percentage oxidation with time

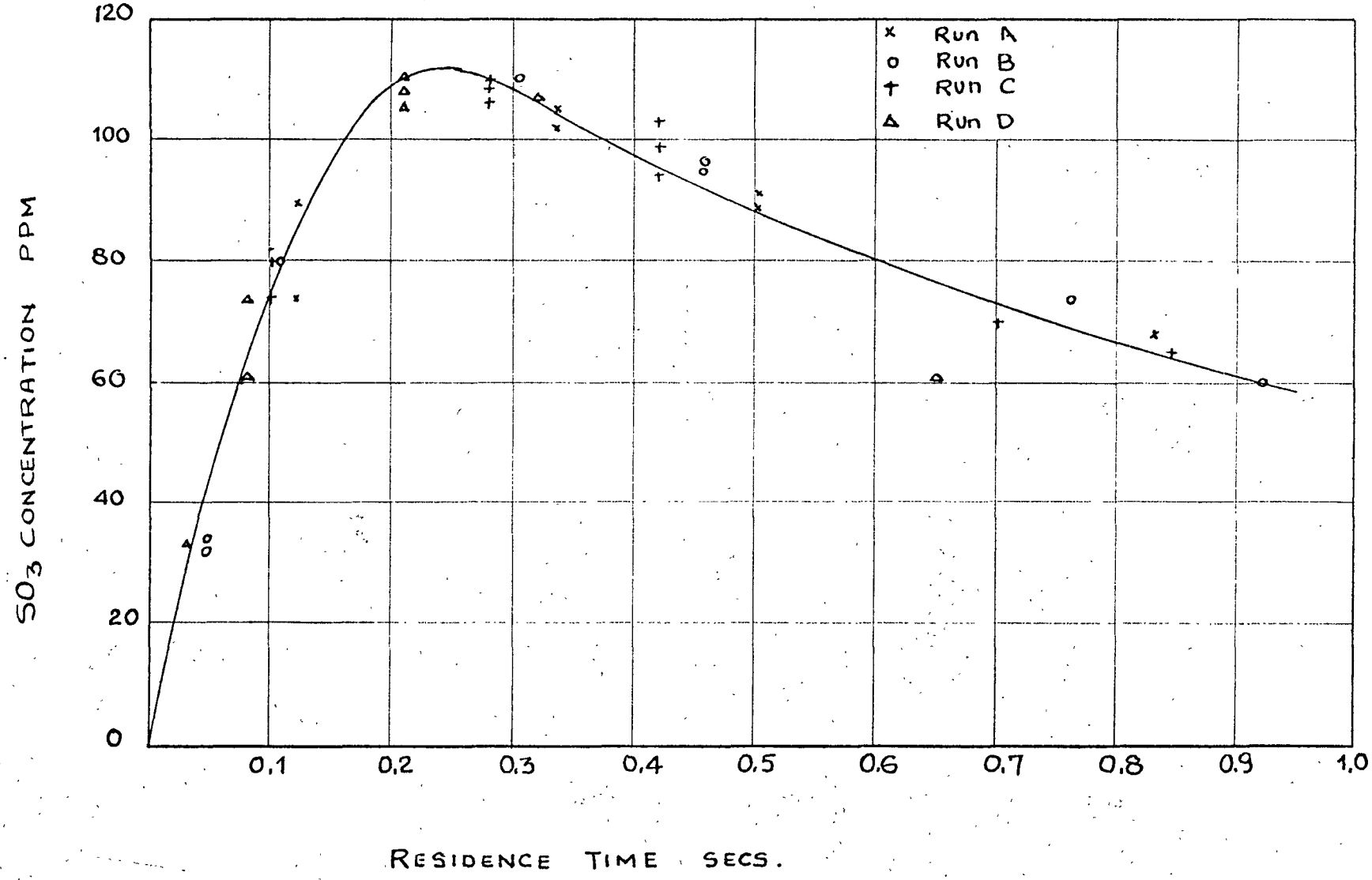

FIG. 6.11 Variation of SO_3 concentration with time.

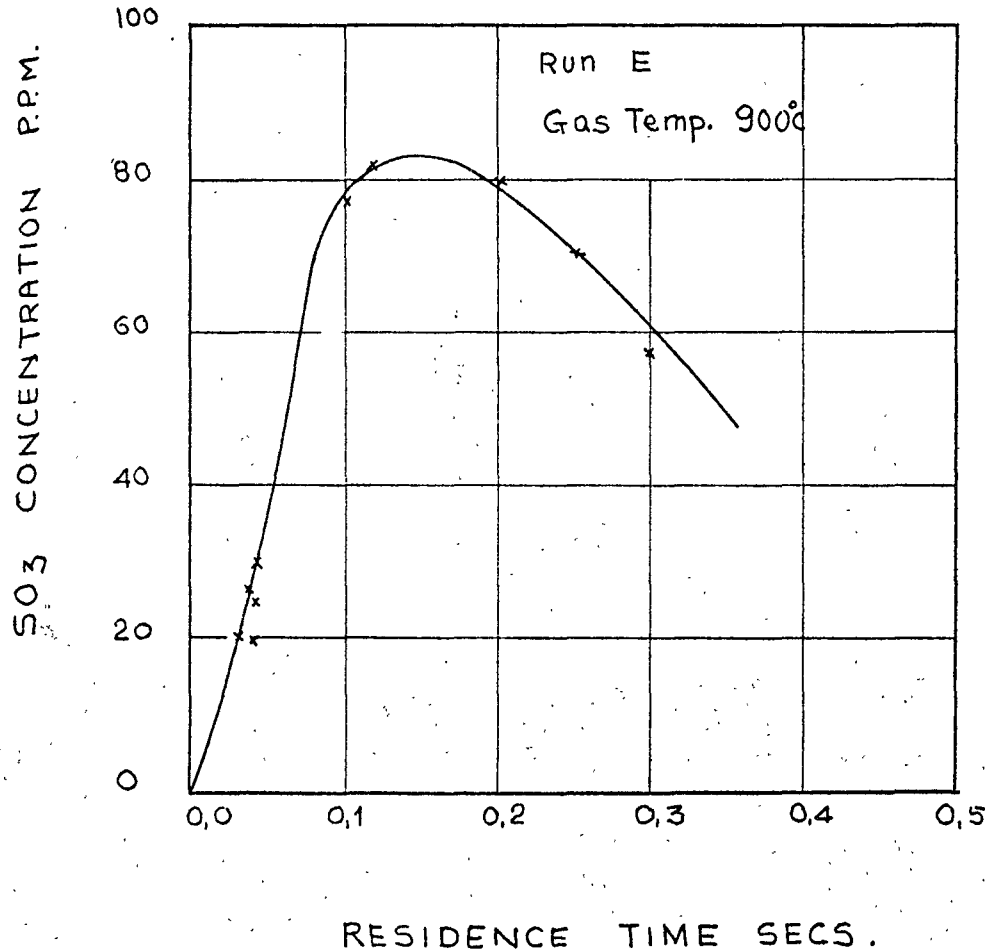

FIG. 6.12 Variation of SO_3 concentration with time

CHAPTER 7

DISCUSSION AND INTERPRETATION OF RESULTS

7.1. Introduction

The experiments described in the previous Chapter can be divided into three main classes.

a) Effect of oxygen content in the combustion gases on the formation of SO_3 was determined and the value of oxygen concentration for optimum SO_3 formation was obtained.

b) Fuels with different ignition properties were burnt and SO_3 concentration in the combustion gases were determined at various oxygen content of the flue gases (varying air-fuel ratio). Thus effect of ignition properties on the formation of SO_3 was determined.

c) In the third series of experiments, the measurement of SO_3 was made at different sampling ports for a specific fuel. The rate of fuel flow, and the excess air was kept constant.

Hence, the effect of residence time of combustion gases on the formation of SO_3 was determined.

7.2 Discussion

7.2.1 Effect of excess oxygen on SO_3 formation

The reduction of excess oxygen concentration in the flue gases towards zero, causes a reduction of SO_3 concentration to zero. This has been reported by a number of workers and it is generally reasonable to assume that under fuel rich conditions, in the absence of excess oxygen, carbonmonoxide reaction with oxygen will take preference over SO_2 reaction with oxygen.[12] The work of Rosborough indicated that there is an oxygen concentration between 3% to 6% at which SO_3 level would be maximum. In the present series of experiments, this value appears to be 4.5%. It can be concluded that conditions most favourable for the production of SO_3 is when combustion takes place when oxygen concentration in the flue gases is around 4.5% and all of the excess air has been added prior to combustion.

7.2.2 Effect of ignition properties on the formation of SO_3

Processes involved in the oxidation of even the simplest hydrocarbon, i.e. methane has not been fully understood.[69] In the pre-mixed, high temperature (flame) combustion of hydrocarbons, the mechanism of combustion differs markedly from that responsible for low temperature slow oxidation, the majority of enthalpy of reaction is released rapidly in a narrow reaction zone leading to the production of high temperatures. It is evident that the problem of finding exact mechanism of combustion of hydrocarbon is extremely difficult.

The complex nature of the intermediate reactions during the short region of 'reaction zone' deters any absolute assessment of the mechanism of formation of SO_3 in flames. However in - direct methods of assessment can be employed.

In order to understand the phenomena better, three zones, a pre-heat, a true reaction and a recombination zone - may be distinguished in the structure of a pre-mixed flame[69] (Appendix Fig. A.1.) With the majority of hydrocarbons, in the pre-heat zone, degradation occurs and the fuel fragments leaving this zone will comprise mainly lower hydrocarbons, olefins and hydrogen. In the reaction zone proper, owing to the short time available, the radical concentration will still be very high and oxidation will proceed mainly to carbon monoxide rather than carbon dioxide, and this zone will terminate in a quasi-equilibrium state. In the post-flame or the recombination zone, carbon monoxide will oxidise to carbon dioxide depending on the fuel-oxygen ratio. Concentration of radicals and atoms in the more extended post-flame region where recombinations are still taking place is therefore a determining factor in the final concentration of stable spicies. Considering these assumptions, it is possible that hydrocarbons which tend to initiate early reactions bring forward the recombination region of the flame and thus allow greater time for CO to compete with SO_2 for reacting with available atomic oxygen.

It is also known that standard fuel energy change for the carbon monoxide oxidation is much greater than that for sulphur dioxide oxidation. Therefore it would be expected that former

reaction would take preference over the latter, and under the circumstances oxidation of SO_2 will be reduced.

Four hydrocarbons with different ignition properties were used in the experimental programme. It was found that although the production of SO_3 reached its maximum value at around 4.5% excess oxygen in all four cases, the actual values of SO_3 however, differed appreciably from each other. It may be noted that sulphur content in the fuel was the same in all the four cases. Therefore it appears reasonable to assume that ignition properties have an effect on the formation of SO_3. It was decided to find the respective ignition delay times of the fuels used in the present series of experiments to find evidence in support of the above argument.

7.2.3 Effect of residence time on the formation of SO_3

It is evident from the experimental results that the degree of oxidation of SO_2 in flames is dependent upon the residence time of combustion gases, other variables like nature of the fuel, its sulphur content and excess air remaining constant. It was also found that flame gases contained SO_3 very much in excess of the equilibrium concentration and therefore a mechanism involving oxygen atoms seems likely.[8,12].

7.2.4 Kinetic consideration of mechanism of formation of SO_3 in flames

Let us first consider the oxidation of carbon monoxide which is of major importance since carbon monoxide is one of the major products of the partial oxidation of hydrocarbons and their

derivatives. During the initial stage in the oxidation of organic compounds, carbon monoxide is formed which is then further oxidised to carbon dioxide depending upon the availability of oxygen. The exact mechanism, however, by which CO is oxidised to CO_2 has been the subject of controversy for many years and is still in dispute.[70,71,72] It was suggested by Lewis and Von Elbe that chain branching under some conditions was due to the reactions -

$$O + O_2 + M \longrightarrow O_3 + M \qquad (1)$$

$$CO + O_3 \longrightarrow CO_2 + 2O \qquad (2)$$

But there were strong objections to this view particularly due to the inability to detect ozone by ultraviolet absorption during the explsion of a $2CO + O_2$ mixture.[73] The theory of Semenov[74] was however, thought to be more likely explanation. He suggested the reactions:

$$CO + O \longrightarrow CO_2^* \qquad (3)$$

$$CO_2^* + O_2 \longrightarrow CO_2 + 2O \qquad (4)$$

are responsible for branching. This view was criticized by Lewis and Von Elbe on the grounds that excited CO_2 molecules dissociate too rapidly to be able to act as chain carriers. Other evidence[75] indicated that at least some molecules formed in the reaction (3) would have sufficiently long time to take part in the reaction (4). The results of Avramenko and Kolesnikova[76] suggested strongly that the rate determining step in the formation of carbon dioxide was the bimolecular

association of CO and O, with an activation energy of 3Kcal/mole. On examination of these mechanisms, it is clear that each time a single CO molecule burns, a surplus oxygen atom is released into the system.

The principal source of oxygen atom for SO_2 oxidation is therefore either from thermal decomposition of excess oxygen.

$$O_2 + 117 \text{ K cal g mol.}^{-1} \longrightarrow O + O$$

or the dissociation of excess oxygen molecules by collision with excited CO_2* molecules which has been suggested to exist in flames as discussed earlier.

The presence of a third body M is known to be necessary for the combination of two colliding oxygen atoms to form O_2 molecule.[89] On the other hand, the presence of this third body is not necessarily imperative when an oxygen atom and a SO_2 molecule collide to form a SO_3 molecule [70]. The excess energy is absorbed by the extra bonds in the molecule which would then lose energy by radiation or by later molecular collisions. The process can be represented as [12]

$$SO_2 + O \longrightarrow SO_3^* \qquad (5)$$

$$SO_3^* \longrightarrow SO_3 + h\gamma \qquad (6)$$

$$SO_3^* + M \longrightarrow SO_3 + M \qquad (7)$$

This activated molecule will subsequently collide with a third body (e.g. (H_{2O}) to give normal SO_3.

The mechanism proposed by Levy and Merryman[20] of the formation of SO_3 in H_2S flames also involved O-atom chain operating in the following manner:

$$SO + O_2 \rightleftharpoons SO_2 + O \qquad (8)$$

$$O + H_2S \rightleftharpoons OH + SH \qquad (9)$$

$$OH + H_2S \rightleftharpoons H_2O + SH \qquad (10)$$

$$SO_2 + O \rightleftharpoons SO_3 \qquad (11)$$

Gaydon[78] agreed with the view[8] that the amount of SO_3 formed would depend on the composition of the flame gases as well as upon concentration of atomic oxygen.

The most likely overall process of formation of SO_3 thus appears to be that proposed by Hedley[12]. Oxygen atoms are reacting with the most easily oxidisable substance available which happens to be SO_2. This results in the formation of excited sulphur trioxide which subsequently collides with a third body to give normal SO_3. This transient quantity of SO_3 is considerably in excess of the equilibrium concentration, and therefore begins to dissociate. The dissociation continues until the theoritical concentration is reached which will be governed by the gas temperature. It would appear that if the gases are kept at a high temperature to allow longer time for the SO_3 to be dissociated, then the SO_3 concentration will be low. Experimental results confirm this hypothesis.

The theory can be represented as:

$$SO_2 + O \xrightarrow{K_1} SO_3 \xrightarrow{K_2} SO_2 + \tfrac{1}{2} O_2 \qquad (12)$$

where K_1 and K_2 are two specific rate constants (units of $K = sec^{-1}$). If we assume that the concentrations of atomic oxygen and sulphur trioxide are small compared with that of sulphur dioxide, we can take the kinetics of the primary process producing SO_3 as those of first order reaction. On similar grounds, the dissociation of SO_3 can also be taken as first order reaction. Thus we have two consecutive first order reactions with the rates dependent solely on (O) and (SO_3) respectively. This case has been treated by Harcourt and Essen[79].

The situation can be represented as

$$A \xrightarrow{K_1} B \xrightarrow{K_2} C$$

Let $[A]_o$ = initial concentration of A

$[B]$ = concentration of SO_3 after time t

$[C]$ = concentration of reaction products after time t

The rate of disappearance of A is given by

$$-\frac{d[A]}{dt} = K_1 [A] \qquad (13)$$

which integrated to

$$[A] = [A]_o e^{-K_1 t} \qquad (14)$$

The rate of formation of C is given by

$$\frac{d[C]}{dt} = K_2 [B] \qquad (15)$$

while the net rate of production of B, which is the rate of its formation from A minus that of its reaction to give C, is

$$\frac{d[B]}{dt} = K_1[A] - K_2[B] \qquad (16)$$

Introduction of equation (14) into equation (16) gives

$$\frac{d[B]}{dt} = K_1[A]_o e^{-K_1 t} - K_2[B] \qquad (17)$$

which contains only the variables B and t. It integrates to

$$[B] = [A]_o \frac{K_1}{K_2 - K_1} (e^{-K_1 t} - e^{-K_2 t}) \qquad (18)$$

substituting $[SO]_3$ for $[B]$, and let a is the initial concentration of atomic oxygen, we get

$$[SO]_3 = a \frac{K_1}{K_2 - K_1} (e^{-K_1 t} - e^{-K_2 t}) \qquad (19)$$

The quantities known from the experimental results which can be substituted in equation (19) are the SO_3 concentrations at various time t along the length of the combustion chamber. The data obviously is not enough for the direct solution of the equation.

However, mathematical method of separation of exponentials derived by Lonzos was used for the determination of K_1, K_2 and a. A detailed solution is given in Appendix 6.

The values obtained for a, k_1, and k_2 from the experimental results are given below:

FIG. 6.7

$k_1 = 11.8\ Sec^{-1}$ $k_2 = 1.24\ Sec^{-1}$

a = 118 p.p.m.

FIG.6.9

$k_1 = 11.52\ Sec^{-1}$ $k_2 = 1.5\ Sec^{-1}$

a = 120 p.p.m.

FIG.6.11

$k_1 = 10.53\ Sec^{-1}$ $k_2 = 1.4\ Sec^{-1}$

a = 128 p.p.m.

An examination of these values show that the rate of formation of SO_3 is approximately eight times the rate of its dissociation.

CHAPTER 8

CALCULATIONS OF THE THEORETICAL PERCENTAGE OXIDATION OF SO_2 TO SO_3 UNDER EQUILIBRIUM CONDITIONS

Consider the formation of sulphur trioxide by reaction of sulphur dioxide and molecular oxygen represented by the equation

$$SO_2 + \tfrac{1}{2} O_2 \rightleftharpoons SO_3 + 22.6 \text{ K cal/g.mol } (\Delta H)$$

This reaction has been extensively studied and Reference (80) gives two equations taken from Bodenstein and Pohl[19] and Kapustinsky and Samovsky[81]. They have related the thermodynamic equilibrium constant K_p with absolute temperature.

(Reference 19) $$\log K_p = \frac{5185.5}{T} + 0.611 \log T - 6.7497 \quad \ldots (1)$$

(Reference 81) $$\log K_p = \frac{5005}{T} - 4.743 \quad \ldots (2)$$

where $$K_p = \frac{p\ SO_3}{p\ SO_2 \times p\ O_2^{\frac{1}{2}}} \quad \ldots (3)$$

$T = {}^{o}K$

and p = atms.

Macfarlane[82] states that there is little to choose between these two sets of sources for obtaining the value of K_p as the difference in the value of K_p from the two sources is 2 per cent at 700°K and 3 per cent at 1500°K.

From equation (3), we have

$$K_p \cdot p\,O_2^{\frac{1}{2}} = \frac{p\,SO_3}{p\,SO_2} \qquad \ldots (4)$$

Here the quotient $\frac{p\,SO_3}{p\,SO_2}$ is independent of the units of measure since they cancel from both the numerator and denomenator. Therefore the units might equally be parts per million instead of partial pressure. The object first is to relate the equilibrium conversion of SO_2 to SO_3 with the availability of oxygen and the thermodynamic equilibrium constant K_p. Multiplying l.h.s. of equation (4) by

$$\frac{p\,SO_2 + p\,SO_3}{p\,SO_2 + p\,SO_3}, \quad \text{we have}$$

$$K_p \cdot p\,O_2^{\frac{1}{2}} \frac{p\,SO_2 + p\,SO_3}{p\,SO_2 + p\,SO_3} = \frac{p\,SO_3}{p\,SO_2} \qquad \ldots (5)$$

$$\text{or} \quad \frac{K_p \cdot p\,O_2^{\frac{1}{2}} \cdot p\,SO_2}{p\,SO_2 + p\,SO_3} = \frac{p\,SO_3}{p\,SO_2 + p\,SO_3} \qquad \ldots (6)$$

Dividing both nomenator and denominator of l.h.s. of equation (6) by $p\,SO_2$, we get

$$\frac{K_p\,p\,O_2^{\frac{1}{2}}}{1 + \frac{p\,SO_3}{p\,SO_2}} = \frac{p\,SO_3}{p\,SO_2 + p\,SO_3} \qquad \ldots (7)$$

Substituting the value of $\frac{p\ SO_3}{p\ SO_2}$ from equation (4) to equation (7), we get

$$\frac{p\ SO_3}{p\ SO_2 + p\ SO_3} = \frac{K_p \times p\ O_2^{\frac{1}{2}}}{1 + K_p\ p\ O_2^{\frac{1}{2}}} \qquad \ldots (\varepsilon)$$

$$\frac{p\ SO_3}{p\ SO_2 + p\ SO_3} = \frac{K_p}{K_p + \frac{1}{p\ O_2^{\frac{1}{2}}}} \qquad \ldots (9)$$

the expression arrived at relates the conversion of SO_2 to SO_3 with the equilibrium constant and the partial pressures. We now calculate quantitively the variation of the per cent conversion with partial pressures of oxygen and temperature.

Let us consider the composition of the fuel by wt. as :

Carbon	83.5% wt.
Hydrogen	13.1% wt.
Sulphur	3.4% wt.

Basic 1g. of fuel :-

Constituent	wt. fraction	g mol/ g fuel	Mol O_2 / g fuel	Products	Mols products/ g fuel
C	0.835	.0694	.0694	CO_2	.0694
H	0.131	.0655	.0327	H_2O	.0655
S	0.034	.00106	.00106	SO_2	.00106
Total			.10316		.13596

Therefore, one 1g. of the fuel would require .10316 g.mol. of O_2.

Composition of dry air (at sea level[84])

oxygen	....	20.99 per cent vol.
carbon dioxide	....	0.03 per cent vol.
nitrogen	....	78.98 per cent vol.

Hence, g mol. atmospheric nitrogen/g fuel

$$= 0.10316 \times \frac{78.98}{20.99}$$

$$= 0.388$$

Therefore, stoichiometric air = .10316 + .388 = .49116 g.mol/g.fuel

Also, wt. of O_2 required/g. fuel = 0.10316 x 32

= 3.3 g

wt. of air required/g fuel = $3.3 \times \frac{100}{23.1}$ = 14.3 g.

At stoichiometric conditions,

quantity of combustion products formed by combustion of 1g. of fuel:

1g. of fuel on combustion produced .0694 g mols of CO_2

also 1g. of fuel on combustion produced .0655 g mols of H_2O

and 1g. of fuel on combustion produced .00106 g mols of SO_2

Therefore, the total combustion products formed, including nitrogen was,

$$= .388 + .0694 + .0655 + .00106$$

$$= 0.52396 \text{ g mols/g fuel.}$$

TABLE 8.1

Excess O_2 % wt.	Excess Air % wt.	Mols excess Air / g fuel	Mols excess O_2 / g fuel	Mols total products / g fuel	$p\,O_2$ atmos.	$p\,O_2^{\frac{1}{2}}$ atmos.
0.11	0.476	0.00234	0.000531	0.52630	0.001029	0.0322
1.1	4.76	0.0234	0.00531	0.54736	0.01029	0.1028
2.2	9.52	0.0468	0.01062	0.53488	0.02058	0.1415
3.3	14.28	0.0702	0.01593	0.53989	0.03087	0.1750
4.4	19.04	0.0936	0.02024	0.54420	0.04116	0.202
5.5	23.80	0.1170	0.02655	0.55051	0.05145	0.227
6.6	28.56	0.1404	0.03186	0.55582	0.06174	0.248
8.8	38.08	0.1872	0.4148	0.56544	0.08232	0.287

TABLE 8.2

From equation (2), $\log K_p = \frac{5005}{T} - 4.74$

Temp. ^oK	$\frac{5005}{T}$	$\log K_p = \frac{5005}{T} - 4.74$	K_p
700	7.15	2.41	257.0
800	6.26	1.52	33.11
900	5.56	0.82	6.61
1000	5.01	0.27	1.86
1100	4.56	$\bar{1}.82$	0.661
1200	4.17	$\bar{1}.43$	0.269
1300	3.85	$\bar{1}.11$	0.129
1400	3.58	$\bar{2}.84$	0.0692
1500	3.34	$\bar{2}.60$	0.0398
1600	3.13	$\bar{2}.39$	0.0246

TABLE 8,3

Temp. ^{o}K	$K_p \; p\,O_2^{\frac{1}{2}} = \frac{p\,SO_3}{p\,SO_2}$							
	% wt. excess oxygen							
	0.11	1.1	2.2	3.3	4.4	5.5	6.6	8.8
700	8.28	26.5	36.5	45.0	52.0	58.4	63.8	73.9
800	1.065	3.405	4.69	5.8	6.7	7.51	8.21	9.5
900	0.213	0.679	0.937	1.16	1.335	1.50	1.64	1.9
1000	0.0558	0.191	0.263	0.326	0.379	0.422	0.461	0.534
1100	0.0213	0.068	0.0935	0.1160	0.135	0.150	0.164	0.190
1200	.00866	0.0277	.0381	0.0471	0.0555	0.0611	0.0667	0.0774
1300	.00415	0.0132	0.0183	0.0226	0.0263	0.0293	0.0320	0.0370
1400	.00223	.0071	0.00980	0.0121	0.0141	0.157	.0172	0.0199
1500	.00128	.00409	0.00563	0.00695	0.0081	0.00904	.00987	0.0114
1600	.000792	.00253	0.00348	0.0043	0.00502	0.00559	.0061	.00706

TABLE 8.4

Temp. ^{o}K	$\left[\frac{K_p \cdot p\,O_2^{\frac{1}{2}}}{1 + K_p \cdot p\,O_2^{\frac{1}{2}}}\right] 100 = \left[\frac{p\,SO_3}{p\,SO_2 + p\,SO_3}\right] \times 100$							
	% Excess oxygen							
	0.11	1.1	2.2	3.3	4.4	5.5	6.6	8.8
700	89.5	96.1	97.4	97.9	98.4	98.4	98.4	98.6
800	51.4	77.4	82.5	85.3	87.0	88.2	89.4	90.5
900	17.6	40.4	48.5	53.7	57.2	60.0	62.0	65.4
1000	5.29	16.0	20.8	24.5	27.5	29.6	31.5	34.7
1100	2.08	6.38	8.54	10.5	11.9	13.0	14.1	16.0
1200	0.866	2.70	3.68	4.5	5.2	5.75	6.25	7.2
1300	0.415	1.30	1.80	2.20	2.56	2.85	3.10	3.58
1400	0.223	0.71	0.98	1.20	1.40	1.55	1.69	1.95

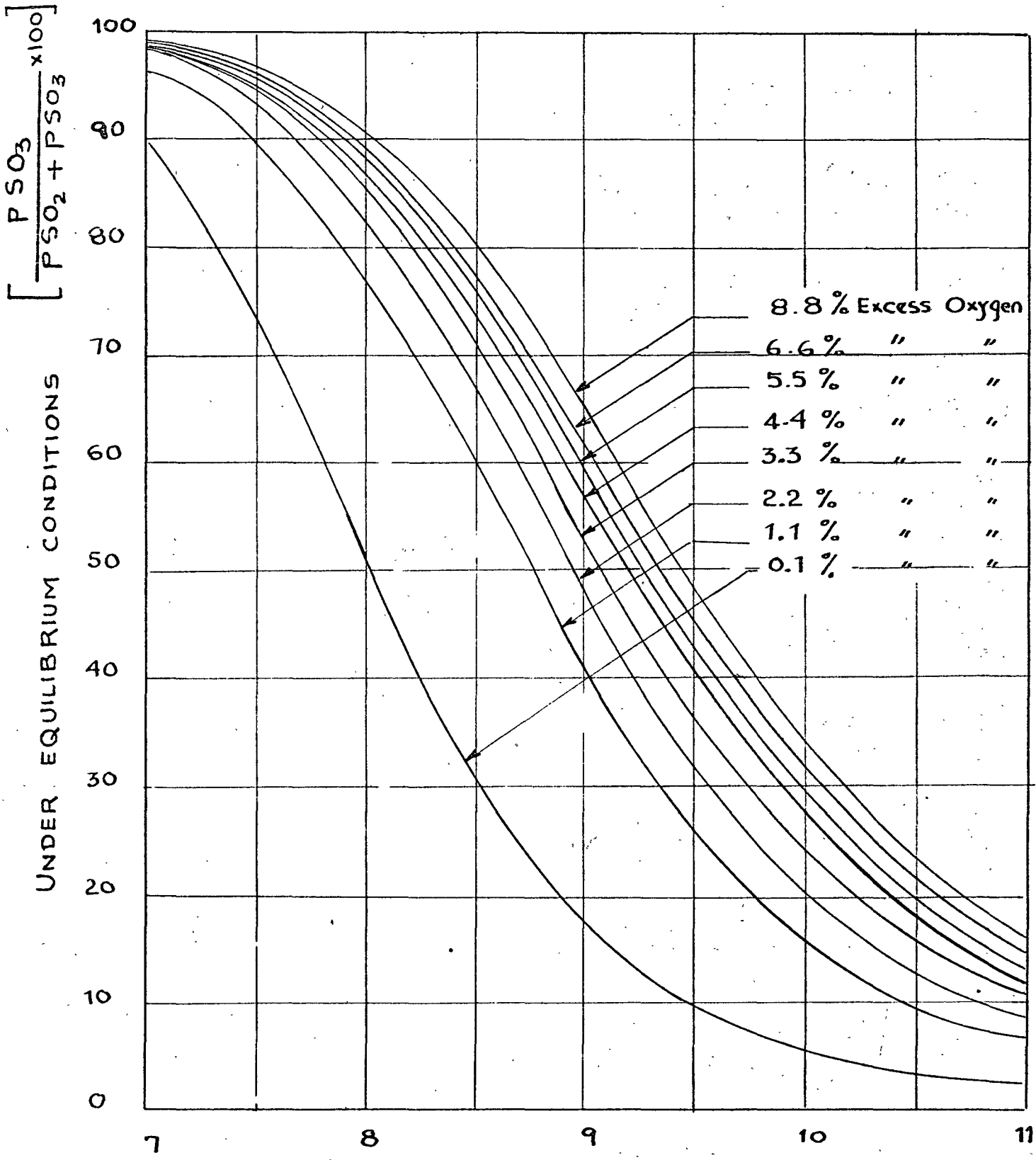

FIG. 8.1 The Effect Of Temperature And Excess Oxygen On The Theoretical Oxidation Of SO_2 to SO_3 Under Equilibrium Conditions.

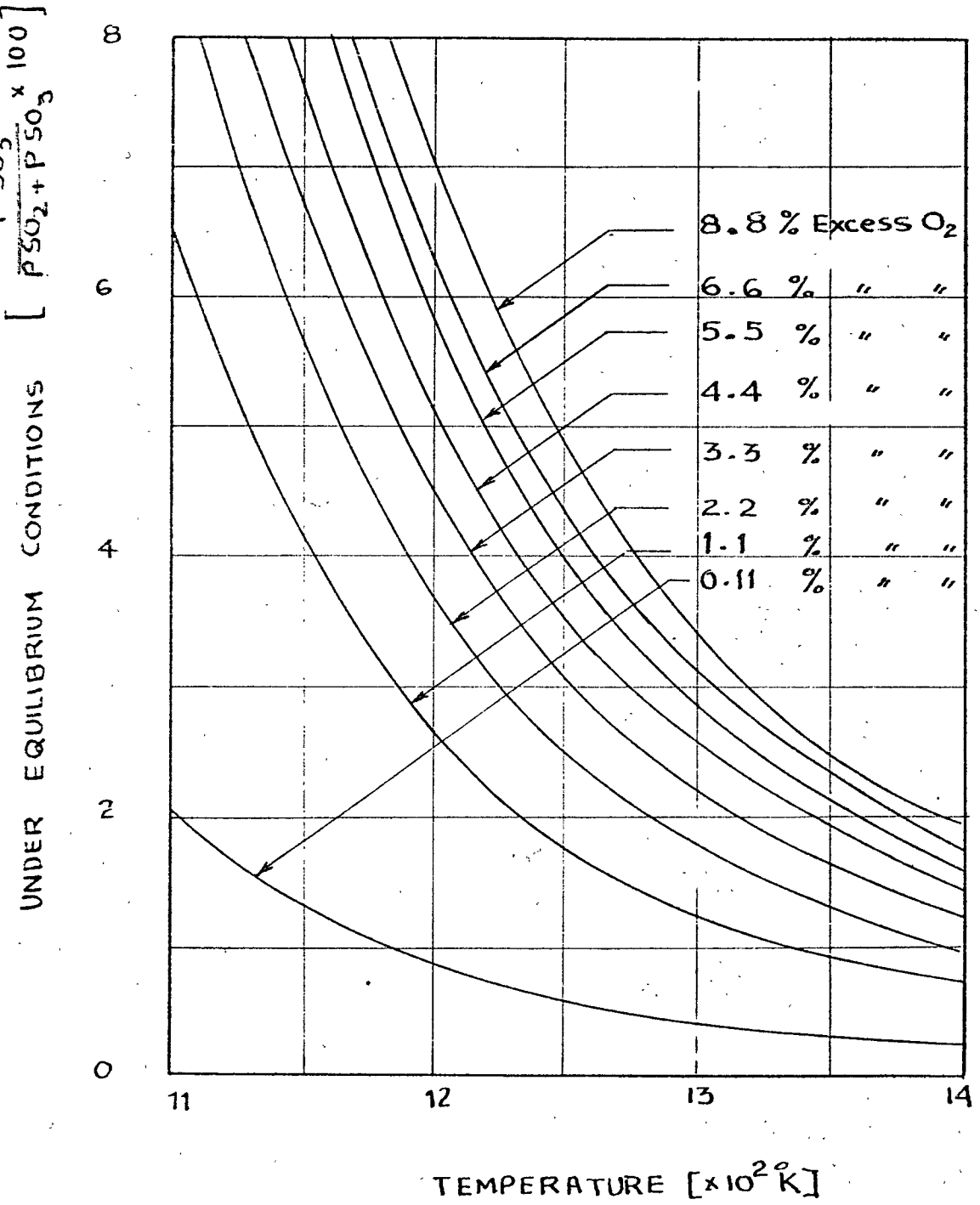
UNDER EQUILIBRIUM CONDITIONS [$\frac{P_{SO_3}}{P_{SO_2}+P_{SO_3}} \times 100$]
8
6
4
2
0
11
12
13
14
8.8 % Excess O_2
6.6 % " "
5.5 % " "
4.4 % " "
3.3 % " "
2.2 % " "
1.1 % " "
0.11 % " "
TEMPERATURE [$\times 10^2$ °K]

FIG. P.1.(Cont'd.)

PART II

CHAPTER 9

EXPERIMENTS ON IGNITION DELAY MEASUREMENTS

9.1 INTRODUCTION

This chapter deals with the study of ignition delay time of the different fuels used in the previous experiments. The ignition delay time or simply the Ignition Delay is termed as the time lapse between the introduction of a fuel droplet into a heated atmosphere and its eventual ignition.

The need for the measurement of ignition delays of individual liquid fuels has been discussed earlier. Techniques used for the measurement of ignition delay was similar in principle to that used by Satcunanathan and Zaczek.[87]

9.2 Description of Apparatus

The general arrangement of the apparatus and associated equipments are shown in Plate 9.1.

9.2.1 Electric furnace and heated surface

The apparatus used in the investigation is shown in Fig. 9.1. The electric furnace consisted of a vertically placed stainless steel cylindrical tube closed at the bottom and heated by means of an insulated electrical heating coil. The cylinder was then placed in a cubical asbestos chamber filled with asbestos wool. This was done to protect

associated equipment from heat of the furnace. Temperature of the furnace was controlled through a voltage regulator. The flat machined surface of the bottom of the chamber acted as a 'heated surface' on which fuel droplets under test were allowed to fall. A cover 50mm diameter, machined from stainless steel fitted over the top of the cylinder and was securely fixed by means of a screw. The enclosed cylinder served as an 'ignition space'. A stainless steel tube was fitted to the cover. The top end of the tube was connected through a stop valve to compressed air supply for purging combustion products after ignition. Three more holes were drilled in the top cover, a central one 5mm in diameter for the introduction of fuel droplets, a second one 3mm diameter and 10mm from the centre for the introduction of thermocouple and one 5mm diameter and 10mm from the centre on the other side for the detection of explosion.

9.2.2 Fuel Container and Droplet formation

Fuel container consisted of a 50 cm^3 graduated burette as shown in Fig. 9.1 and the arrangement is also shown in Plate 9.1. The end of the burette was surrounded by a cooling chamber with inlet and outlet openings for allowing cooling water to flow through the chamber to maintain a constant temperature of the fuel. The temperature of the fuel at the tip of the burette would rise due to its proximity with the furnace. It was found that consistent results was achieved when droplets collected near the end of the burette were

discarded and fourth or fifth droplet was used for test. The wt. of a single droplet was determined by collecting a known number of droplets and then weighing them on a torsion balance. The fuel height in the burette was kept constant by filling in more fuel under test after every successive experiment.

9.3 Temperature Measurement

The temperature of the surface of the bottom of the chamber was measured by means of Ni Cr/Ni Al thermocouple attached to an electronic thermometer supplied by COMARK of Type 1602 and of range - 120°C to 1100°C in 12 steps of 100°C. The thermocouple was so placed as to make contact with the bottom surface of the cylindrical chamber.

9.4 Ignition Delay Measurement

The ignition delay i.e. the time lapse between the introduction of the fuel droplets through the central hole of the cover into the 'combustion space' and its eventful ignition was measured by means of a Venner Digital Trimmer triggered by two photo-transistor circuits. The circuit diagram is shown in Fig. 9.6.

A fuel droplet just before entering the furnace breaks a beam of light focussed on a photo-transistor and sends an impulse to the digital counter as a short impulse. The drop of fuel ignites in the hot chamber and a small explosion occurs. This sends a pressure signal through another opening in the

furnace cover thereby deflecting a very light shutter (made of a thin sheet of aluminium) pivoted in such a manner that it interrupts another light beam focussed on a second photo-transistor and an impulse is relayed to the counter as a stop pulse.

Main errors involved in the measurement of ignition delay time could be classified as follows:-

a) response time of the electrical circuits,

b) the time taken by the droplet to reach the surface after breaking the 'starting beam of light',

c) the response time of shutter after ignition and explosion had occurred.

Two relays were employed in the trigger circuit. Since both relays reacted subsequent to the breaking of the corresponding light beams and assuming the reaction time for both relays were the same, the errors would cancel out. The time taken by the fuel droplet to reach the surface after breaking the 'starting beam' would be the same for every test and as the study was concerned with the relative values of ignition delay times, results were not effected. The error involved in the response time of the pointer was difficult to evaluate but here again, it did not effect the relative ignition delay values, assuming the response time was the same in every case. However to minimise this error, the pointer was made of a thin tin foil and was sensitive to even a minor below of air.

9.5 Experimental Procedure

Temperature of the combustion space was raised at a rapid rate initially until a liquid fuel droplet started igniting when allowed to fall in the space. After locating this temperature approximately which was found to be about 380°C for Kerosine droplets, the current supply to the heater was reduced to lower the temperature of the 'heated surface'. The temperature was then raised gradually and the rise in temperature was recorded. When steady conditions were reached and no change in temperature was observed, a fuel droplet was admitted and ignition delay time was noted in the digital timer. After each droplet, the ignition space was scavenged by means of compressed air flowing through the chamber. This brought down the temperature inside the chamber by a few degrees of centigrade. The air supply was then closed and the temperature of the 'heated surface' was again allowed to stabilize for about 5 minutes. Fuel droplets collected near the tip of the burette was drained and the tip now contained fresh cooler fuel from above. Another test was conducted by introducing another fuel droplet into the chamber, and ignition delay time and the surface temperature of the chamber was noted. The above procedure was repeated until the temperature of the heated surface was raised to about 700°C. The same procedure was carried out for decreasing surface temperature and the values shown are the mean of the two values.

9.6 Experimental Programme

The following experimental programme was decided:

1) Determination of ignition delay curve for Kerosine droplets with respect to change in the surface temperature of the chamber.

2) Determination of ignition delay vrs surface temperature of hydrocarbons used in the previous programme of experiments (Part I), namely Cyclohexane, n-hexane, and n-Pentane.

3) Determination of minimum ignition temperature of Kerosine, Cyclohexane and n-Pentane and comparison with the results of other workers.

It was decided to investigate the ignition delay curve for Kerosine most thoroughly and to make this curve as a basis for comparison with the curves of other hydrocarbons used. Appropriate amount of carbon-disulphide (CS_2) was added in each fuel under investigation to make it 3.4% S(wt).

9.7 Experimental Results

The results obtained of the ignition delays with varying surface temperatures are shown in Fig. 9.3. The curve of ignition delay for Kerosine droplets covered the whole range of ignition, i.e., the lowest temperature at which ignition was obtained to the highest temperature possible under the limit of experimentation. Fig. 9.4 shows the results obtained

for cyclohexane, n-hexane and n-Pentane and also includes the curve for Kerosine obtained earlier. Table 9.1 shows the spontaneous ignition temperature of Kerosine, cyclohexane, n-hexane and n-Pentane obtained experimentally and it compares the results of other workers.

9.8 Discussion

Before the results can be discussed, the behaviour of droplets on a hot surface is considered here. Fig. 9.2 shows a typical curve obtained by Tamura and Tanasawa[85], in the form of lifetime of droplet versus surface temperature. This has been discussed in detail elsewhere[86]. Three distinct regions are recognised, namely contact evaporation stage from θ_0 to θ_1, transition stage from θ_1 to θ_2, and spheriodal evaporation stage from θ_2 to θ_3. (These notations are introduced to denote specific points on the life curves). It is argued that up to θ_1 evaporation takes place by physical contact of the liquid with the hot surface. From θ_1 to θ_2 boiling takes place and θ_2 is the maximum boiling rate point, and θ_3 is the Leidenfrost point, after which the droplet evaporates in spheroidal state and spheroidal evaporation stage begins.

The data of reference[85] was used by Satcunanathan to obtain values of θ_1, θ_2 and θ_3, and these values when plotted against θ_B (the boiling point) gave linear relationship.

The equations to these straight lines are given below

$$\theta_1 = (1.055\ \theta_B + 6)\ ^{o}C$$

$$\theta_2 = (1.156\ \theta_B + 27)\ ^{o}C$$

$$\theta_3 = (1.4\ \theta_B + 78)\ ^{o}C$$

where θ_B = the boiling point of the liquid.

Taking the above theory as a guide line, there appears to be obvious resemblance between the ignition delay-temperature curve shown in Fig. 9.3 and the lifetime curve shown in Fig. 9.2. The results show that the ignition delay is critically dependent on the temperature of the heated surface. It decreases initially, reaching a minimum at a temperature near maximum boiling rate point. The ignition delay then increases with rise in temperature of the heated surface reaching a maximum, and then decreases with the rise in temperature of the heated surface. This pattern was possible to achieve only with Kerosine droplets. The ignition delay curves of hydrocarbons, cyclohexane, n-hexane and n-Pentane exhibit no such definite characteristics. This had been earlier predicted[86,87], and the results appear to be in complete agreement.

Careful study and comparison of the curves of the ignition delay v. surface temperature of light hydrocarbons with that of Kerosine show that after a temperature of say 500°C, the rate of decrease of ignition delay is slower with Kerosine than with light hydrocarbons. This can be more clearly seen in Fig. 9.4.

The purpose of the whole exercise was to determine whether fuels producing less SO_3 compared to Kerosine have shorter ignition delays. It can be seen that fuels, viz. cyclohexane, n-hexane, and n-Pentane, those that produced less SO_3 have steeper slope of their ignition delay curves compared with Kerosine. It is therefore reasonable to expect that these fuels have shorter ignition delays compared with those of Kerosine at temperatures prevailing in flames.

Here it may be pointed out that magnitude of ignition delay may differ with a change in the form of apparatus and other conditions. However the shape of the curves is not expected to vary as was proved in the case of Kerosine droplets. The measurement of ignition delay at higher temperatures was not possible due to the difficulty in minimizing response time, and other techniques are under consideration for future research. The general shape of the curves of different fuels can give an indication of the likely values of ignition delays at higher temperatures. Thus fuels having steeper slope of ignition delay curve compared with Kerosine will be expected to have less SO_3 formation on combustion than Kerosine.

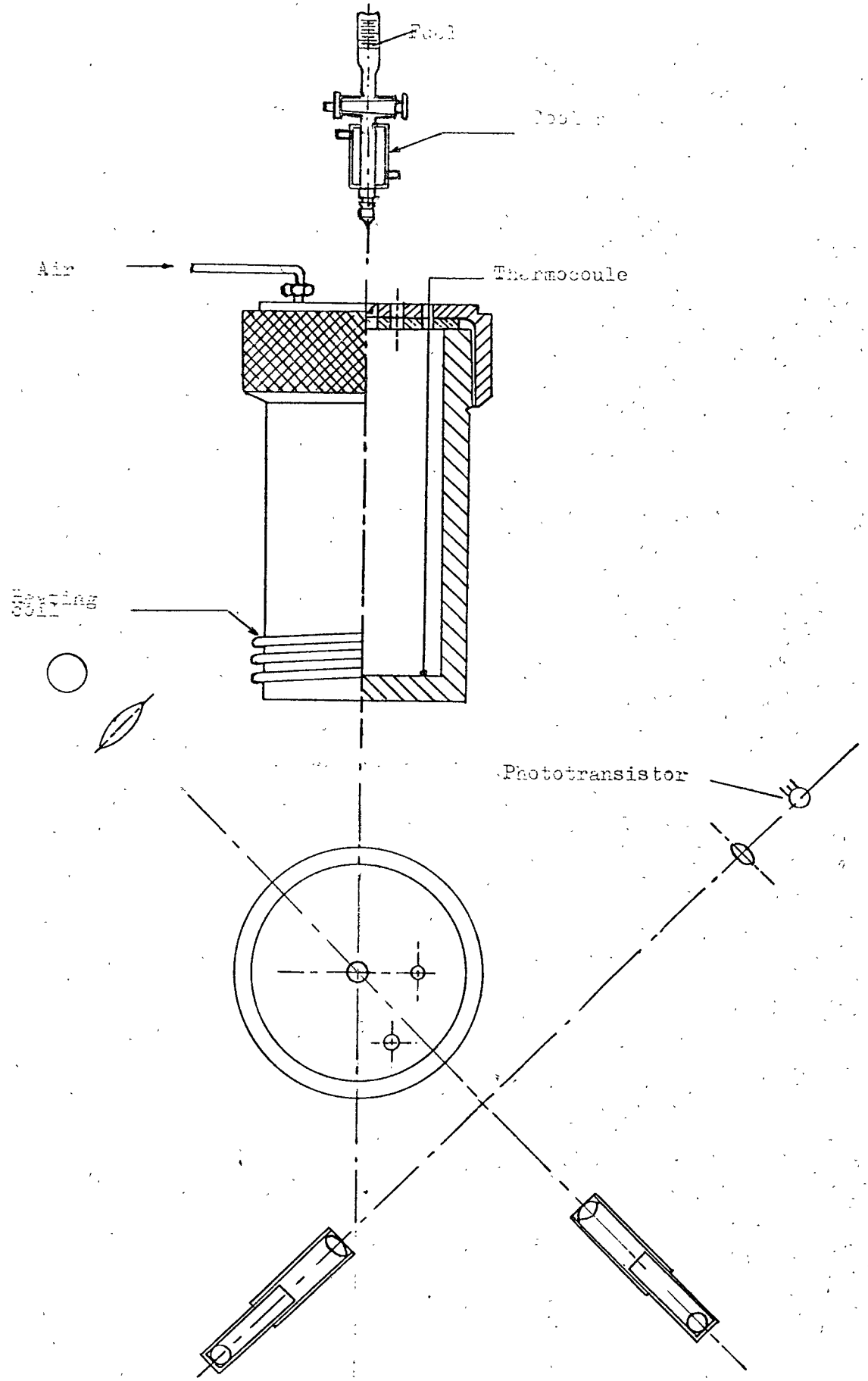

Fig. 3.1. Diagrammatic View Of Apparatus.

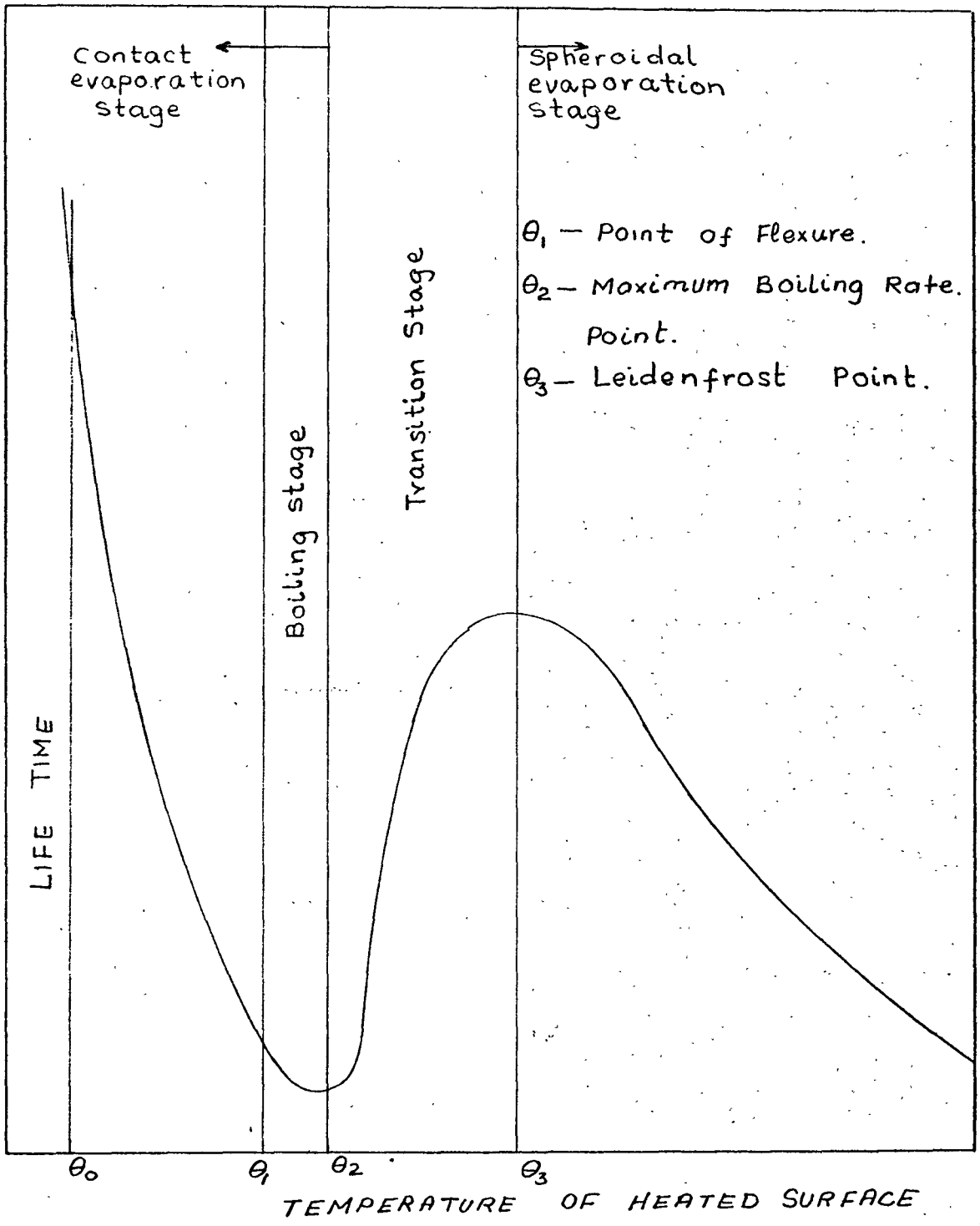

FIG. 9.2. Typical life curve of a droplet evaporating on a heated surface.

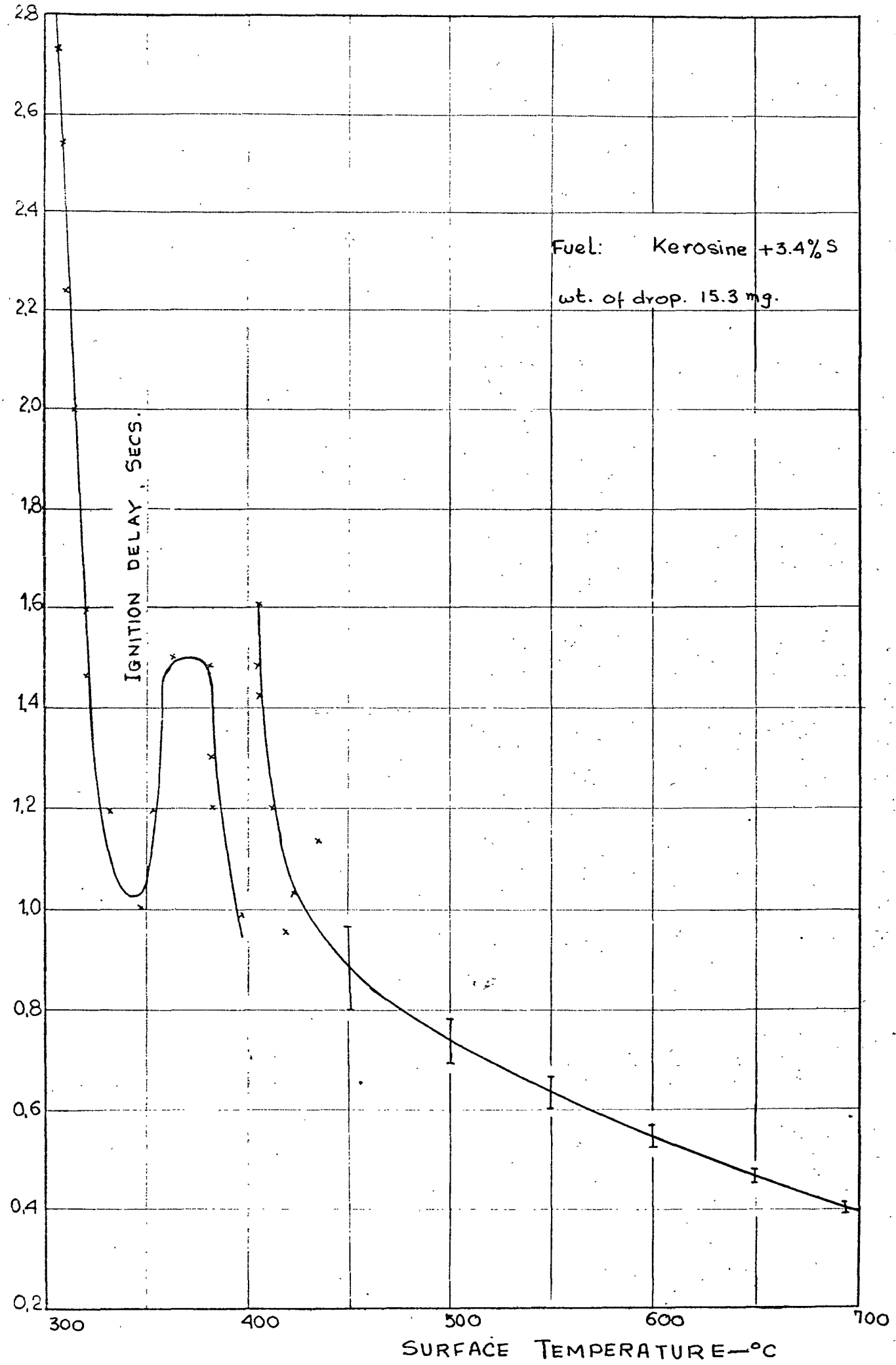

FIG. 9.3. Variation of ignition delay with surface temperature

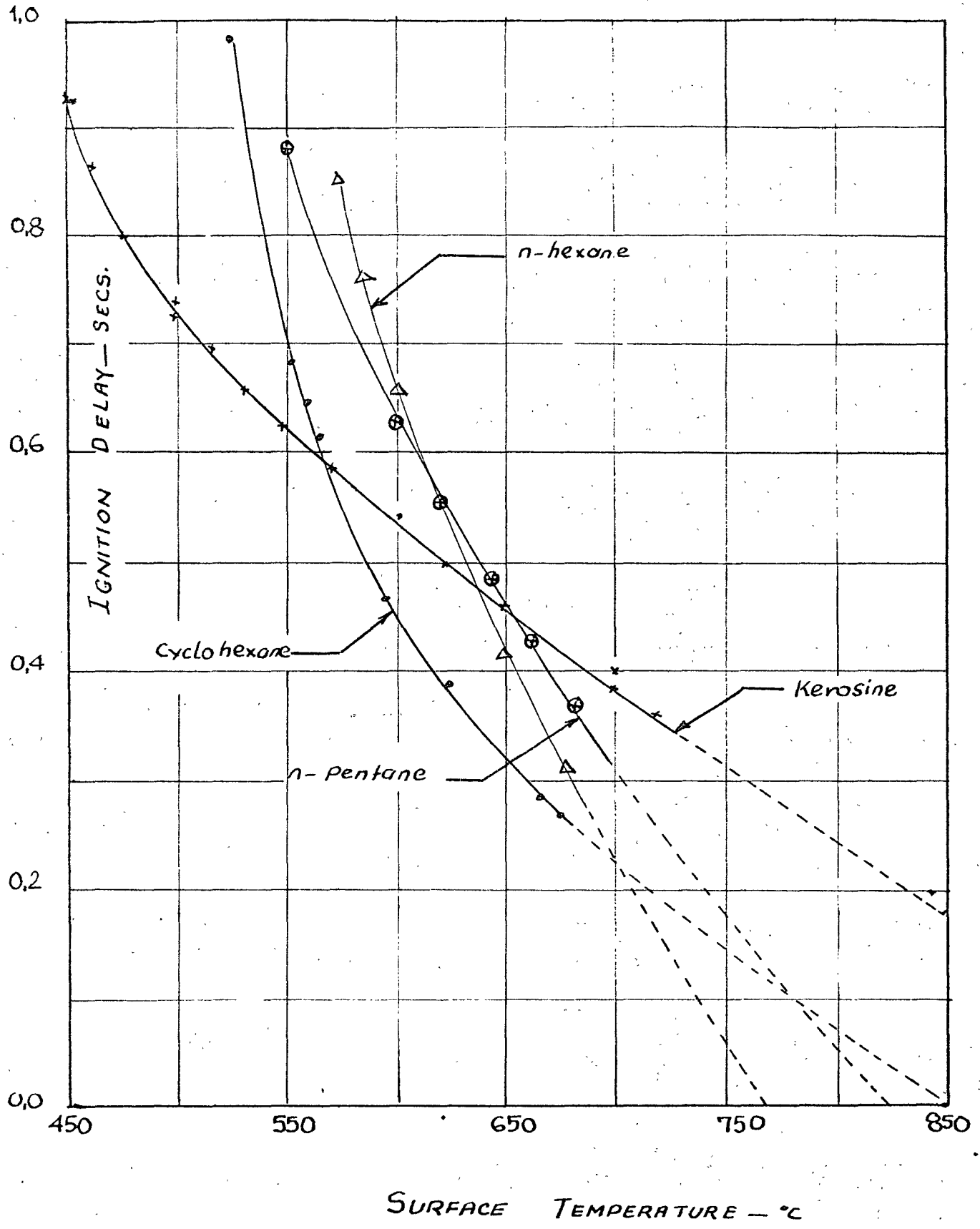

FIG. 9.4. Variation of ignition delay with surface temperature for various fuels.

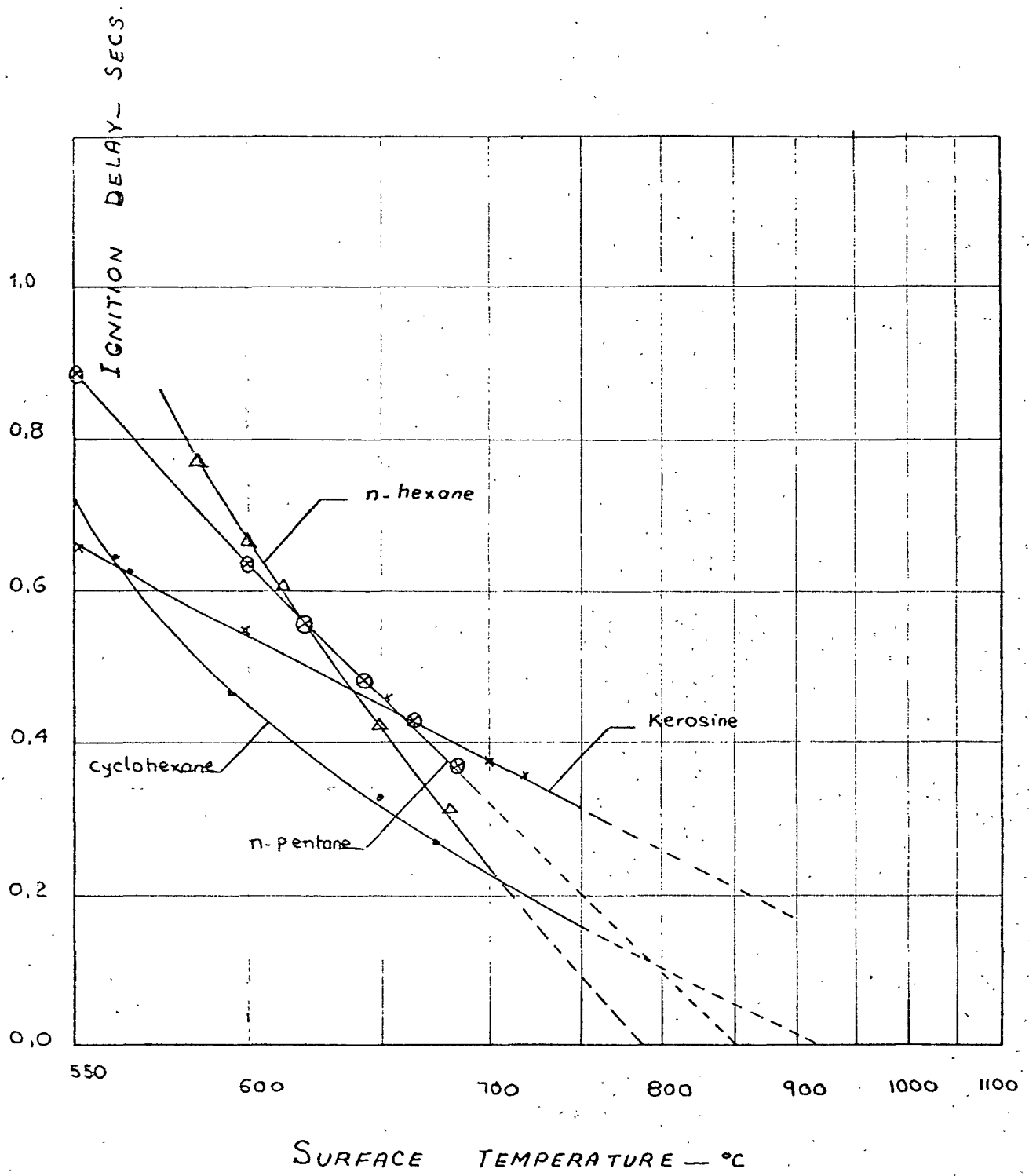

FIG. 3.3. Ignition delay Vs 1n (surface temperature)

FIG. 9.6

Circuit diagram for light operated switches controlling Timer.

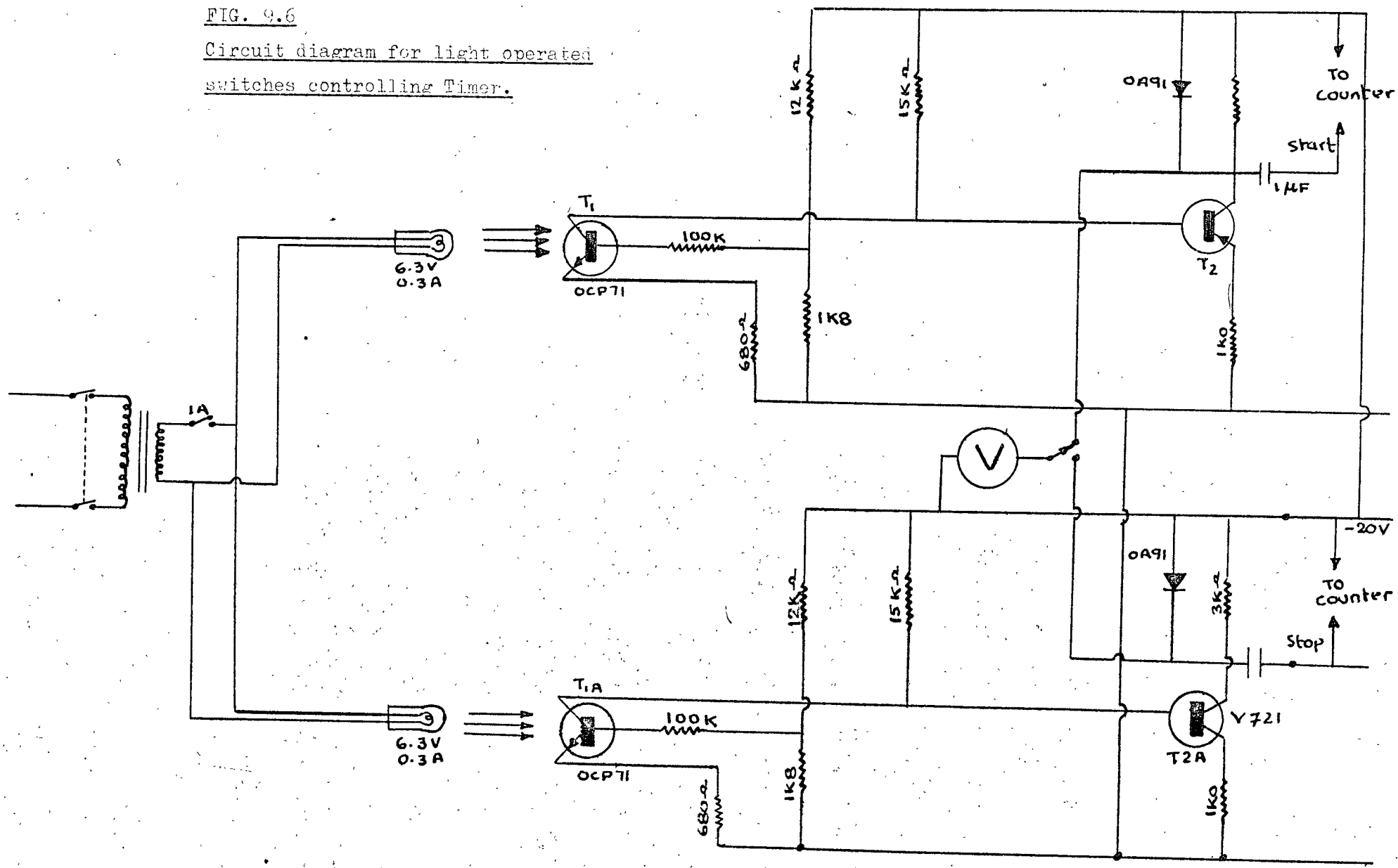

TABLE 9.1

Physical and combustion properties of fuels used in the experiments

Fuels	Formula	Molecular Weight	Specific gravity at 15°C	Boiling Point* range (95%) °C	Spontaneous ignition temperatures			
					Ref.(1)	Ref.(2)	Ref.(3)	Ref.(4)
Kerosine	-	-	0.79	160-290	254	-	295	260
Cyclohexane	$CH_2(CH_2)_4CH_2$	84.16	0.776	80-82	-	510	516	512
n-hexane	$CH_3(CH_2)_4CH_3$	86.18	0.670	67-70	248	500	478	482
n-pentane	$CH_3(CH_2)_3CH_3$	72.15	0.625	35-37	290	510	-	523

Reference (1) - Scott, G.S., Jones, G.W., and Sctt, F.E, Analytical chemistry, 1948, 20 , 238.

Reference (2) -Townend and Maccormac, J. Inst. Pet., 1939, 25 . 495.

Reference (3) - Satcunanathan,S.,

(4) - Author

* Technical Data on Fuel - Spiers, H.M.

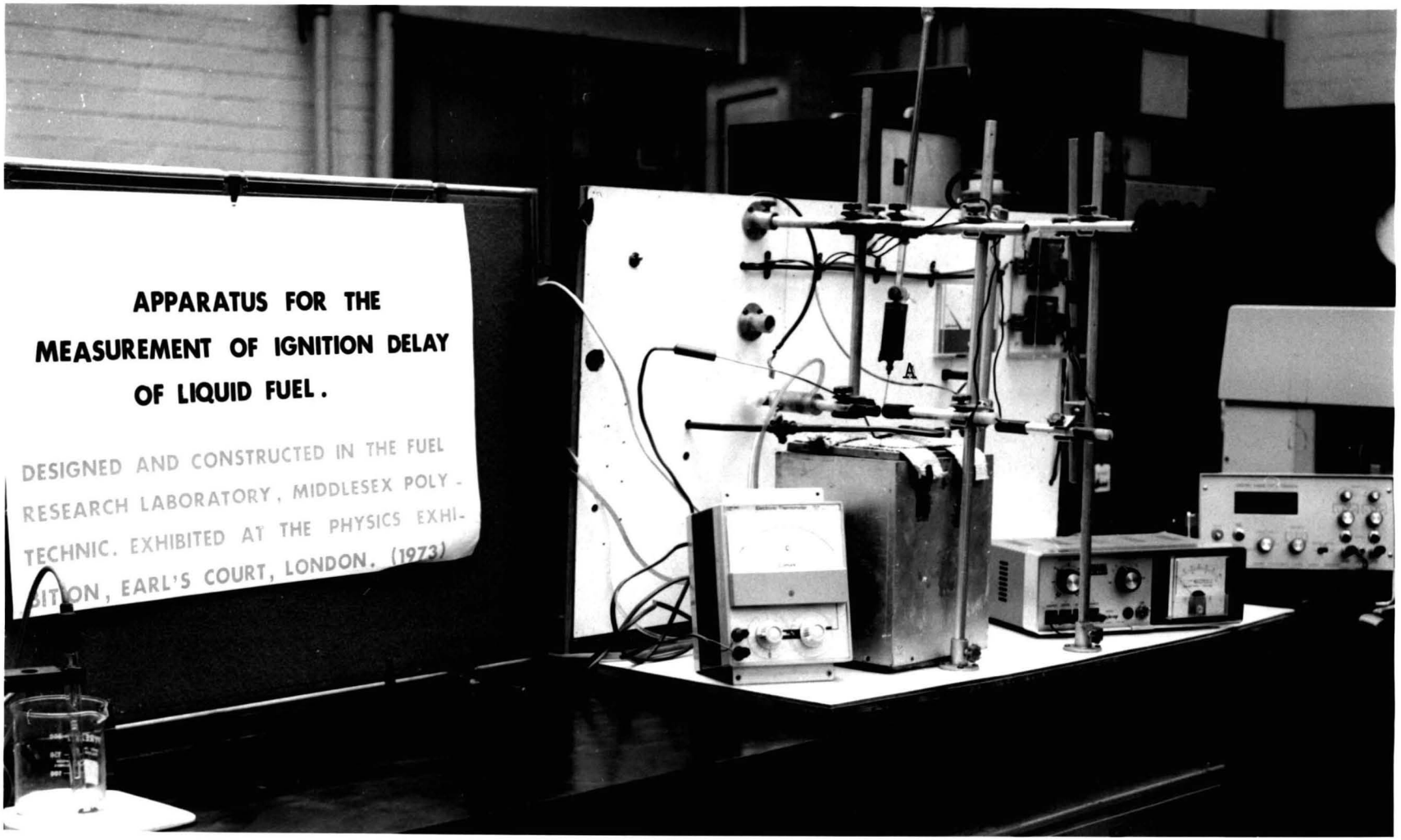

PLATE 9.1 General Arrangement of the apparatus.

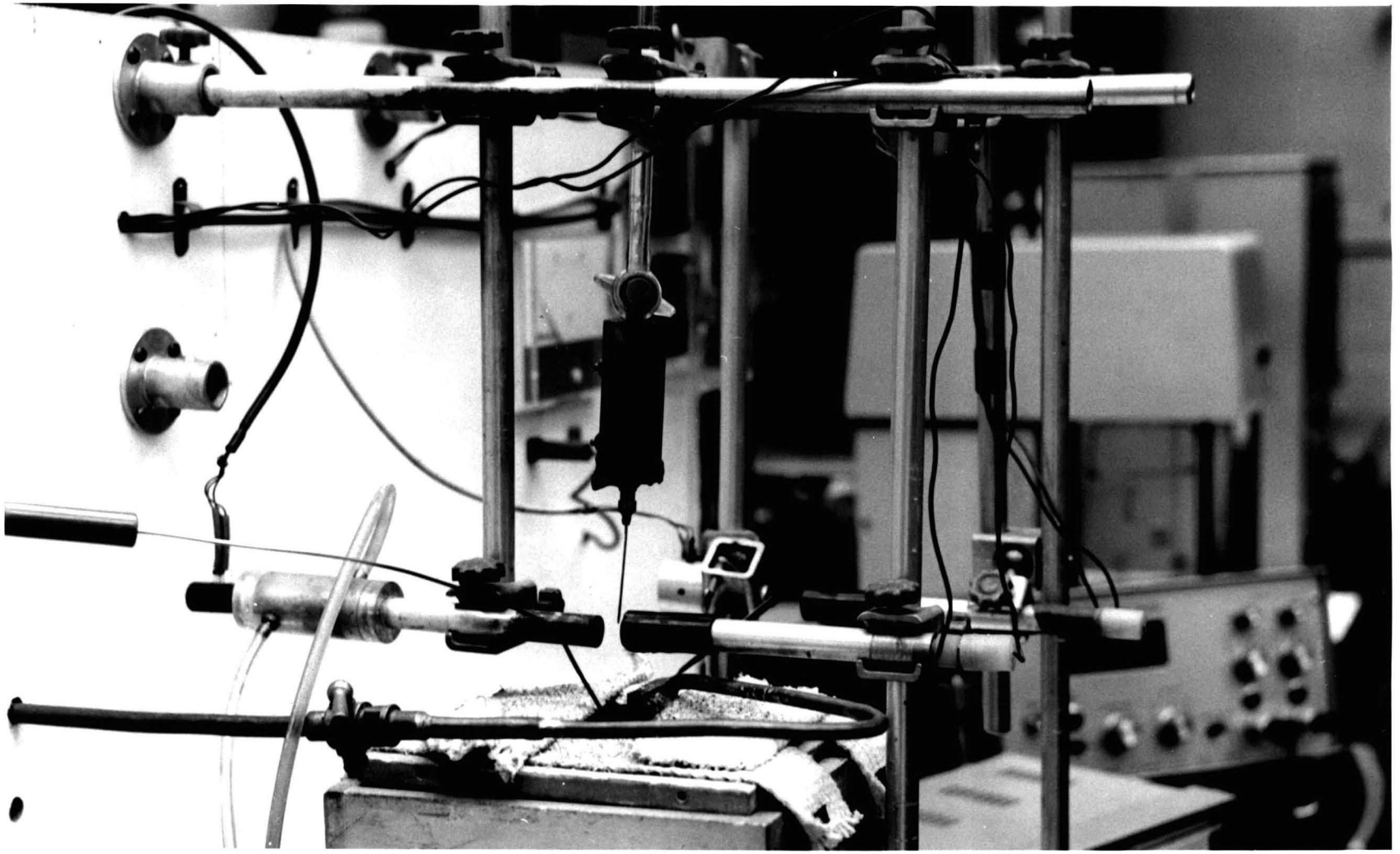

PLATE 9.2 Enlarged view of (A) (Plate 9.1).

CHAPTER 10

CONCLUSIONS

The mechanism of formation of sulphur trioxide in combustion gases produced during combustion of liquid fuels bearing sulphur has been investigated. A laboratory combustor was designed and constructed when this phenomena was studied using a pre-mixed flat flame eliminating physical effects of evaporation and mixing in the combustion zone. Thus it was possible to investigate purely chemical effects on the formation of SO_3. No results have so far been published when formation of SO_3 was studied under these conditions. By the use of a laboratory combustor, the phenomena was studied in an actual combustion system, and therefore the results reported can be applicable in the field of combustion.

The effect of ignition properties of fuel on the formation of sulphur trioxide has also not been reported previously, and therefore the present work breaks new ground in the field of combustion.
It was found that hydrocarbons producing less sulphur trioxide on combustion compared with burning of Kerosine (having same level of sulphur content and under identical combustion conditions) have steeper slope of their ignition delay curves and thus shorter ignition delay times near temperatures prevailing in flames compared with those of Kerosine. It was also found that the hydrocarbon which produced least amount of sulphur trioxide on combustion has the highest slope of its ignition delay curve. (See Fig. 9.5).

Based on the results of these studies, the following main conclusions can be derived :-

1. Reduction of combustion air in excess of stoichiometric requirements had a marked effect on the formation of SO_3. When combustion takes place under fuel rich conditions, SO_3 formation ceases.

2. Level of SO_3 content in the flue gases reaches a maximum at about 4% excess oxygen concentration in the combustion gases after which it starts declining.

3. It has been noticed that ignition properties of hydrocarbons have a considerable effect on the oxidation of sulphur dioxide to sulphur trioxide. It was found that hydrocarbons of lower ignition delay properties and having steeper slope of ignition delay versus surface temperature curve produced less SO_3 on combustion. This evidence supports the view that primarily it is the combination of atomic oxygen with sulphur dioxide in the flame which governs the formation of sulphur trioxide.

4. The results obtained of SO_3 concentration with respect to residence time supports consecutive reaction theory, i.e.

$$SO_2 + O \xrightarrow{K_1} SO_3 \xrightarrow{K_2} SO_2 + \tfrac{1}{2} O_2$$

where K_1 and K_2 are specific rate constants (unit of $K = sec^{-1}$).

This assumes a process in which sulphur is formed as a result of the combination of sulphur dioxide and atomic oxygen. Sulphur trioxide thus formed, dissociates into sulphur dioxide and molecular oxygen. The rate of formation of SO_3 has been found to be nearly eight times that of its dissociation.

5. The reduction of SO_3 in the system can be brought about by the introduction of any substance that can mop up atomic oxygen near the flame zone or change the ignition characteristic of the fuel used by initiating early reactions.

CHAPTER 11

APPENDIX 1

I. Calculation of stoichiometric air/fuel ratio

Combustion Reactions :

$$C + O_2 \longrightarrow CO_2$$

$$12g\ C + 32g\ O_2 \longrightarrow 44g\ CO_2$$

or per gram of carbon (fuel),

$$1g\ C + 2.67g\ O_2 \longrightarrow 3.67g\ CO_2$$

Similarly, for the combustion of Hydrogen and Sulphur,

$$H_2 + \tfrac{1}{2} O_2 \longrightarrow H_2O$$

$$1g\ H_2 + 8g\ O_2 \longrightarrow 9g\ H_2O$$

and

$$S + O_2 \longrightarrow SO_2$$

$$1g\ S + 1g\ O_2 \longrightarrow 2g\ SO_2$$

On mass basis, the combustion equation for carbon is as follows considering oxygen is taken from atmosphere,

$$1g\ C + 2.67g\ O_2 + 8.83g\ N_2 \longrightarrow 3.67g\ CO_2 + 8.83g\ N_2$$

Therefore, the theoretical amount of air required to burn 1g of C = 2.67 + 8.83 = 11.5g ;

to burn 1g of Hydrogen, amount of air required = 34.5g ;

and to burn 1g of Sulphur, amount of air required = 4.31g.

(a) Fuel - Diesel Oil.

The chemical composition of the fuel after doping with carbon disulphide to raise sulphur content was as follows :

Carbon	83.6%
Hydrogen	13.0%
Sulphur	3.4%

Basis 1g of fuel.

Combustion of 0.836g C requires 0.836 x 11.5 = 9.63g of air.

Combustion of 0.13g of H_2 requires 0.13 x 34.5 = 4.49g of air.

Combustion of 0.034g S requires 0.034 x 4.31 = .147g of air.

Therefore, the combustion air required for stoichiometric burning = 14.27g of air.

Air/Fuel mass ratio for stoichiometric burning = 14.27

(b) Fuel - Kerosine.

Carbon	83.2%
Hydrogen	13.4%
Sulphur	3.4%

The combustion air required for stoichiometric burning is 14.34g per g of fuel.

II. Calculation of composition of fuel from a typical exhaust gas analysis

Fuel: Kerosine

Exhaust gas analysis

CO_2	11.7
CO	NIL
O_2	4.6
SO_2	0.17
Balance N_2	83.54

Consider 100 moles of dry exhaust gases and let 100 X moles of air be used with the fuel.

The combustion equation is :

$$a\,C + b\,H_2 + c\,S + 21\,X\,O_2 + 79\,X\,N_2 = 11.7\,CO_2 + 4.6\,O_2 + 83.54\,N_2 + d\,H_2O + 0.17\,SO_2$$

By molar balance,

Carbon	a	=	11.7
Hydrogen	b	=	d
Oxygen	21 X	=	$11.7 + 4.6 + \frac{d}{2} + 0.17$
Nitrogen	79 X	=	83.54
Sulphur	C	=	0.17

Solving these equations, we get

$$X = 1.06 \; ; \quad \text{and} \quad d = 11.66$$

Therefore, the mass analysis of the fuel,

$$\text{Carbon} = \frac{11.7 \times 12}{11.7 \times 12 + 11.66 \times 2 + 0.17 \times 32} = 83.10\%$$

Hydrogen = 13.7%

Sulphur = 3.2%

III. Calculation of exhaust gas composition from a typical reading of air and fuel supply.

Fuel: Diesel Oil.

Rate of fuel flow = 2.55cc/min. = 2.55 x 0.84

= 2.14g/min.

where density of fuel = 0.84 at 15.5°C

Rate of air flow = 29 lit/min. at N.T.P.

= 29 x 12.93 x 10^{-1} g/min = 37.5g/min.

where density of air at N.T.P. = 12.93 x 10^{-4} g/cc

Air/Fuel mass ratio = 17.5

$\therefore$ X = $\frac{17.5}{28.96}$ = 0.604

where X is moles of air supplied per g of fuel.

Composition of fuel being:

C, 83.6% ; H, 13.0% ; S, 3.4%

The combustion equation is:

$$\frac{0.836}{12}(C) + \frac{0.13}{2}(H_2) + 0.21\,X\,(O_2) + 0.79\,X\,(N_2) + \frac{0.034}{32}(S) = a\,(CO_2) + H_2O + d\,(O_2) + f\,(N_2) + e\,(SO_2)$$

By molar balance,

C Balance a = $\frac{0.836}{12}$ = 0.0697

H_2 Balance b = $\frac{0.13}{2}$ = 0.065

O_2 Balance $\quad 0.21X = a + \frac{b}{2} + d + e$

S Balance $\quad e = \frac{0.034}{32} = .00106$

N_2 Balance $\quad f = 0.79\ X$

From these equations,

$d = .02324$; $f = .477$

$\therefore \quad \sum a + d + f + e = .571$

$\therefore$ % CO_2 in the dry flue gases $= \frac{.0697}{.571} = 12.2\%$

% O_2 in the dry flue gases $= \frac{0.02324}{0.571} = 4.07\%$

% SO_2 in the dry flue gases $= \frac{.00106}{.571} = 0.185\%$

Experimental values :

$CO_2 = 11.9\%$

$O_2 = 4.1\%$

$SO_2 = 1610$ p.p.m.

IV. Sample calculation for residence time of combustion gases.

Say fuel used is Kerosine and the rate of flow = 2.14×10^{-3} kg/min. From 'spiers' combustion gases at $0^{o}C$ and 760 mm Hg produced on burning Kerosine with stoichiometric are 12.13 m^3 per kg of fuel.

Therefore, combustion gases produced at

N.T.P. = $12.13 \times 2.14 \times 10^{-3}$ m^3/min.

= 26×10^{-3} m^3/min.

Theoretical combustion air required for burning 1kg of Kerosine at N.T.P. = 11.35 m^3 (spiers)

at 20% excess air = 11.35×0.2

= 2.27 m^3/kg of fuel

Actual excess air = $2.27 \times 2.14 \times 10^{-3}$ m^3 = 4.85×10^{-3} m^3 (N.T.P)

Total volume of combustion gases using 20% excess air

= $(26 + 4.85) \times 10^{-3}$ m^3 at N.T.P.

= 30.85×10^{-3} m^3 at N.T.P.

Volume of combustion gases at $600^{o}C$ (say),

= $30.85 \times 10^{-3} \times \frac{873}{283}$

= 98.7×10^{-3} m^3/min.

Cross sectional area of the combustion tube

= 8×10^{-4} m^2

$\therefore$ velocity of combustion gases

$$= \frac{98.7 \times 10^{-3}}{8 \times 10^{-4} \times 60}$$

$$= 2.06 \text{ m/s}$$

$\therefore$ Residence time at post 3, 1m from the burner plate, $\tau_3 = \frac{1}{2.06}$ secons

$$= \underline{0.484} \text{ s}$$

APPENDIX 2

The Evaporating Chamber

The main criteria for the design of the evaporating chamber was that it should be able to evaporate at least 10 cm^3 of Kerosine per minute and mix it with air prior to entering the combustion zone.

Taking the sp gravity of Kerosine as 0.78 at 15°C, which is assumed as room temperature, mass flow rate of Kerosine,

$$= 10 \times 0.78 = 7.8 \text{ g/min.}$$

From 'spiers'[69], mean sp. heat of Kerosine

$$= 2.0 \text{ KJ/Kg K}$$

Say, the final temperature of Kerosine = 180°C,

Heat required to raise the temperature of Kerosine from 15°C to 180°C = m x sp. heat x $(T_2 - T_1)$

where m = mass flow rate of Kerosine

T_2 = final temperature of Kerosine

T_1 = initial temperature of Kerosine

Taking latent heat of evaporation of Kerosine

$$= 355 \text{ KJ/Kg,}$$

Total heat required by Kerosine,

$$= 7.8 \times 10^{-3} \quad (355 + 2.01 \ (180 - 15))$$

$$= 5.37 \text{ KJ/min}$$

$$= 0.0895 \text{ KJ/sec} = 0.0895 \text{ KW}$$

Stoichiometric air required for burning

1 Kg of Kerosine = 14.7 Kg

Total air required using 20% excess air

$= 7.8 \times 14.7 \times 1.2 \times 10^{-3}$ Kg/min.

$= 138 \times 10^{-3}$ Kg/min.

Taking, sp. heat at constant volume of air

= 0.714 KJ/Kg K

Heat required by air

$= 0.714 \times 138 \times 10^{-3} \times 165$

= 16.2 KJ/min.

= 0.27 KJ/sec.

= 0.27 kW

Therefore total heat required = 0.27 + .089

= 0.359 kW

Therefore a 0.5 kW electric heater should be sufficient for this purpose.

APPENDIX 3

Calculations of maximum combustion gas velocity and fuel flow for laminar conditions

All calculations are duplicated for two temperatures of:

(a) $1000^{o}C$

(b) $600^{o}C$

(A) Combustion gas density

Taking the density of combustion gases at $0^{o}C$ and 760 mm Hg to be 1.257 Kg/m^3, the density of the combustion gases at the two temperatures are:

(a) at $1000^{o}C$, the gas density

$$= \frac{1.257 \times (273 + 0)}{(1000 + 273)} = 0.269 \text{ Kg/m}^3$$

(b) at $600^{o}C$, the gas density,

$$= \frac{1.257 \times (273 + 0)}{600 + 273} = 0.393 \text{ Kg/m}^3$$

(B) Absolute viscosity of the combustion gases

Assume viscosity of the combustion gases

= viscosity of nitrogen.

(a) Absolute viscosity of N_2 at $1000^{o}C = 461 \times 10^{-6}$ poises (ref. 89)

$= 461 \times 10^{-7}$ NS/m^2

(b) Absolute viscosity of N_2 at $600^{o}C = 386 \times 10^{-7}$ NS/m^2

(c) Velocity of combustion gases

Assume R_e = 2000 (for laminar flow)

$$R_e = \frac{\rho DV}{\mu}$$

where R_e = Reynolds No.

ρ = Density Kg/m^3

D = Diameter m

V = Velocity m/s

μ = Abs. viscosity NS/m^2

Choosing a pipe of internal diameter = 32×10^{-3} m

Case a) $$V = \frac{R_e \cdot \mu}{P.D} = \frac{2000 \times 461 \times 10^{-7}}{0.269 \times 32 \times 10^{-3}} \text{ m/s}$$

$$= \underline{\underline{10.4}} \text{ m/s}$$

Case b) $$V = \frac{2000 \times 368 \times 10^{-7}}{0.393 \times 32 \times 10^{-3}} \text{ m/s}$$

$$= \underline{\underline{5.85}} \text{ m/s}$$

i.e. the maximum velocity for laminar flow at 1000°C

= 10.4 m/s

and the maximum velocity for laminar flow at 600°C

= 5.85 m/s

(D) Combustion gas quantity flow

Quantity per second = cross sectional area m^2 x velocity m/s

cross sectional area = $\frac{\pi}{4} D^2 = \frac{\pi}{4} \times 32^2 \times 10^{-6}$ m^2

$= 804 \times 10^{-6}$ m^2

Case a) $\therefore$ $Q = 804 \times 10^{-6} \times 10.4^4 = 8.35 \times 10^{-3}$ m^3/s

Case b) $Q = 804 \times 5.85 \times 10^{-6} = 4.7 \times 10^{-3}$ m^3/s

(E) Calculation for the maximum quantity of diesel and Kerosine flow for laminar conditions.

Diesel.

From spiers(89) combustion gases at N.T.P. produced on burning 1 Kg of Diesel fuel with stoichiometric air are 12.20 m^3.

Theoretical air required for combustion

$= 11.46$ m^3/Kg of fuel at N.T.P.

Assuming combustion takes place with 20% excess air, the total volume of combustion gases

$= 12.2 + 0.20 \times 11.46$

$= 14.49$ m^3/Kg of fuel at N.T.P.

Case a) at 1000°C,

the volume of combustion gases

$= 14.49 \times \frac{1273.15}{273.15} = 67.4$ m^3/Kg of fuel

$\therefore$ maximum amount of fuel flow for laminar conditions

$$= \frac{8.35 \times 10^{-3}}{67.4} \quad \frac{m^3/s}{\frac{m^3}{Kg}}$$

$$= 124 \times 10^{-6} \text{ Kg/s}$$

Taking s.g. of Diesel fuel as 0.84, at N.T.P.

$$Q_{diesel} = \frac{124 \times 10^{-6}}{0.84} \times 1000 \times 60 \text{ cc/min}$$

$$= \underline{\underline{8.85}} \text{ cc/min.}$$

Case b) at 600°C

the volume of combustion gases

$$= 14.49 \times \frac{873 \cdot 15}{273 \cdot 15}$$

$$= 46.4 \text{ m}^3/\text{Kg of fuel}$$

Maximum amount of fuel flow for laminar conditions

$$= \frac{4.73 \times 10^{-3}}{46.4} \quad \frac{m^3/s}{m^3/Kg}$$

$$= 102 \times 10^{-6} \text{ kg/s}$$

$$Q_{diesel} = \frac{102 \times 10^{-6} \times 1000 \times 60}{0.84} = 7.3 \text{ cc/min.}$$

Kerosine

Combustion gases at N.T.P. produced on burning 1 Kg of Kerosine with stoichiometric air (89) = 12.13 m^3

Theoretical air required for combustion

$$= 11.35 \text{ m}^3/\text{Kg pf fuel at N.T.P.}$$

Assuming combustion takes place with 20% excess air, the total volume of combustion gases

$$= 12.13 + 0.2 \times 11.35 = 14.40 \text{ m}^3/\text{Kg of fuel at N.T.P.}$$

Case a) at 1000°C

Total volume of combustion gases

$$= 14.4 \times \frac{1273.15}{273.15}$$

$$= 67.2 \text{ m}^3/\text{Kg of fuel}$$

$\therefore$ maximum fuel flow for laminar conditions,

$$= \frac{8.35 \times 10^{-3}}{67.2} = 124.5 \times 10^{-6} \text{ Kg/s}$$

Assuming sp. gravity of Kerosine as 0.78,

$Q_{Kerosine}$ = Quality flow of Kerosine

$$= \underline{\underline{9.6}} \text{ cc/min.}$$

Case b) at 600°C

$$Q_{Kerosine} = \underline{\underline{7.9}} \text{ cc/min.}$$

APPENDIX 4

General principle of operation of analyser used for the measurement of carbonmonoxide, carbon dioxide and oxygen concentrations in the combustion gases

Infralyt III Gas Analyser for the Analysis of CO and CO_2

Purpose and application:

The Infralyt is a recording gas analyser operating on a Physical principle used for continuous quantitative determination of gas concentrations. It can be used in principle for the evaluation of gases consisting of 2 or more types of atoms. Excluded from the measurement are gases consisting of equal atoms such as O_2, N_2, H_2, Cl_2, etc. as well as inert gases and metal vapours. The results of the measurement in % v/v or g/m^3 are recorded and indicated on a moving coil instrument.

Principle of operation:

The operation of the Infralyt analyser is based on the absorption of infra-red radiation. Infra-red radiation forms part of the electro-magnetic spectrum; the range from 2 to 15 µm is used in the infra-red analyser. Gases which consist of at least two different types of atoms exhibit characteristic absorption bands in the infra-red regions. The infra-red radiation passing through a cell filled with a gas suffers a reduction in intensity over a wavelength range appropriate to the gas concerned, according to the Lambert-Beer Law :

$$I = I_{oe}^{-Acd}$$

where I_o represents the incident radiation,

C is the gas concentration,

d length of the absorption distance (cell length),

and A is the extinction constant.

The characteristic of the material which is responsible for the absorption is represented solely by the extinction constant A. Its value is usually dependent on the wavelength. If the concentration C of the measured component is increased or if the absorption distance d is extended, the absorption and therefore measuring effect increases. The product Acd is often referred to as extinction.

The emerging radiation I is therefore dependent on the gas concentration and the cell length.

Measuring Principle:

The schematic diagram is shown in Fig. (Appdx. 4.1).

The Infralyt operates without dispersion of the infra-red radiation. The required specific indication is achieved by using a selective radiation receiver. The heat radiation is emitted by two chrome-nickel filaments heated to red heat (700°C) and is concentrated into two beams by parabolic mirrors (1) and (7); these pass through a measuring cell (8) and a comparison cell (3) to the radiation receiver(5). The comparison cell (3) contains a gas which does not absorb the infra-red radiation. Pure nitrogen is used for this purpose.

The test gas mixture to be analysed passed through the measuring cell (8). If the test gas exhibits the property of absorbing infra-red radiation the two radiation beams emerging from the two cells differ in intensity in the appropriate wavelength range.

The principle of selective measurement in this instrument consists of measuring the intensity difference of the infra-red

radiation not with bolometers or photocells but by using as radiation receiver a sealed volume of the actual gas to be measured.

The radiation receiver consists of two chambers (4)(9) which are sealed off from the outside by windows transparent to infra-red radiation and which are separated by a diaphragm condenser. This diagram condenser consists of a thin metal foil (10) mounted under tension at a distance of a few hundredths of a millimeter from a carefully insulated metal plate (6).

When determining the CC content of a gas, for example, the two chambers are filled with a 15% mixture of CO in Argon. If the test gas contains some of the receiver gas the resulting difference in the radiation produces a selective pressure and temperature difference between the two chambers of the receiver which give rise to a change in capacity. A rotating chopper (2) interrupts the two beams periodically in synchronism. The interruption takes place 6.25 times per second. This measure excludes the slow and non-selective heating of the cell walls so that only the temperature rise of the gas is measured. The resulting periodic variation in capacity Δc is concerted into an a.c. voltage charge Δu which is more suitable for further processing than a fixed capacity corresponding to a particular concentration.

The low-level a.c. voltage output now available at the radiation receiver is amplified in a value amplifier (11), rectified and then fed to indicating or recording instruments (12).

Permolyt Oxygen Analyser for the analysis of oxygen concentration in the combustion gases

The Permolyt magnetic oxygen analyser is used to determine the oxygen content in gas mixtures and the results of the analysis (Vol. % O_2) is recorded on potentiometric recorders.

Principle of Operation

Oxygen differs from all other gases by its paramagnetic behaviour. The magnitude of the paramagnetic effect varies inversely with the absolute temperature, while the diamagnetic properties are independent of temperature. For this reason a gas containing oxygen placed in a magnetic field will suffer a smaller attraction at elevated temperature than a colder gas of the same composition. The measurement of the oxygen content and the conversion of the result into a voltage corresponding to the oxygen content takes place in a ring chamber.

This chamber (See Fig. Appdx. 4.2) is made from a non-magnetic material and consists of an annular gas channel connected by a horizontal glass tube. This tube carries on its outside two platinum windings adjacent to each other which are connected together with two Rheostan resistance into a Whetstone bridge circuit. When heated electrically, the tube becomes hotter in the centre than at its ends. A powerful magnetic field is placed at one end of the tube. If gas containing oxygen passes through the ring chamber, it is attracted more strongly at the left end of the tube than at the heated right end. A gas flow from left to right is produced which is proportional to the oxygen content.

The resulting thermal and resistance changes in the two arms of the bridge circuit unbalances the bridge and gives rise to a deflection of the recording instrument connected in the diagonal which is calibrated in % O_2 by volume. The measured value is determined mainly by the oxygen content of the test gas but its remaining composition must also be taken into account. The flow through the measuring tube is affected by the coefficient Cp ρ/η which therefore influences the measured value, Cp, being specific heat, and ρ is the density of gas and η is the viscosity of the test gas.

When calibrating the Permolyt, it is necessary therefore to use a gas corresponding to the actual test gas.

The constant-temperature measuring system (1), the transistorised constant voltage supply with temperature controller (6) and the control unit (10) are designed as separate sub assemblies and are contained in a sheet steel dust and splash-proof housing which is mounted on an aluminium base plate.

The oxygen content is recorded and indicated on instruments which are installed separately from the Permolyt.

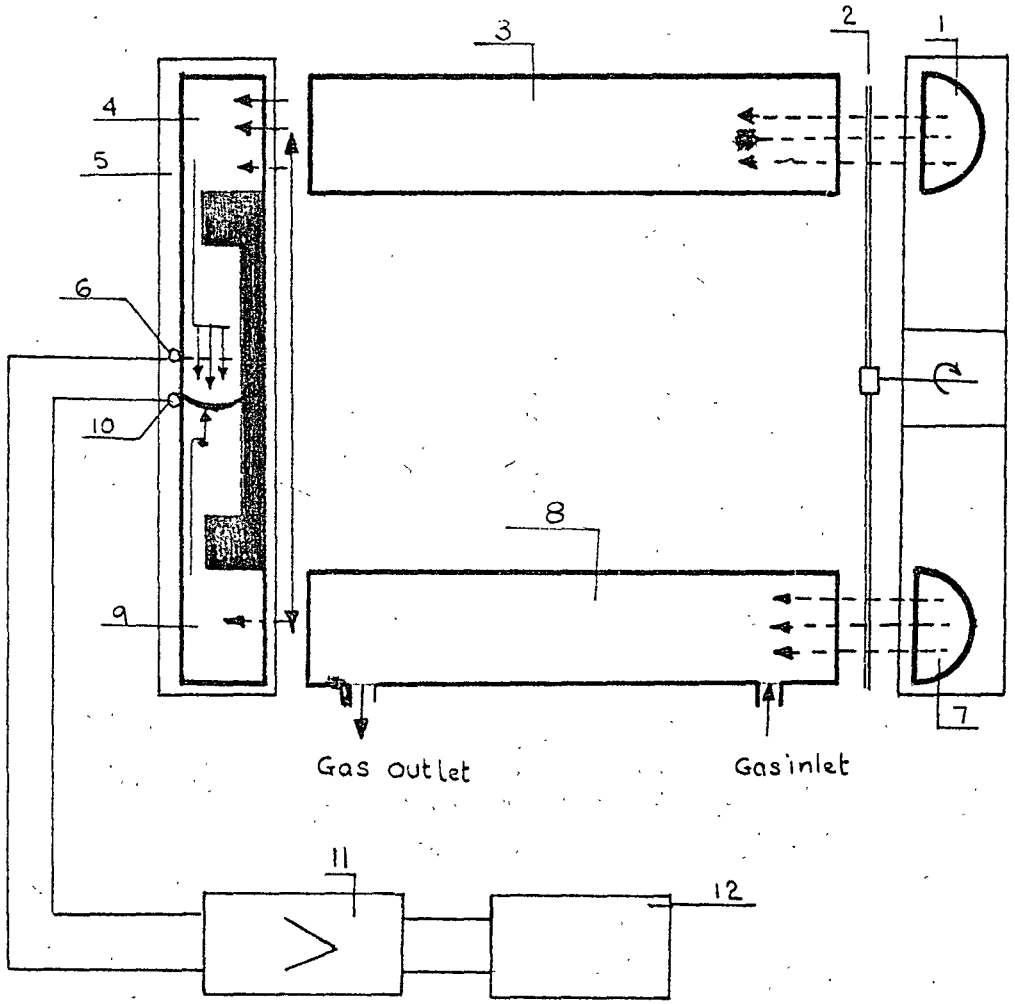

APP. A.1

FIG. Measuring Principle of Infralyt III.

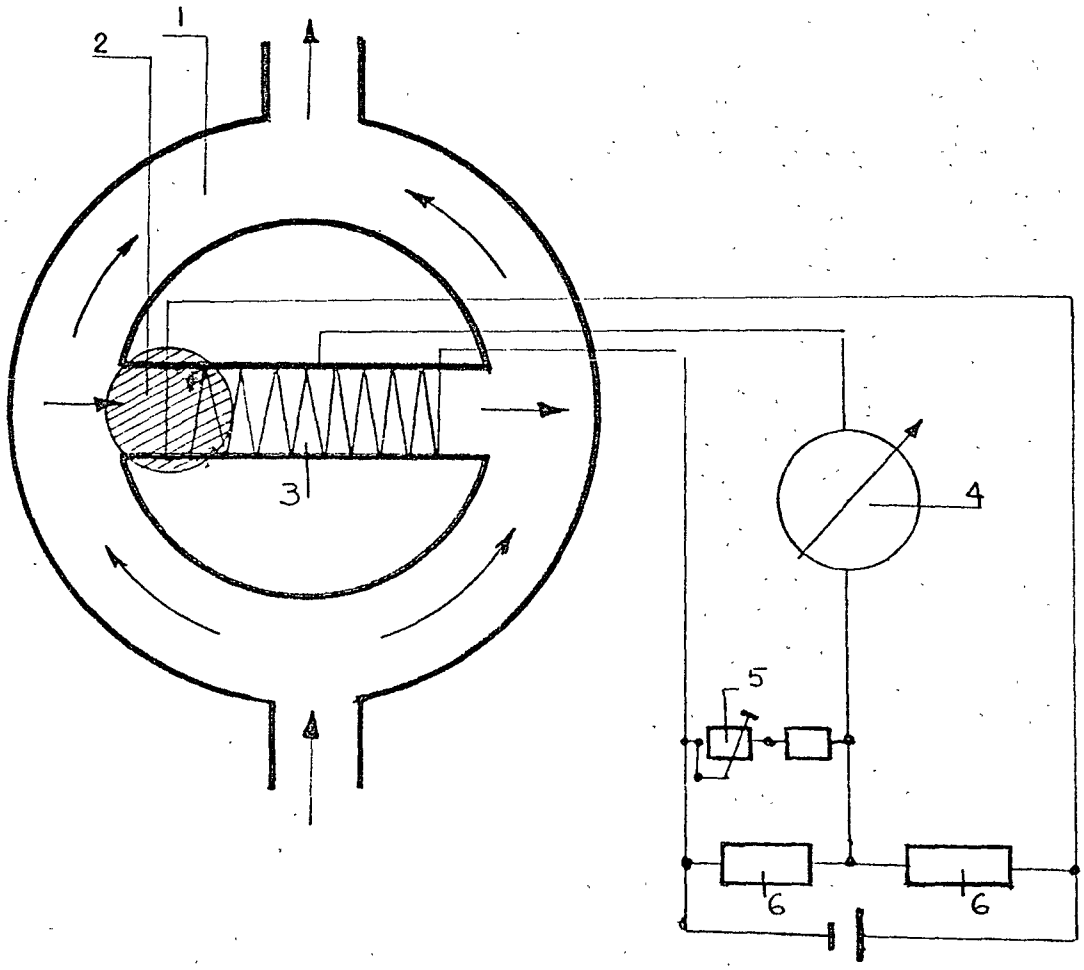

App 4.2

Fig. Ring chamber ; 1. Ring chamber ; 2. Magnetic field ; 3. Glass tube with heater windings ; 4. Measuring instrument; 5. Zero adjustment ; 6. Bridge resistances.

APPENDIX 5

Calculation for the thickness of the insulating blanket

Theory.

Consider Fig. A5-1 below which shows the cross-section of the insulation on the pipe. The outside radius of the insulation and the pipe being r_i and rp respectively. The corresponding temperatures are t_i and tp where $t_i > tp$ and the heat transfer rate Q is in the direction shown.

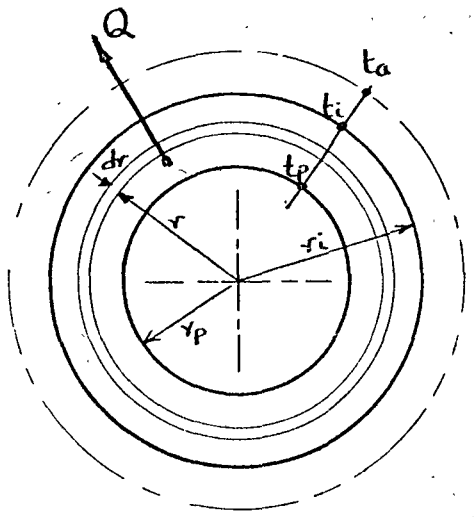

FIG. A5-1

Consider unit length of the tube and an elementary thickness of insulation dr at radius r. Let dt be the temperature fall across dr, then considering the heat transfer rate Q is constant through each successive layer of material,

$$Q = - K A \frac{dt}{dr} \quad \ldots (1)$$

where K = thermal conductivity ($^{W}/_{mK}$)

A = surface area (m^2)

For unit length of pipe, $A = 2 r \times 1 = 2 r$

$$\therefore \quad Q = K 2 r \frac{dt}{dr} \quad \ldots (2)$$

Integrating:

$$\text{Heat transfer rate per unit length} = Q = \frac{2 K(tp - ti)}{\ln \frac{r_i}{r_p}} \quad \ldots (3)$$

Now, considering heat transfer from the outer surface of the lagging to the surroundings, and applying the equation:

$$Q = h A \theta$$

where h = surface transfer coefficient ($^{W}/_{m^2K}$)

A = surface area (m^2)

θ = temperature difference between the surface and its surroundings (K)

For unit length, $A = 2 r_i$

$$\therefore \quad Q = h 2 r_i (t_i - t_a) \quad \ldots (4)$$

Transposing equation (3) and (4) we have,

$$\frac{Q \ln \frac{r_i}{r_p}}{2 K} = t_p - t_i$$

$$\frac{Q}{2 r_i h} = t_i - t_a$$

Adding both sides:

$$\frac{Q}{2}\left[\frac{\ln \frac{r_i}{r_p}}{K} + \frac{1}{r_i h}\right] = t_p - t_a \qquad \ldots (5)$$

Application to the present problem:

Heat lost per meter length of the pipe is also

= = m x cp x dT

where m = rate of mass flow of combustion gases (g/s)

cp = sp. heat of combustion gases (J/g deg.C)

dT = temperature drop per meter length of the tube.

A gas temperature of 1000°C at the beginning of the combustion tube and a temperature drop of 100°C along 1 meter length of the tube are assumed.

Taking sp. heat of combustion gases as that of air, the sp. heat of air at 1000°C, from Spiers[89] = cp = 1.21 J/g deg.C, the density of combustion gases at 1000°C, calculated in App. 3 = 269 g/m^3, and the rate of volumetric flow of combustion gases at 2000°C was calculated = 8.3×10^{-3} m /s. Therefore the rate of mass flow = m

= $8.3 \times 10^{-3} \times 269$

= 2.23 g/s

Therefore heat lost per meter length of the tube = Q = m cp dT

Here, m = 2.23 g/s = 2.23 x 1.21 x 100

cp = 1.21 J/g deg.C = 270 J/s

dT = 100°C

This heat is conducted through the insulation and is also converted from the outside surface, and this value of Q is used in equation (5).

Here t_a = ambient temperature = 20°C

r_p = outside radius of the pipe = 19×10^{-3} m

K = thermal conductivity of the insulating blanket

= 0.238 J/sm°C

h = surface transfer coefficient = 1.08 J/sm²c

Substituting the above values in equation (5) we get,

$$\frac{\ln r_i/19 \times 10^{-3}}{0.238} + \frac{1}{r_i \times 1.08} = (1000-20)$$

Q = 270 J/s

K = 0.238 J/sm°C

h = 1.08 J/sm²C

tp = 1000°C

ta = 20°C

From above, the value of r_i was calculated to be 50.8 mm (using trial and error method) i.e. a thickness of 31.8 mm of blanket. In practice, an insulating blanket of 50.8 mm thickness was used for lagging purposes.

APPENDIX 6

Finite Difference Equations

Lanczos[90] gives a method of fitting exponential curves of the type

$$u(t) = A_1 e^{\lambda_1 t} + A_2 e^{\lambda_2 t} + A_3 e^{\lambda_3 t} \ldots + A_n e^{\lambda_n t}$$

to ordinates (evenly spaced) supplied by experimentation.

In our case, theoretical consideration of the number of exponentials involved is 2, and we also require that $u(o) = o$.

It follows that we are assuming that the differeme equation relating consecutive equally spaced ordinates is of form

$$a\,u(t + 2h) + b\,u(t + h) + c\,u(t) = o \qquad \ldots (1)$$

$u(t)$ is function we are looking for

t is independent viable

h is step between successive ordinates

a, b, c are real constants.

It can be demonstrated that solutions of form $u(t) = A\,\alpha^t$ of equation (1) must satisfy

$$A\,\alpha^t (a\,\alpha^{2h} + b\,\alpha^h + c) = 0 \qquad \ldots (2)$$

If we put $Z = \alpha^h$ ... (3)

then we look for solutions of auxiliary equation

$$a Z^2 + b Z + c = o \qquad \ldots (4)$$

and we can find α using equation (3)

$$\log_e \alpha = \log_e Z/h$$

putting $\alpha = e^{\lambda}$

then $$\lambda = \log_e Z/h \qquad \ldots (5)$$

Since (4) is quadratic, we will expect two solutions for Z which must both be positive to satisfy (5). It can be shown that if $A e^{\lambda_1 t}$, $B e^{\lambda_2 t}$ are solutions of (1) then

$$u(t) = A e^{\lambda_1 t} + B e^{\lambda_2 t} \qquad \ldots (6)$$

is also a solution and a general solution if $\lambda_1 \neq \lambda_2$

Since in this problem we also require $A = - B$ ... (7)

then it follows that it is necessary to put $u(o) = o$

To obtain a unique solution of the problem we require 4 ordinates (including $u(o) = o$) (See Fig. Ap.6-1)

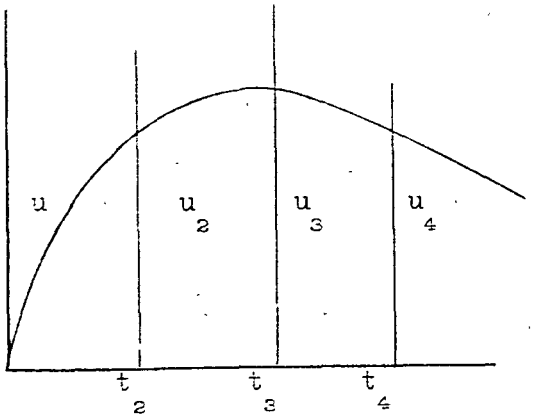

Table of data required

ot	u(t)
o	o
h	u_2
2h	u_3
3h	u_4

FIG. Ap. 6-1

Rearrange difference equation (1)

$$b_o\, u(t) + b_1\, u(t + h) + u(t + 2h) = o \qquad \ldots (8)$$

we substitute values of u_i into (8) with 1st. case $u(t) = o$

$$b_o\, u_1 + b_1\, u_2 + u_3 = o \qquad \ldots(9)$$

But $u_1 = o$

$$\therefore \quad b_1\, u_2 + u_3 = o \qquad b_1 = \frac{-u_3}{u_2} \qquad \ldots(10)$$

2nd. case

$$u(t) = u(h) = u_2$$

$$b_o\, u_2 + b_1\, u_3 + u_4 = o \qquad \ldots(11)$$

whence

$$b_o = \frac{- b_1\, u_3 - u_4}{u_2}$$

$$= \left(\frac{u_3}{u_2}\right)^2 - \left(\frac{u_4}{u_2}\right) \qquad \ldots (12)$$

With the new notation, equation (4) becomes

$$Z^2 + b_1 Z + b_o = o \qquad (4a)$$

Substituting b_o and b_1 into (4a) we find necessary and sufficient conditions for solutions of the difference equation to be

$$\left.\begin{array}{l} b_o > 0 \\ b_1 < 0 \\ \text{and} \quad b_1^2 - 4b_o > 0 \end{array}\right\} \quad 11$$

Given satisfactory values of b_o b_1 for solution we obtain solutions of (4a) as follows:

$$Z_1, Z_2 = \frac{u_3}{2u_2} \pm \frac{1}{2} \sqrt{4\left(\frac{u_4}{u_2}\right) - 3\left(\frac{u_3}{u_2}\right)^2} \qquad \ldots (13)$$

values of corresponding λ can be obtained from (5).

From (6) and (7), we obtain

$$u(t) = A\left(e^{\lambda_1 t} - e^{\lambda_2 t}\right) \qquad \ldots (14)$$

replacing λ_i by $-k_i$ and A by a $\frac{k_1}{k_2 - k_1}$ we can evaluate a,

$$a = \frac{u_3 (k_2 - k_1)}{k_1 \left(e^{-k_1 3} - e^{-k_2 3}\right)} \qquad \ldots (15)$$

To facilitate the calculation of the results a short computer program has been written by Mr. Chris Abbess of the Middlesex Polytechnic Computing staff, using the algorithm described above.

The following pages show a listing of the FORTRAN program and specimens of computer output.

```
C       SEPARATES  EXPONENTIALS INTO  FORM:
C           U(T)   =A*K1*(EXP(-K1*T) - EXP(- K2*T))/(K2 - K1 )
C       DATA:
C           1ST CARD  INTERVAL BETWEEN ORDINATES(= H) (F10.3)
C           2ND- 4TH CARDS   ITH CARD CARRIES  VALUES OF ORDINATE
C                      U(I)   LO, MID HI VALUES ARE RECORDED  (3F10.3)
C                      E.G.  2ND CARD  RECORDS VALUES  OF U2
C       PROGRAM ATTEMPTS TO FIND CURVES OF STATED TYPE TO FIT  LO, MID
C           OR HI SET OF ORDINATES. FAILURE LEADS TO MESSAGE:
C                     'DID NOT COMPUTE '
            JOB NAME   *DISK0
```

```
001             DIMENSION U(3,3), V(2,3), A(3), LAB(3)
002             DATA LAB/ 3HLO , 3HMID,3HHI /
003              DO1 NN = 1,2
004             READ(2,21) H,((U(I,J),J=1,3),I=1,3)
005     21      FORMAT(F10.3/(3F10.3))
006             WRITE(3,31) H, (LAB(I),(U(J,I),J=1,3),I=1,3)
007     31      FORMAT(1H1,10X,26HSEPARATION OF EXPONENTIALS/
                1(1H2,    6HINPUT:/
                2(1H2,5X,3HH =,F10.3/
                3(1H2,12X, 2HU2,10X, 2HU3,10X, 2HU4/ 3
                4(1H2, A3,2X, 3F12.4/),
                X  8H2OUTPUT:/
                5(1H2,12X, 1HA, 11X, 2HK1,10X, 2HK2 )
010             DO I I = 1,3
011             CALL AHMED (H,U(1,1),U(2,1),U(3,1),V(1,1),V(2,1),A(I),IND)
012             IF(IND.EQ.2) GO TO 2
013             WRITE(3,32) LAB(I), A(I), V(1,I), V(2,I)
014     32      FORMAT(1H2, A3, 2X, 3F12.4 )
015             GO TO 1
016     2       WRITE(3,33)
017     33      FORMAT(16H2DID NOT COMPUTE)
020     1       CONTINUE
021             STOP
022             END
```

```
001             SUBROUTINE AHMED(H,U2,U3,U4,V1,V2,A,IND)
002             P= U3/U2
003             Q= 4.*U4/U2 - 3.*P*P
004             IF(P*P.GT.U4/U2.AND.Q.GT.0.) GO TO 1
005             IND = 2
006             RETURN
007     1       V1 = - ALOG((P-SQRT(Q))/2.0)/H
010             V2 = - ALOG((P+SQRT(Q))/2.0)/H
011             A  = U3*(V2 - V1)/V1/(EXP(-2.*V1*H) - EXP(-2.*V2*H) )
012             IND = 1
013             RETURN
014             END
```

SEPARATION OF EXPONENTIALS

INPUT:

m = .150

	U2	U3	U4
LO	100.0000	103.0000	90.0000
MID	102.0000	105.0000	92.0000
HI	104.0000	107.0000	94.0000

OUTPUT:

	A	K1	K2
LO	138.2220	11.0015	1.1783
MID	139.7896	11.1669	1.1456
HI	141.3868	11.3279	1.1148

SEPARATION OF EXPONENTIALS

INPUT:

m = .200

	U2	U3	U4
LO	107.0000	98.0000	78.0000
MID	109.0000	100.0000	80.0000
HI	111.0000	102.0000	82.0000

OUTPUT:

	A	K1	K2
LO	147.0910	9.7604	1.2815
MID	148.6257	9.8927	1.2477
HI	150.1915	10.0213	1.2157

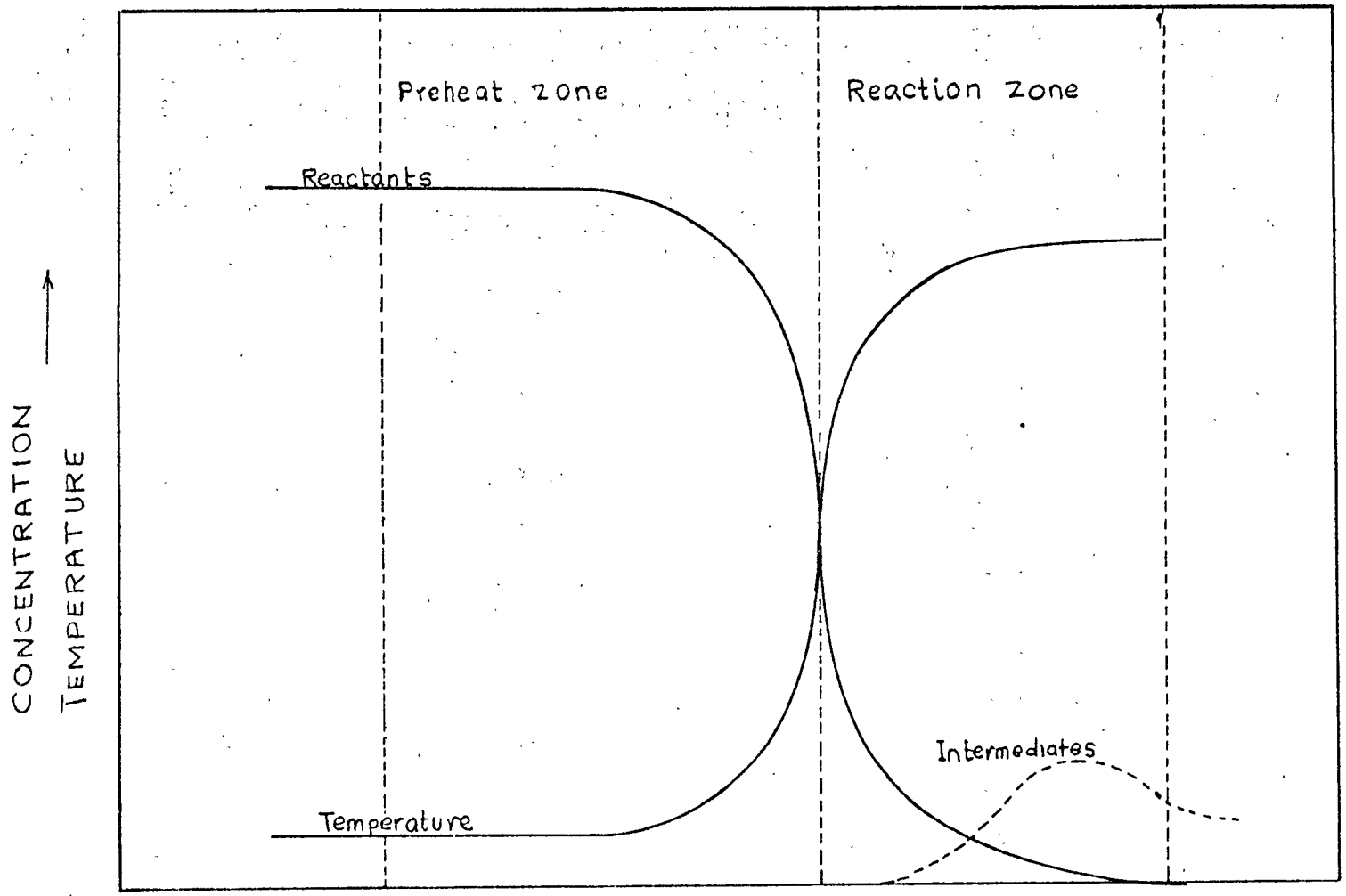

FIG. A-1. Concentration and temperature profiles through the pre-mixed flame. After ref. [6].

CHAPTER 12

REFERENCES

1. Williams, F.A. and Cawley, C.M. See Reference (2) Paper 2, Page 24.

2. Johnson, H.R. and Littler, D.J. Proceedings of International Conference 'Mechanism of corrosion by fuel impurities'. Marchwood Engineering Laboratories, Marchwood, 20th to 24th May 1963. Butterworths Sci. Publ. London.

3. Nelson, H.W. "Corrosion and deposits in coal and oil fired boilers and gas turbines" A.S.M.E. Publication 1959.

4. Jackson, P.J. Researches in the C.E.G.B. into fireside fouling and corrosion in boiler plants. J.Inst.Fuel, 1967, 40, 335.

5. Crossley, H.E. "External fouling and corrosion of boiler plant" A. commentary. J.Inst.Fuel, 1967, 40, 342.

6. Barrett, R.E. "High-temperature corrosion studies in an oil-fired Laboratory Combustor". Trans. of A.S.M.E. J.Engn. for Power. April 1967, Pages 288-296.

7. Laxton, J.W. "The influences of excess oxygen and metallic additives on the formation and deposition of sulphur oxides in flue gas" See Reference (2) Paper 1 Page 228.

8. Dooley, A and Whittingham, G. "The oxidation of SO_2 in gas flames". Trans. Faraday Soc. 1946, 42, 354.

9. Hedley, A.B. "Factors affecting the formation of SO_3 in flames" J.Inst.Fuel, 1967, 40, 142.

10. Nettleton, M.A. and Stirling, R. "The formation and decomposition of SO_3 in flames and burnt gases". Proc. 12th Int.Symp. on Combustion, 1969, Academic Press, New York, U.S.A.

11. Harlow, W.F. "Causes of flue gas deposits and corrosion in modern boilers". Proc.Inst.Mech.Engrs. 151, 293-309 (1944)

12. Hedley, A.B. Ph.D. Thesis, Sheffield University, 1961.

13. Gaydon, A.G. and Whittingham, G. Trans.Farad.Soc. A., 1947, 189, 313-325.

14. Rylands, J.R. and Jenkinson, J.R. "The acid dew-point" J.Inst.Fuel. 27, 299 (1954).

15. Alexander, P.A., Fielder, R.S., Jackson, P.J., Raask, E., and Williams, T.B., "Acid deposition in oil-fired boilers: Comparative trials of additives and testing techniques" J.Inst.Fuel, 34, 53 (1961).

16. Gaydon, A.G. Proc.Royal Soc.A., 1944, 183, 111.

17. Crumley, P.H., and Fletcher, A.W. J.Inst.Fuel, 1956, 29, 322.

18. Hedley, A.B. "A kinetic study of sulphur trioxide formation in a pilot scale furnace". See Reference 2 Paper 11.

19. Bodenstein and Pohl, Z. Electrochem. 11, 373 (1905)

20. Levy, A and Merryman, E.L., "SO_3 formation in H_2s flames" Journal of Engineering for Power, Trans. A.S.M.E., Vol. 87, Series A, 1965, pp.374-378.

21. Barrett, R.E., Hummell, J.D., and Reid, W.T. "Formation of SO_3 in a non-catalytic combustor". Trans. A.S.M.E., J.Eng.,Power, 1966, 88, (2), 165.

22. Wiedersum, G.C., "Corrosion and deposits from combustion gases: a review" Mechanical Engineering, August 1968, pp. 22-27.

23. Halstead, W.D., "Progress Review No. 60: some chemical aspects of fireside corrosion in oil-fired boilers" J. Inst. Fuel, July 1970, Pages 234-239.

24. Whittingham, G., "Oil-fired boilers" Paper presented at the I.Mech.E. 8th March 1961.

25. Shaw, J.T., and Green, P.D.," Oxidation of SP_2 in air at 950°C Co-operative influence of CO and NO" Nature 1966, 211, 1171.

26. Harlow, W.F., "Formation of sulphuric acid in boiler flue gases". Trans. A.S.M.E., 1958, 80, 225.

27. Anderson, D.R., and Manlick, F.P., Trans.A.S.M.E. 1958, 80, 1231. "Sulphuric Acid corrosion in oil-fired boilers - studies on SO_3 formation"

28. Rendle, L.K., and Wilsdon, R.D., "The prevention of acid condensation in oil-fired boilers". J.Inst. Fuel., 1956, 29, 372.

29. Corbett, P.F., "The SO_3 content of the combustion gases from an oil-fired water tube boiler". J.Inst.Fuel, 1953, 26, 92.

30. Flint, D., Lindsay, A.W. and Littlejohn, R.F., "The effect of metal oxides smokes on the SO_3 content of combustion gases from fuel oils". J.Inst.Fuel, 1953, 26, 122.

31. Taylor, R.P., and Lewis, A., "SO_3 formation in oil firing" International Congress on Industrial Heating (Paris 1952), Group II, Section 24, No. 154.

32. Jarvis, W.D., "The solution and use of additive in oil-fired boilers". J.Inst.Fuel, November 1958.

33. Ahmed, S.H., "Low-temperature corrosion by flue gases from burning fuel oil" M.Sc. Thesis, University of London, 1962.

34. Crossley, H.E., "Prevention of corrosion and deposits" Paper No. 16, Proceedings at the Residential Conference on Major Developments in Liquid Fuel Firing, May 1959, pp. D-9-12. Published by the Inst. of Fuel.

35. Remeysen, J., "Low-excess combustion of fuel oil at Merksem Power Station (Belgium)" A.S.M.E. Paper No. 63-WA-163, November 1963.

36. Chaikivsky, M., and Siegmund, C.W., "Low-excess air combustion of heavy fuel-high-temperature deposits and corrosion" J.Engng. for Power, October 1965, pp. 379-388.

37. Glaubitz, F., "The Economic combustion of sulphur-containing Heating Oil". Combustion, March 1963, pp. 25-32.

38. Neipenberg, H.P. "Combustion control of oil-firing systems operated at low excess-air levels". Paper 5. Third Liquid Fuels Conference, Torquay, April 1966.

39. Lees, B., "An Investigation into the air-heater corrosion of oil-fired boilers". J.Inst.Fuel, 1956 (April) 29, 171.

40. Fielder, R.S., Jackson, P.J. and Raask, E., "The determination of sulphur trioxide and sulphur dioxide in flue gases" J.Inst. Fuel, Vol. No. 229, February 1960, pp. 84-89.

41. Rosborough, D.F., Discussion of Ref. 15. J.Inst. Fuel, June 1961, pp. 250-251.

42. Reese, J.T., Jonakin, J., and Caracristi, V.Z., "Prevention of residual oil combustion problems by use of low excess air and magnesium additive" A.S.M.E. Paper No. 64-Pwr-3, April 1965, pp. 229-235.

43. Holland, W.H., and Rosborough, D.F. "High temperature corrosion trials at Marchwood Power Station - effect of low-excess air and magnesium hydroxide" J.Inst.Fuel, June 1971, Papers 300-308.

44. Exley, L.M., "A practical review of residual oil firing problems and solutions" Combustion, March 1970, pp. 16-23.

45. Wheeler, W.H., "Developments in the application of two stage combustion" Proceedings of Conference on Application of Liquid Fuels. Inst.Fuel, 1966, 1, 95.

46. Archer, J.S., and Eisenklam P., "Multistage combustion of residual fuel oil, Part I : The effects of using air or steam for the atomization of residual fuel in a high intensity first stage gasifier". J.Inst.Fuel, October 1970. pp. 397-404.

47. Whittingham, G., "The influence of carbon smoke on the dew-point SO_3 content of flame gases" J.Appl.Chem. 1951, 1, 382.

48. Rosahl, O., VI K. Mitt. No.4,(1956) pp. 53-61. "The state of Development of steam-boiler technology in Germany"

49. Marskell, W.G., "The work of the boiler availability Committee - Contribution No. 6" J.Inst.Fuel, No. 218, March 1959, pp. 130-132.

50. Laxton, J.W., "The influences of excess oxygen and metallic additives on the formation and deposition of sulphur oxides in flue gases" Paper 13. See Reference (2).

51. Volkov, V.L., and Fotiev, A.A. "Characteristic features of the reaction of V_2O_5 with $CaCO_3$ in vacuum" J.Inorg.Chem. U.S.S.R. 1969, 14, 184.

52. Hansen, W., "A successful additive against high-temperature corrosion by residual fuel oil ash" J.Inst.Fuel, 1967, 40, 348.

53. Niles, W.D., and Siegmund, C.W., "Reaction between fuel ash components and additive combinations" Paper 22 - See Reference (2).

54. Whittingham, G., "The influences of silica smokes on the dew-point of combustion gases containing sulphur oxides". J.Soc.Chem.Ind., 1948, 67, 411.

55. Brett Davies, E., and Alexander, B.J. "The use of Heterocyclic tertiary amines for the control of corrosion caused by flue gases" J.Inst.Fuel, No.231 April 1960 pp. 163-173.

56. Jenkinson, J.R., and Zaczek, B.J., "Anti-corrosion additives in oil fired boilers" Convention of European Federation of Corrosion in Frankfurt (Main), March 1965.

57. Lees, G.K., Friedrich, G.K., and Mitchell, E.R., "Control of SO_3 in low-pressure heating boilers by an additive" J.Inst.Fuel, February 1969, 67-74.

58. Lavell, P.S., "Selection of metal oxides for removing sulphur dioxide from flue gas" Ind. & Engng. Chem. 10 (3) July 1971, pp. 384-390.

59. Macfarlane, J.T., "The relationship between combustion conditions and the corrosion of metal surfaces by fuel oil ash deposits" Paper 16 - See Reference (2).

60. Attig, R.C., and Sedor, P., "A pilot-plant investigation of factors affecting low-temperature corrosion in oil-fired boilers" J.Engng. for Power. April 1965, pp. 197-204.

61. Dunn, D.C. "Contribution No. 3 - The work of the Boiler Availability Committee" J.Inst. Fuel. March 1959, pp. 123-126.

62. Raylands, J.R., and Jenkinson, J.R., Proc. Instn.Mech.Engrs. London, 1948. 158, 405.

63. Johnstone, H.F., University of Illinois Engineering Experimental Station Bulletin, 228, 1931, p.45.

64. Zaczek, B.J., and Grindley, R., "Fuel additive in the fight against corrosion" Paper presented at the Corrosion Convention, 15th October 1957.

65. Levy, A., and Merryman, E.L., "Interactions of sulphur oxide-iron oxide systems" J.Engng. for Power, Trans. A.S.M.E. Ser.A., 1967, 89, 297.

66. Minkoff, G.J., and Tipper, C.F.H., "Chemistry of combustion reactions". Butterworth Publication 1962.

67. Semenov, N.N., "Some problems in chemical kinetics and reactivity". (a) Vol.2 (1959), Princeton University Press.

68. Goksoyr, H., and Ross, K., "The determination of Sulphur Trioxide in the Flue Gases," Journal of the Institute of Fuel, vol. 35, 1962, pp.177-179.

69. Bradley, J.N., "Flame and Combustion Phenomena" Methuen & Co Ltd., New Fetter Lane, London E.C.4

70. Lewis, B., and Elbe, G. Von. Combustion, Flames and Explosions of Gases (1951) Academic Press, New York.

71. Lewis, B., and Elbe, G. Von., and Roth, W., 5th Symp. p.610.

72. Gordon, A., and Knipe, R.H., J.Phys.Chem., 1955, 59, 1160.

73. Minkoff, G.J., and Everett, A.J., and Broide, H.P., 5th Symp. p. 779.

74. Semenov, N.N., Chemical kinetics and chain reactions Oxford University Press (1935)

75. Gordon, A.G., and Knipe, R.H.J., Phys.Chem. 59 (1955) 1160.

76. Avramenko, L.I., and Kolesnikova, R.V., Bull. Acad. Sci. U.S.S.R., Dir Chem.Sci (1959)

77. Malcahy, M.F.R., Steven, J.R., Ward, J.C., and Williams, D.J., "Kinetics of interaction of oxygen atoms with sulphur oxides" 12th. Int.Symposium Combustion, 1969.

78. Gaydon, A.G., General discussion on the paper by Dooly and Whittingham, Reference (8).

79. Harcourt, A.V., and Esson, W., Proc.Roy.Soc.(London), 14, 470 (1865); Phil.Trans., 156, 193 (1866); 157, 117, (1867).

80. Gmelias Handbuch der anorganischan chemie, 8th edition (1953) System No.9, schwefel. Teil Ap 325, Published by Verlag Chemie, Gmbh Weinheim, Bergstrasse.

81. Kapustinsky, A.F., Samovsky, L.M., Acta Physicochim, U.R.S.S., 1936, 4, 791.

82. Macfarlane, J.J., "The formation of sulphur trioxide in the combustion products from petroleum fuel oils" J.Inst.Fuel, 1962, 35, 502.

83. Htun, M.N., "Residual fuel oil combustion: the effect of air/fuel ratio on the products of combustion". Ph.D. Thesis, University of London, 1960.

84. Fowle, F., Smithsonian Physical Tables, 8th edition (1934) Published by Smithsonian Institution, Washington, D.C.

85. Tamura, Z., and Tanasawa, Y., "Evaporation and combustion of a drop contacting with a hot surface" Seventh Symp. (International) on Combustion. Butterworth Scientific Publications, London 1959.

86. Satcunanathan, S., Ph.D. Thesis, University of London, 1966.

87. Satcunanathan, S., Zaczek, B.J., "The spontaneous ignition and ignition delay of liquid fuel droplets inpinging on a hot surface" Paper 41, Thermodynamics and Fluids Mechanics Convention, Bristol 27-29 March 1968. Published by the Inst. of Mechanical Engineers.

88. Laidler, K.J., Chemical kinetics. McGraw-Hill, p.69 (1950).

89. Spiers, H.M., "Technical data on fuel" 6th edition, 1962 British National Committee World Power Conference.

90. Lanczos, C " Applied Annalysis" PITMAN & SONS. LTD.